EXPERIMENTAL AND COMPUTATIONAL INVESTIGATION OF THE EMERGENCY COOLANT INJECTION EFFECT IN A CANDU INLET HEADER

A THESIS SUBMITTED TO
THE GRADUATE SCHOOL OF NATURAL AND APPLIED SCIENCES
OF
MIDDLE EAST TECHNICAL UNIVERSITY

BY

K. ZAFER TURHAN

IN PARTIAL FULFILLMENT OF THE REQUIREMENTS
FOR
THE DEGREE OF MASTER OF SCIENCE
IN
MECHANICAL ENGINEERING

FEBRUARY 2009

Approval of the thesis:

EXPERIMENTAL AND COMPUTATIONAL INVESTIGATION OF THE EMERGENCY COOLANT INJECTION EFFECT IN A CANDU INLET HEADER

submitted by **K. ZAFER TURHAN** in partial fulfillment of the requirements for the degree of **Master of Science in Mechanical Engineering Department, Middle East Technical University** by,

Prof. Dr. Canan Özgen _____
Dean, Graduate School of **Natural and Applied Sciences**

Prof. Dr. Suha Oral _____
Head of Department, **Mechanical Engineering**

Prof. Dr. A. Orhan Yeşin _____
Supervisor, **Mechanical Engineering Dept., METU**

Dr. Enis Pezek _____
Co-Supervisor, **Engineer, EÜAŞ**

Examining Committee Members:

Assoc. Prof. Dr. Cemil Yamalı _____
Mechanical Engineering Dept., METU

Prof. Dr. A Orhan Yeşin _____
Mechanical Engineering Dept., METU

Dr. Enis Pezek _____
EÜAŞ

Prof. Dr. Taner Altunok _____
Turkish Military Academy

Assist. Prof. Dr. İlker Tarı _____
Mechanical Engineering Dept., METU

Date: 11.02.2009

I hereby declare that all information in this document has been obtained and presented in accordance with academic rules and ethical conduct. I also declare that, as required by these rules and conduct, I have fully cited and referenced all material and results that are not original to this work.

Name, Last name : K. Zafer TURHAN

Signature :

ABSTRACT

EXPERIMENTAL AND COMPUTATIONAL INVESTIGATION OF
THE EMERGENCY COOLANT INJECTION EFFECT
IN A CANDU INLET HEADER

Turhan, K. Zafer

M.S., Department of Mechanical Engineering

Supervisor : Prof. Dr. A. Orhan Yeşin

Co-Supervisor: Dr. Enis Pezek

February 2009, 110 pages

Inlet headers in the primary heat transport system(PHTS) of CANDU type reactors, are used to collect the coolant coming from the steam generators and distribute them into the reactor core via several feeders. During a postulated loss of coolant accident (LOCA), depressurization and vapor supplement into the core may occur, which results a deterioration in the heat transfer from fuel to the coolant. When a depressurization occurs, "Emergency Coolant Injection(ECI)" system in the PHTS in CANDU reactors, is automatically become active and supply coolant is fed into the reactor core via the inlet header and feeders. .

This study is focused on the experimental and computational investigation of the ECI effect during a LOCA in a CANDU inlet header. The experiments were carried out in METU Two-Phase Flow Test Facility which consists of a scaled CANDU inlet header having 5 connected feeders. The same tests were simulated with a one

dimensional two-fluid computer code, CATHENA, developed by Atomic Energy of Canada Limited(AECL).

The average void fraction and the two phase mass flowrate data measured in the experiments are compared with the results obtained from CATHENA simulation. Although a few mismatched points exist, the results coming from two different studies are mostly matching reasonably. Lack of three-dimensional modeling for headers in CATHENA and experimental errors are thought to be the reasons for these dismatches.

Keywords: Two-phase flow, CATHENA, CANDU inlet header, METU Two-Phase Flow Test Facility

ÖZ

ACİL SOĞUTUCU TEDARİK SİSTEMİNİN
CANDU SOĞUTUCU DAĞITMA HAZNESİ ÜZERİNDEKİ ETKİSİNİN
DENEYSEL VE HESAPLAMALI OLARAK ARAŞTIRILMASI

Turhan, K. Zafer

Yüksek Lisans, Makina Mühendisliği Bölümü

Tez Yöneticisi : Prof. Dr. A. Orhan Yeşin

Ortak Tez Yöneticisi : Dr. Enis Pezek

Şubat 2009, 110 Sayfa

CANDU tipi nükleer reaktörlerin ana ısıl aktarım sistemlerinde bulunan soğutucu dağıtma hazneleri (inlet header) tanımlı alt bileşenler, buhar üreteçlerinden çıkan nispeten soğumuş suyu haznesi içinde toplayıp, reaktör kalbine, kendisine bağlı birçok besleme borusu üzerinden dağıtmaktadır. Olası bir soğutucu kaybı kazası anında, sistemde oluşan basınç kaybı nedeniyle, bir miktar su sıvı fazdan buhara dönüşebilmekte ve yakıt kanallarında ısı transferini azaltmaktadır. Bu tarz bir durum için CANDU reaktörleri "Acil Kalp Soğutma Sistemi(AKSS)" adı verilen sistemleri ile donatılmıştır. Ana ısıl aktarım sisteminde herhangi bir basınç düşmesi anında, AKSS kendisini otomatik olarak aktif hale getirir ve soğutucu takviyesini, aynı soğutucu dağıtma hazneleri ve besleme kanalları üzerinden reaktör kalbine gönderir.

Bu çalışma, bahsi geçen soğutucu kaybı kazası anında Acil Kalp Soğutma Sistemi'nin, soğutucu dağıtma hazneleri ve besleme kanalları üzerindeki etkilerini deneysel ve nümerik olarak incelemektedir. Deneysel çalışma, ODTÜ- İki Fazlı Akış Test Düzeneği'nde bulunan, 5 adet besleme çıkış kanallı, gerçeğinin ölçeklendirilmişi bir soğutucu dağıtma haznesi üzerinde gerçekleştirilmiştir. Aynı

deneyler, Atomic Energy of Canada Limited(AECL)'de geliştirilmiş tek boyutlu, iki akışkanlı nümerik kodu CATHENA ile simüle edilip, nümerik sonuçlar elde edilmiştir.

Deneysel çalışmadan elde edilen ortalama boşluk oranları ve iki fazlı akış hızları, CATHENA simülasyonu sonuçları ile karşılaştırılmış ve yorumlanmıştır. Nümerik ve deneysel çalışmalar arasında bazı uyumsuz noktalar olsa da, iki ayrı çalışmadan elde edilen sonuçlar genelde memnun edici derecede uyuşmaktadır. CATHENA'da geometrinin üç boyutlu modellenememesi ve bazı deneysel kısıt ve hatalar bu uyumsuz noktaların nedeni olarak gösterilebilirler.

Anahtar Kelimeler: iki-fazlı akış, CATHENA, CANDU soğutucu dağıtma haznesi, ODTÜ İki Fazlı Akış Test Düzeneği

To My Wife & My Parents

ACKNOWLEDGEMENTS

Firstly, I would like to express my sincerest gratitude to my supervisor Prof. Dr. A. Orhan Yeşin not only for his invaluable guidance, support and encouragement but also for the patience he has shown throughout my thesis work.

I am grateful to my co-supervisor Dr. Enis Pezek for his unbelieveable effort on helping me in any means while preparing this dissertation and for giving his time whenever I needed it. Without his contributions, this work wouldn't come true.

I would like to thank Turkish Atomic Energy Agency (TAEK), Atomic Energy of Canada Limited (AECL) and Middle East Technical University (METU) for this Joint Research Project and providing the needed instruments in the experiments.

Very special thanks go to my managers Ercüment Dokanakoğlu, Hayrettin Karabudak and Dinar Öztürk for their endless tolerance and support. Without their support, work and school would not have been possible.

I thank the technicians Mehmet Erili and Ufuk Cengizel for their big support during the experiments in the Two-Phase Flow Test Facility.

I would like say a big "Thank you!" to my fellow and co-worker Teoman Ünal for giving his time to check the thesis outline and format.

I owe my warmest thanks to all of my close friends who have been right next to me whenever I needed.

I also need to thank my parents-in-law Ertan Baş and Perihan Baş for the support they gave me throughout my study. They have been the source of patience and encouragement.

I am grateful to my beloved parents Ayfer and Salih Turhan and my sister Seda Turhan who have endlessly been behind me in any means in my whole life. Nothing would have come true without them.

Lastly but most importantly, I owe my deepest gratitude to my wife, Ceren Zeynep Turhan, for being the source of love and patience, also for standing by me everytime.

TABLE OF CONTENTS

LIST OF TABLES

TABLES

LIST OF FIGURES

FIGURES

LIST OF SYMBOLS

$\dot{m}_{TP}$	mass flow rate , (kg/s)
$\dot{m}_{ECI}$	mass flow rate, Emergency Coolant Injection,(kg/s)
$\dot{m}_{NN}$	mass flow rate - Neural Network , (kg/s)
$\dot{m}_{EXP}$	mass flow rate – Experimental , (kg/s)
$\dot{m}_{CATHENA}$	mass flow rate – CATHENA , (kg/s)
$\dot{m}_{FxNN}$	mass flow rate in Feeder x-Neural Network, (kg/s)
$\dot{m}_{FxEXP}$	mass flow rate in Feeder x-Experimental, (kg/s)
V_{DP}	voltage generated at DP-transmitter, (Volt)
α	average void fraction
$\overline{\alpha}_{INLET}$	average inlet void fraction
P	pressure, (Pa)
t	time, (s)

CHAPTER 1

INTRODUCTION

1.1 An Overview of Two-Phase Flow and CANDU Reactors

Two-phase flows occur in several engineering processes, such as heat exhangers, boilers, air-water flow in cooling towers and coolant distributing headers in nuclear reactors. In the design of the two-phase flow systems, it is very important to know the effects of different variables to the flow conditions.

In CANDU(**CAN**ada **D**euterium **U**ranium) type nuclear reactors, primary heat transport system contains components named “inlet headers” where the coolant is collected and distributed to the fuel channels in the reactor core (Calandria) via large amount of feeders.

Flow distribution from a header to multiple feeders has been not only an interesting subject but also a complex question to answer. It is generally investigated by different types of experiments, analytical and numerical studies. In case of two phase fluid flow distribution, the problem becomes more complicated.

In CANDU, the coolant removes heat from the fuel rods and flows through the outlet header to the steam generators. In case of a loss of coolant accident (LOCA), a tendency of mal-distribution of coolant flow among the inlet header outlets may

occur and water vapor may be introduced into the core, so that the system may run in short of enough coolant to cool the fuel rods.

The emergency coolant injection(ECI) system in CANDU reactors are designed to lead the system in a safer state in case of a loss of coolant accident. When a depressurization occurs in the Primary Heat Transport System, supplementary coolant is injected into inlet headers according to the differential pressure originating, so it helps cooling the core.

This dissertation describes the experimental and computational investigation of the effect of the emergency coolant injection when two-phase flow appears in the header, which may represent a LOCA, taking place in the system. For this purpose, some experiments are done in selected ranges within the limits of the METU Two-Phase Flow Test Facility. Four steady state test cases may be described as:

- the single phase (water) flow
- two phase (water-air) flow initiated from a fictitious LOCA

and then,

- low flow rate ECI and
- high flow rate ECI introduced to the reactor cooling system which undergoes a LOCA.

Also computational modeling of the experimental setup is made in a two-fluid code, named CATHENA. The same four test cases are simulated by using CATHENA and the results obtained from the experiments and the computer simulation are compared.

In this chapter, an introduction is made to the general Primary Heat Transport System(PHTS) of a CANDU type reactor. Some more details will follow in the on going parts of the introduction. The motivation behind the present work and the literature survey are also discussed in this chapter.

1.2 Background

This study is part of a joint research project between Atomic Energy of Canada Limited(AECL), TAEK (Turkish Atomic Energy Agency) and METU (Middle East Technical University). It's aim is to investigate the two-phase flow behaviour in the inlet header and feeders in different two-phase flow conditions. The studies in this joint research project will reduce the uncertanties associated with existing header models and provide experimental data to compare with the past studies .

1.3 CANDU Heat Transport System

In CANDU reactors there are pressure tubes containing the fuel rods that forms the reactor core which is called Calandria (Figure 1.1) The coolant (heavy water- D_2O) passes through those channels removing the heat originating from nuclear fission. Hot coolant is collected in the outlet header passing through the feeders and with the driving force of the main primary system pumps (no.3 in Figure 1.1) it is sent to the steam generators. The secondary side takes the heat from the primary side and produces steam in the steam generators. The main circulation pumps take cold D_2O from the steam generators and pump it to a reactor inlet header. (the horizontal component between no.3 and no.4 in Figure 1.1)

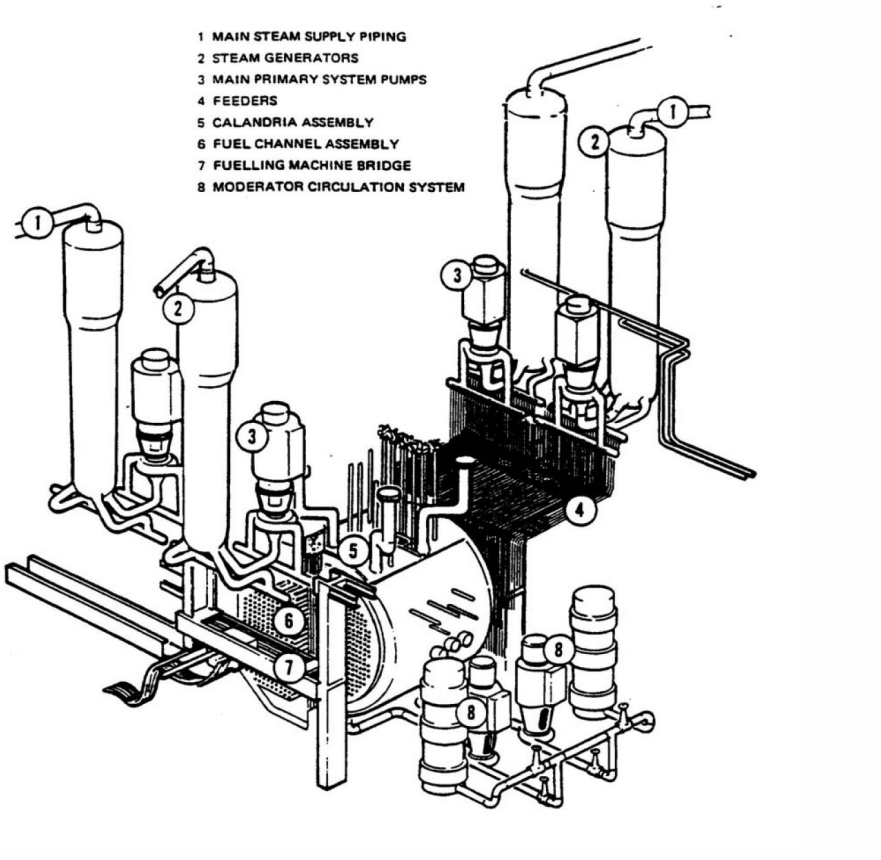

Figure 1.1 Primary Side CANDU Heat Transport System.

The header distributes the coolant through feeder pipes to the individual fuel channels in the opposite direction. This vice-versa direction in the flow keeps the two sides of the calandria equal in temperature which form a symmetrical power generation in the core. Each HTS loop has a “figure of eight” configuration and has an inlet and outlet headers in either end of the reactor core [4].

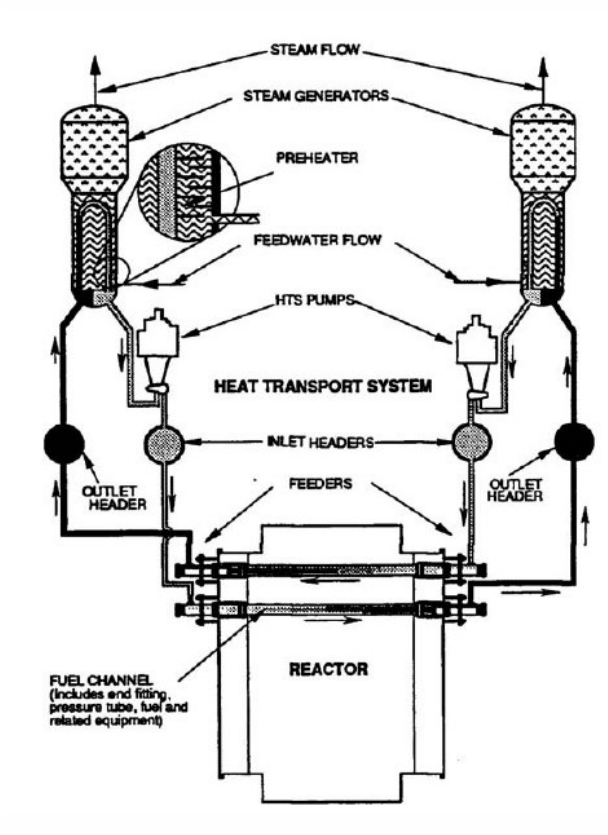

Figure 1.2 CANDU Heat Transport System

As it is seen in the Figure 1.2, the inlet headers are located between the steam generator outlet and the reactor core. An inlet header of a CANDU-6 reactor is a cylinder of 6 m lenght. Its both ends are capped. It is connected to the calandria via feeder banks which are exiting from the header at different angles and elevations. Each feeeder bank consists of five 50.8 mm i.d. tubes attached to the header at angles of $0^0, 45^0, 90^0, 135^0, 180^0$ measured from a horizontal line [6].

In some postulated loss of coolant accidents, the inlet header may experience some two phase flow (water-steam) conditions which would eventually result in a decrease of coolant flow into the core. The more void fed into the reactor, the hotter the fuel rods are. The emergency coolant injection(ECI) is introduced to the inlet headers to

make up lost coolant in the PHTS. Different elevated and angled exits will eventually have different void behaviours and flow distributions. The distribution of the two-phase flow in the headers and feeders is a determining factor for the adequate removal of heat from the core [22].

1.4 Motivation

AECL's (Atomic Energy of Canada Limited) Whiteshell Laboratories in Manitoba, Canada has been a place for the investigation of header behaviour. The RD14-M test facility has served for the studies pointing the question marks in the two-phase flow behaviours of CANDU for years. Several studies have been done. Those studies generally showed that even through feeders with same exit angle and elevation, different two-phase flow behaviours have been observed which eventually showed the flow distribution in the header and through the feeders are to be better understood to obtain a more clear look at the phenomena.

To provide a better understanding in two-phase flow distribution in an inlet header, this thesis study have been initated in Middle East Technical University Two Phase Flow Test Facility. The facility contains a scaled transparent model of a RD-14M inlet header with the feeders connected to it in different angles and elevations(see Fig.2.2). A set of experiments are done in the capability range of the test facility. After that, the set of experiments are simulated by a computer code, CATHENA. The results from the code and the experiments are compared in Chapter 4.

1.5 Literature Survey

This part gives a review of the literature that is relevant to the present study. There are examples of investigations about two phase flow conditions in headers which carried out by both experimental and numerical studies.

1.5.1 Experimental Two-Phase Discharge Investigations

Yonomoto and Tasaka investigated experimentally and theoretically the phenomenon of two-phase flow discharged from a stratified two-phase region through a small break orifice [21]. A horizontal square duct with an inner side length of 190 mm and orifice sizes of 10 or 20 mm were used in the experiments. The experiments were conducted at a maximum system pressure of 0.7 MPa and room temperature in a steady-state condition. The experimental parameters were: orifice orientation (top, side or bottom), orifice diameter, pressure, water level in the duct, differential pressure across the orifice, and inlet and outlet flow rates of air and water. The experimental results agreed to a large extent with their correlations for the quality and mass flux in the break orifice.

By Kim and Han, the air and water flow distribution are experimentally studied for a heat exchanger composed of round headers and 10 flat tubes. The effects of tube protrusion depth as well as header mass flux, and quality were investigated, and the results were compared with previous 30 channel data. The flow at the header inlet was annular. For the downward flow configuration, water flow distribution was significantly affected by tube protrusion depth. For flush-mounted geometry, significant portion of water flowed through frontal part of the header. As the protrusion depth increases, more water is forced to rear part of the header. The effect of header mass flux or quality was qualitatively the same as that of the protrusion depth. Compared with the previous 30 channel configuration, the present 10 channel configuration yields better flow distribution [16].

The flow distribution mechanism of the header for water was studied by Osakabe, Hamada and Hiroki and the calculation procedure for the design was recommended for a single-phase condition. It was also recommended to avoid the bubbles in the header to obtain a uniform water flow rate to each small pipe, but in some cases, the header had to be used to distribute a flow containing bubbles. Distribution behavior of water with or without a gas-phase was studied experimentally in a horizontal header with four vertical pipes. The prediction method developed for a single-phase fluid was extrapolated to the flow containing bubbles. The prediction agreed well with the experimental results at a small amount of bubbles [17].

Kowalski and Krishnan [12] and Kowalski and Hanna [11] studied two-phase water-vapor flow conditions in the CANDU RD-14 test facility. The test facility consisted of inlet and outlet headers connected with 30 feeders. The headers were like a typical CANDU header but they were half size in the length. Vertical inlet branches were connected at the top of the inlet header bringing the two phase mixture to the geometry. The feeders were connected to the header grouped as 6 banks each of which consisted of 5 feeders. Two feeders were exiting the header horizontally while two of them were exiting with 45^0 with the horizontal. One of the feeders were leaving the header vertically i.e. making 90^0 with the horizontal plane. They used three different water mass flow rates of 30, 45 and 60 kg/s, while the vapor mass flow rates varied between 0.05 and 2.4 kg/s. The pressure levels were 1, 2 and 5 MPa, respectively. The header was a non-transparent one so that they couldn't observe and visualize the two phase flow behaviour in the header. They had differential pressure transmitters and conductivity probes that measure the water level inside the header and the void fraction and two phase flow rate in three of six banks. Based on the void fraction and the flow rate measurements, the studies showed flow stratification both in single turret injection and dual turrent injection. The two phase injected side always had a lower level of water while the other side of the header had a higher level of water. When two turrets are used to inject two-phase mixture, the water level was highest between those two turrets. They also simulated the flow conditions on computer codes and compared the results in their studies.

By Teclemariam, an experimental flow loop was designed and constructed to investigate the two-phase flow distribution in a simulated CANDU header-feeder system [22]. The header in this experiment, made of a transparent material, was a scaled-down version of the one used in Kowalski and Krishnan using a scaling ratio of approxirnately 8.5 : 1 [12]. Experiments were conducted using air-water mixtures at room temperature and a nominal header pressure of 170.3 kPa (abs). The test matrix included one and two-turret injection, two inlet water flow rates (15 and 30 kg/min) and four different air flow rates for each water flow rate, giving inlet qualities of 3%, 1.5%, 0.75% and 0.375%. The outlet flow rates of air and water were measured in all the feeders under the condition of equal pressure drop across the feeders. The data shows that there is significant variation in air and water flow rates among the feeders, both in the axial and circumferential directions. The flow distribution among the feeders was found to be strongly dependent on the inlet flow conditions (mass flow rates of air and water) and the type of injection (one or two turrets). The flow conditions in the header were observed and these were able to be used in some circumstances to explain the outlet flow rate distribution in the feeders. Finally, correlations were developed for three quarters of the experimental data using a Lockhart-Martinelli-type parameter and the feeder quality. These equations agreed with the experimental data with approximately 89% of the correlated experimental data falling within +70% of the predicted values.

1.5.2 Numerical Two-Phase Discharge Investigations

Pezek investigated the two-phase flow distribution through multiple outlets from a horizontal drum both numerically and experimentally [4]. He solved three dimensional incompressible finite difference equations in cylindrical coordinates by using two-fluid model to simulate the air-water flow in the header. These equations were then fit into a computer code in which Implicit Multi Field technique was utilized. A couple of benchmark problems were used to test the code that eventually showed well-matched behaviour. A number of test with single and two phase flows were done in the METU TPFTF with different flowrates of air and water introduced into the system. Varying inlet void fraction and inlet flow rates resulted in different

two-phase flow distributions in the connected feeders. The results obtained from the experiments and calculations with the two fluid 3-D code were in good agreement.

Kowalski and Hanna, used the CATHENA code besides the experimental work. The thermalhydraulic model in CATHENA is a one-dimensional, non-equilibrium two fluid model similar to that found in other current state-of-the-art reactor analysis codes. The basic thermalhydraulic model consists of six partial differential equations for mass, momentum and energy conservation—three for each phase [2].

Cho and Juen in 2003 investigated an inlet header break sized 30 mm in RD-14M test facility and the effect of the ECI water surged with a high pressure to the headers. Those work is also validated with a computer code named RELAP5/CANDU which was in a development process at that time. The experiment started as the valve was opened and the reactor trip occured. The break was located in one of the the inlet headers. After the break initiated, the primary system pressure rapidly decreased as the inventory lost. Due to void generation, the slope of the depressurization rate decreased and few second later ECI injection delivered into the system. This overall test is modelled in the code RELAP5/CANDU which used a very similar nodalization design as CATHENA. The results showed that the header where the break situated received more ECI than any other due to the amount of pressure difference associated between the ECI tank and the header. Almost all of the ECI water to be injected into the reverse side header, was injected into header having the break. Those behaviours associated in the experimental scheme also observed in the code output [3].

Lee and Kim (1999) investigated LOCA with a smaller break size associated in one of the inlet headers. The experiment was a benchmark study test previously in AECL RD-14M facility. The results coming from the CATHENA code (AECL) were compared with the Lee and Kim's study. They used RELAP5/Mod3.2 as the numerical modeller of the whole system. Code predictions with the experimental results showed a reasonable consistency but some discrepiancies were observed in

the depressurization after the break and consequent time delay of the major phenomena [9].

1.6 Thesis Outline

In Chapter 1, an introduction is made to the CANDU Heat Transport System. The motivation and the background of the study is also given. The literature survey which represents experimental and computational studies made in the past is presented in this chapter.

In Chapter 2, the experimental setup is introduced with its components. The calibration procedure for each instrument is given and the experiments are presented. Results are compared and discussed.

Chapter 3 is the part where the computational study is described. An introduction is made about the code CATHENA and its input records. It is also described how the test facility is modelled geometrically and how the boundary conditions are set. Simulation results are given in the last section and comments and comparison are made due to the results.

In Chapter 4, a general comparison of the computational and experimental studies is made. A visual understanding is provided in tables and in graphs. In the last section, comments are made on how two different study results match or differ. Suggestions for the future work are also given.

CHAPTER 2

EXPERIMENTAL STUDY

2.1 Introduction

All test cases investigated in this thesis work are done in the Two Phase Flow Test Facility(TPFTF), located in Mechanical Engineering Department of Middle East Technical University. This facility contains a transparent scaled RD-14M inlet header, connected to a water pump and 3 air tanks via water line and air line, respectively. The two-phase experiments are done with air and water. Air simulates the vapor at the onset of a probable LOCA. When LOCA takes place in the primary heat transport system of a reactor, the primary system pressure drops according to the scale of the LOCA which is followed by flashing of coolant (D_2O in a CANDU-6) at high temperatures into vapor.

2.2 Test Facility and Instrumentation

2.2.1 Test Facility

Except for the inlet header, METU TPFTF consists of a water storage tank, three air tanks, water circulating pump, feeders, connecting pipes, the Emergency Coolant Injection Line (ECI), mixing section, while the instrumentation system has a data acquisition system, differential pressure transmitters, pressure transducers, impedance probes, a rotameter and an orificemeter.

A schematic diagram of the test facility is shown in Figure 2.1: [4].

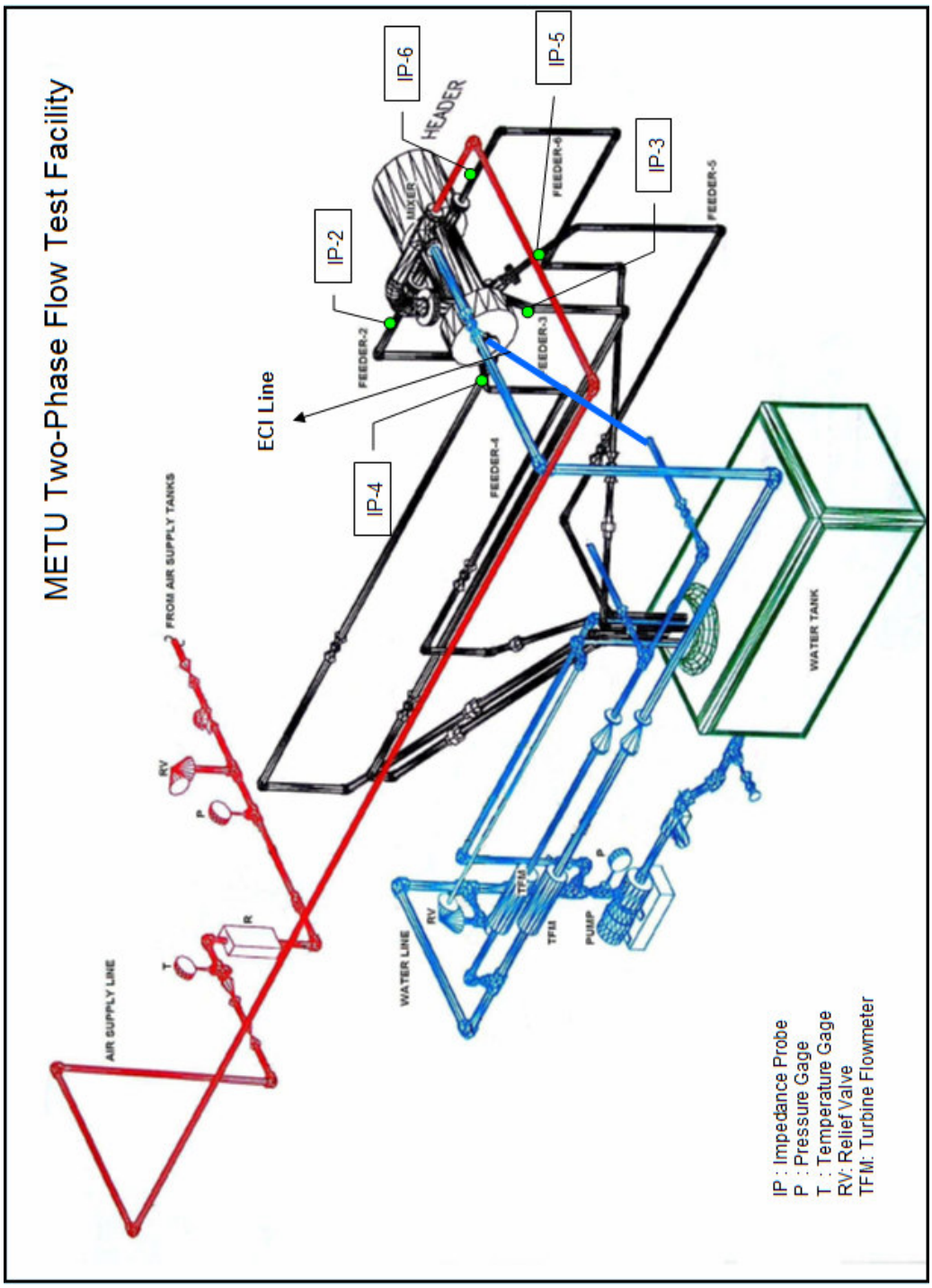

Figure 2.1 METU Two Phase Flow Test Facility (TPFTF).

The test facility consists of a cylindrical header (1100 mm lenght/ 194mm i.d.) connected to five feeders, one main inlet and one ECI injection line. The feeders are connected to the header at different angles and elevations. The feeder diameters are also different. Table 2.1 and Fig. 2.2 show the geometrical configuration of the feeders:

Table 2.1 Inlet and Outlet Feeder Geometrical Configurations

Feeder Title	**Inner Diameter(mm)**	**Angle with respect to Feeder-2 nozzle, anti-clockwise**
Inlet-1	77.9	90^0
ECI line	25.4	-
Feeder-2	34.5	0^0
Feeder-3	34.5	288^0
Feeder-4	25.4	324^0
Feeder-5	25.4	216^0
Feeder-6	25.4	180^0

It should be noted that, Feeder-2 and Feeder-6 of different diameters connect to the header horizontally while Feeder-4 and Feeder-5 are symmetrical and Feeder 3 is in the lowest elevation. The Emergency Coolant Injection(ECI) is provided from the base surface of the header which is near its inlet (See Fig. 2.2).

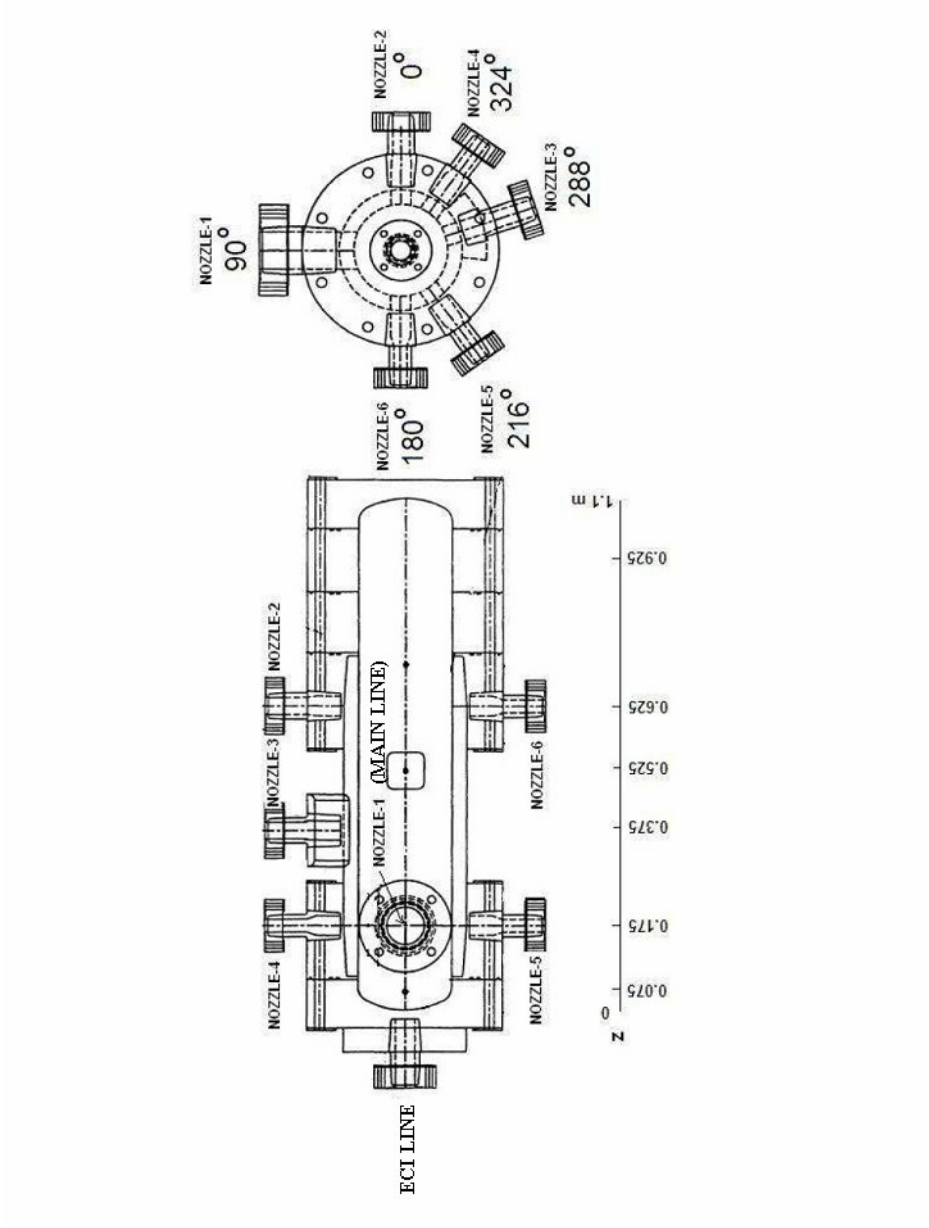

Figure 2.2 Header and Feeder Connections (TPFTF)

The air storage tanks are filled up with the aid of a compressor. The compressed air is injected to the line with a valve regulating the amount of air flow.

The tap water was distilled and collected in a storage tank. Water flows into the system with the help of a pump. The pump inlet is connected to the bottom of the water tank. Also there is a by-pass line and a valve connected to the pump outlet, by which the flow rate to the system is regulated. The pump itself has a water circulating capacity about 8 m^3 / h.

There is a mixing section before the inlet of the header where the distilled water and air are mixed.

2.2.2 Instrumentation

2.2.2.1 Turbine Flowmeter

The water flow rate is measured by 2110 TM Model of Chemline Plastics' turbine type flow meter. There are two of them in the test facility. They are connected to both main water line and ECI line (See Fig. 2.3).

Figure 2.3 Turbine Type Flowmeter

2.2.2.2 Differential Pressure Transmitter

Each feeder line is equipped with a differential pressure transmitter (DP Transmitter) (See Fig. 2.4). There is a globe valve on each feeder line which simulates the flow resistance in the reactor fuel channels. Different flow resistances in different channels may occur and this is done by the means of the globe valves in the experiments. The DP transmitter is placed across the globe valve to measure the two-phase flow rate in the feeder. The flow rate is arranged by opening and closing the valve manually. According to the amount of the valve opening, the pressure difference is varied. The measurement range of DP transmitters is 0-6.89 bar.

2.2.2.3 Rotameter

A rotameter is connected to the air line to measure the air flow rate by eye-read. It is also used to calibrate the orificemeter. It has a measuring range between 1.27 - 15.5 m^3 / h.

2.2.2.4 Orificemeter

The air flowrate is measured by the aid of an orificemeter which has an orifice of 5.9 mm diameter and a differential pressure transmitter connected to the both sides of the orifice. A voltage signal is produced which is proportional to the pressure difference occurring between both sides of the orifice and it is fed into the data acquisition system. (DAS)

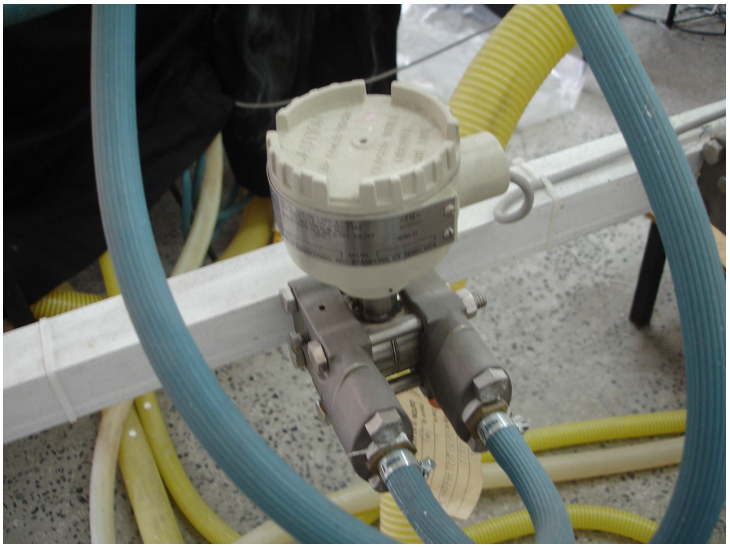

Figure 2.4 Differential Pressure Transmitter

2.2.2.5 Impedance Probes

Average void fraction on each feeder is measured by the impedance probes whose tips are submerged into the center of the flow channel. The main principle is based on the fact that a difference between the excitation voltage and the sensed voltage proportional to the electrical impedance occurs due to the variation of void fraction around the probe [4][19][5].

In 2002, Hosanoğlu investigated the sensitivity of the impedance probes [5] by analyzing the effects of pre-resistance value, excitation frequency, flow regime, fluid temperature and documented a table of parameters for each probe. In this study, the same parameters set by Hosanoğlu[5] are used for the impedance probes [4].

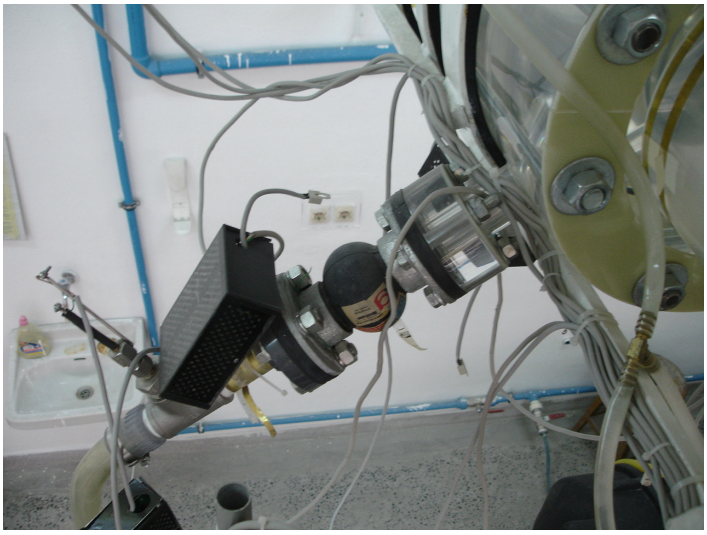

Figure 2.5 Impedance Probe.

2.2.2.6 Pressure Transducers

The gage pressures across the test facility is measured with pressure transducers (See Fig. 2.6). Three transducers are used in different places (at the mixing section , on the water line and on the air line before the mixing section). The measurement range of the transducers is 0-6.89 bar.

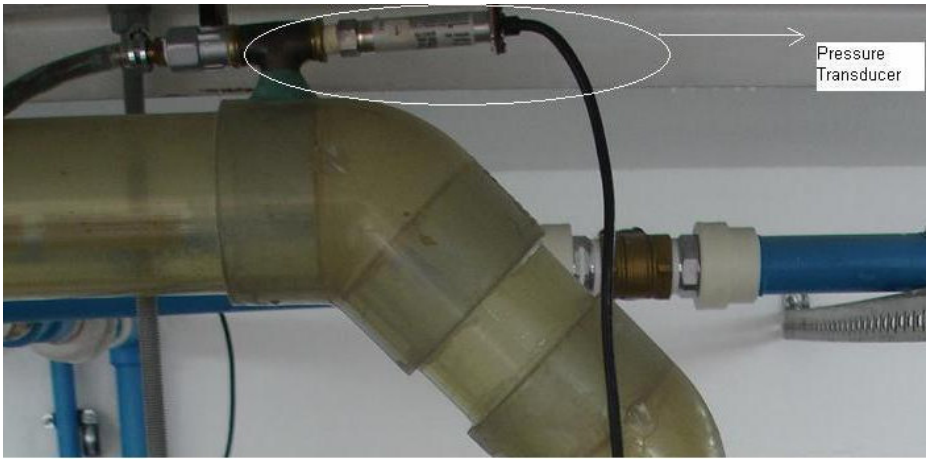

Figure 2.6 Pressure Transducer.

2.2.2.7 Data Acquisition System (DAS)

Each sensor contained in the test facility is generating a propotional voltage according to the value it measures. Those voltage values are fed into a card which acquires all data. The data acquisition system which consists of a Analog/Digital I/O Card and two amplifier-multiplexer cards, sends those packages of data to a software. This software(Advantech GENIE) is capable of screening, logging and recording the data produced by the sensors. GENIE is running on a Windows98 operating system in a Celeron-433 processor 768 MB RAM computer.

The technical properties of all instruments are given in Appendix A.

2.3 Calibration Procedures

The instruments used in the test facility are calibrated one by one prior to the tests.

The turbine flowmeters on the main water line and the ECI line were firstly calibrated. Water was forced to flow through one of the feeders by closing the valves on the other 4 feeders. The calibration was done by collecting water flowing from that feeder into a bucket for a certain period of time. The time was recorded and the mass of water collected in the bucket was measured by an electronic weigher. The set of voltage to volumetric flow rate values were plotted and a linear fit was obtained.

The orificemeter was calibrated by the aid of a rotameter connected to the air line in series with the orifice. The voltage generated by the differential pressure transmitter connected to the orifice was recorded versus the air flow measured by the rotameter. A third degree polynomial fit was obtained.

The impedance probes placed on each feeder line were then calibrated one by one. According to the inlet void fraction introduced into the header by adjusting the air and water flowrates, the impedance probe submerged into the feeder generates

voltage. The minimum amount of void fraction that can be measured due to the facility limitations is 14%. The maximum amount has changed from feeder to feeder according to the range to be used in the tests. The homogeneous flow model assumption is used in this study in calibration procedure of impedance probes [4]. The detailed description of the impedance probes are given by Hosanoğlu [5].

Three pressure transducers to measure the air pressure, air-water mix pressure and water pressure were also calibrated by arranging different flow rates and inlet void fractions.

A differential pressure transmitter on each feeder line was used to measure the two-phase flow rate. The procedure in calibrating the DP transmitter is somehow different from the others. The variables affecting the two-phase flowrate are the void fraction and the DP transmitter voltage signal, provided that globe valve opening ratios on each feeder is kept constant. The general relation is shown below;

$$\dot{m}_{TP} \sim f(V_{DP}, \alpha)$$

$\dot{m}_{TP}$: Two-phase flow rate

V_{DP} : Voltage generated by DP-transmitter

α : Average void fraction

So instead of generating emprical relations between aforementioned variables, a different methodology known as “Neural Network Approach” is used in this study.

2.3.1 Neural Network Use for the Prediction of Two-Phase Flow Rate

Neural networks are composed of simple elements operating in parallel. These elements are inspired by biological nervous systems. As in nature, the network function is determined largely by the connections between elements [7]. The main idea behind neural network is that connections (weights and biases) between input and output elements can be adjusted so that a particular input leads to a specific

target input [4]. The ability of a neural network to analyse any complex functional relationship makes the selection of a suitable regression method unnecessary. Solution of a neural network should generally undergo two steps which lead to final solution, namely learning/training and validation. Learning or training is equivalent to finding a surface in a multidimensional space that provides a best fit to the training data. Validation is equivalent to the use of this multidimensional solution to interpolate data unseen by the network[15].

As data sets are introduced to the network, network is trained for known conditions for different variables. (See Figure 2.7)

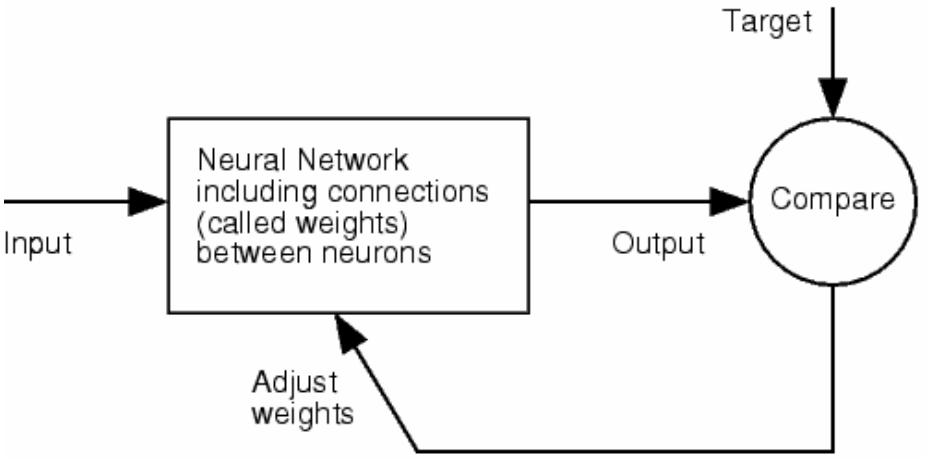

Figure 2.7 Neural Network Block Diagram

A good training is obtained by acquiring and feeding healthy set of data to the system and enough steps of computation made to find the weights and biases. The mechanism here can be explained in two main sessions:

1- Training/Learning Part: Here the set of known input and output data obtained from real tests/applications is used to generate weights and biases until a desired output is provided (in defined error limits). As long as the training phase reaches the desired output, the training is stopped and ready to be tested/validated.

2- Validation/Test Part: The trained network is given new input patterns of which the outputs are already known. Resulting from the calculated training weights&biases, the predictions are made for the needed outputs. The performance of the network is monitored. When acceptable amount of error is reached in test section, the predictions for the unseen data can be made.

In this study, the output needed is the two-phase mass flow rate on each feeder. The inputs consist of void fraction and differential pressure voltage matrices. The network uses three layers, two of which are hidden layers and the third one is the output layer. Increasing the number of hidden layers and the neurons in traning phase helps the accuracy of the predictions to increase[4].

2.3.1.1 Data Source

Data source used in this neural network representation came out from the calibration tests performed in the METU Two Phase Flow Test Facility. The network is based on a total of 329 test results. 146 of which are single phase and the rest 183 tests are two-phase test. Each single phase test has 2 input values (valve opening, DP-Voltage) and an output value, mass flow rate; where each two-phase test includes 3 input values (valve opening, DP-Voltage and void fraction) and one output value, two-phase mass flow rate. Approximately 85% of the data set was used for the training and the rest 15% was used in the validation section. Neural Network Toolbox of MATLAB R2007a was used for the calculations. The toolbox has several learning algorithms. Here in this study Levenberg-Marquardt algorithm was used. Tangent-sigmoid transfer functions for the hidden layers and pure linear function for the output layer were used. Pezek[4] used the same algorithm and network setup for his study.

To give an example for the application of neural network, Table 2.2 represents the Feeder-2 two-phase mass flowrate values for a fixed valve opening ratio and varying

void fraction. Feeder-2 was chosen for the calibration of large diameter feeders. Similarly Feeder-5 was chosen for the calibration of small diameter feeders.

Table 2.2 Feeder-2 Two-phase Flow DP-Transmitter Calibration

Valve Opening Ratio	Void Fraction (%)	DP Voltage Signal (V)	Experimental Data For Water Flow Rate (kg/s)	Neural Network Estimation (kg/s)	Difference	Error (%)
0.1875	0.509	0.570	0.465	0.472	-0.007	-1.51
0.1875	0.364	0.568	0.632	0.613	0.019	3.01
0.1875	0.668	0.521	0.254	0.220	0.034	13.39
0.1875	0.346	0.712	1.154	1.048	0.106	9.19
0.1875	0.313	0.749	1.275	1.196	0.079	6.20
0.1875	0.494	0.564	0.577	0.469	0.108	18.72
0.1875	0.672	0.523	0.275	0.222	0.053	19.27
0.1875	0.750	0.517	0.195	0.196	-0.001	-0.51

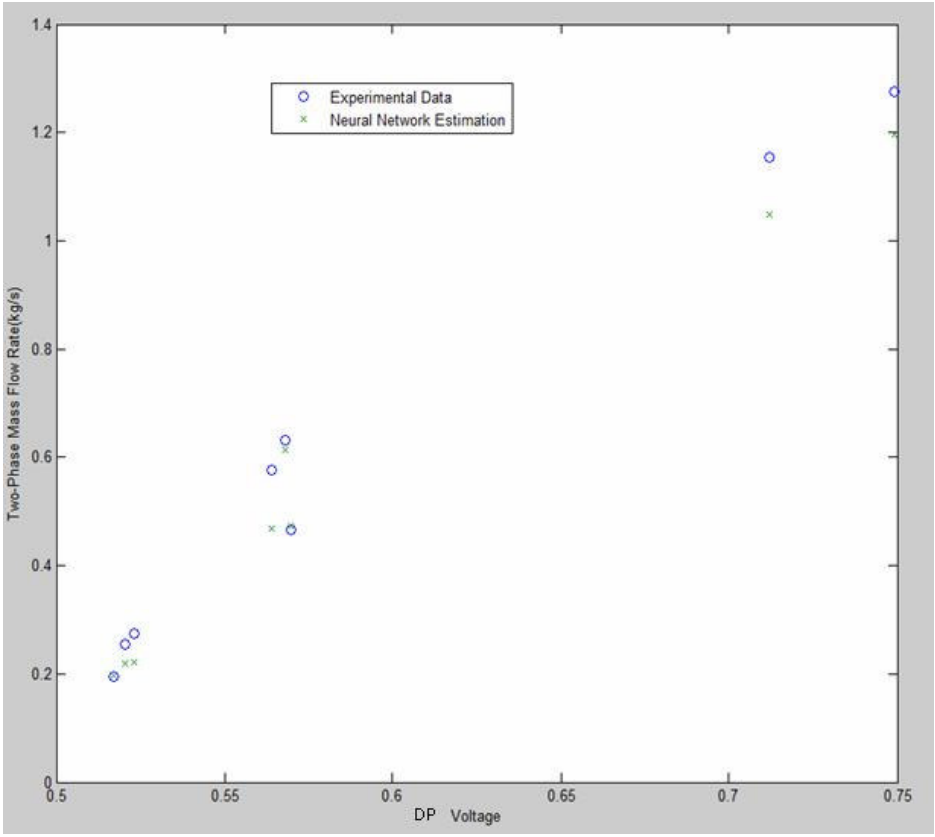

Figure 2.8 Comparison of the Test Data with Neural Network Estimation

The R^2 value in the validation(with linear fit) was 0.9914, which shows the test of the data was rather successful. As seen from Figure 2.8, Figure 2.9 and Table 2.2, when the flow rate decreases and the void fraction increases, neural network guesses for the two-phase flowrate gave relatively high error. If much more training input data for the specified range had been given, the results would have shown a better behaviour.

Figure 2.8 and 2.9 are the outputs of the MATLAB Neural Network Toolbox for the specified feeder and flow conditions.

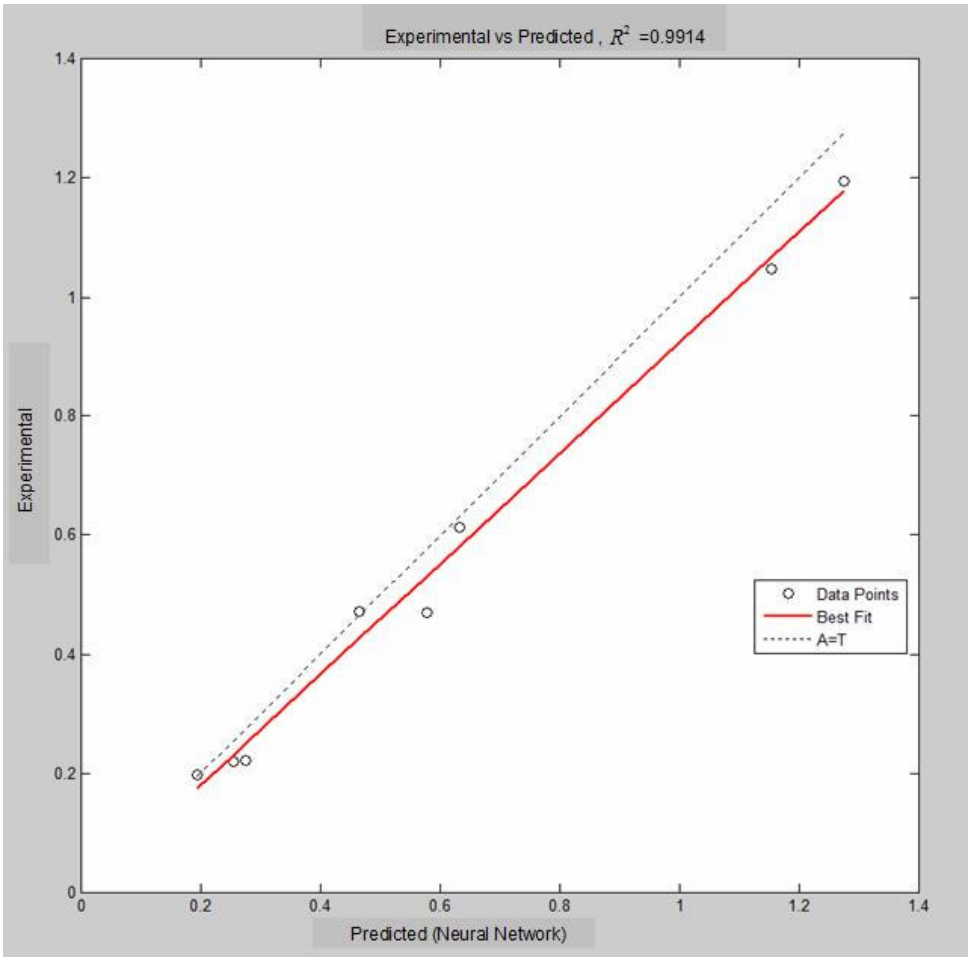

Figure 2.9 Experimental Mass Flow Rates vs Neural Network Predicted Mass Flowrates

2.4 Experiments

2.4.1 Introduction

A series of experiments in METU Two Phase Flow Test Facility have been carried out to simulate the loss of coolant accident effects in a CANDU inlet header. The experiments include four main cases. Single phase flow, two-phase flow, two-phase flow with low flow rate emergency coolant injection (ECI) and two-phase flow with higher flow rate ECI. Throughout the whole experiments, steady state behaviour was investigated.

In the single phase flow case, water flows in the test setup, no air is allowed. This is a simulation of a well conditioned inlet header behaviour of a CANDU reactor. The second case where two phase flow (air + water) conditions are active, is a simulation of a LOCA in the heat transport system(HTS). In a real LOCA, due to the pressure loss occuring in the HTS, water vapor is introduced through the feeders into the fuel channels. In the third and fourth cases, the same two-phase flow conditions of the second case at the inlet are introduced with the addition of the emergency coolant injection. Effects of relatively low and high ECI flowrates are investigated respectively.

The test facility has some limitations for the water flow rate. The pump has a maxium water flow capacity of 2,22 kg/s. The ECI line is also fed by the same pump as the main water line. So the flow rate of ECI water had to be limited. The maximum ECI was selected to be around 0,55 kg/s.
Throughout the tests, all feeders were kept open. The valve opening ratios for large diameter feeders were kept constant at 18,75% while the valve opening ratios for small diameter feeders were kept constant at 25%. The reason for selecting these valve opening ratios was to obtain a fully water occupied header. As the opening ratio increases beyond 18,75% and 25% respectively, the header liquid level in the header drops and a separated air volume forms in the upper region. This is not a desired test condition for the single phase flow case.

Three stages of experiments were carried out. All were done with two different ECI flow rates. Each stage represents a different average inlet void fraction effect. The void fraction at the inlet was varied as almost 28%, 32% and 38%. So the effect of two variables, inlet void fraction and ECI flow rate were observed throughout the experiments.

The temperature of the system for each test was measured nearly $24^0 C$, while the system pressure for each test case is :

Table 2.3 Experimental Pressure Values in Each Test Case

	A-I	A-II	A-III	A-IV	B-I	B-II	B-III	B-IV	C-I	C-II	C-III	C-IV
Pressure(bar)	1,068	1,131	1,163	1,189	1,067	1,135	1,171	1,191	1,068	1,145	1,181	1,206

The uncertainty analysis for the experiments is given in the Appendix C.

2.4.2 Experimental Results and Discussions

In this section, results of experiments are given in three test matrices. Test A, Test B and Test C.

The valve opening ratio was kept constant at 18,75% and 25% for large and small diameter feeders, respectively. To bring the valve opening ratio from 0 to 100 % in the feeders with large diameters (Feeder-2 and Feeder-3) the valve is fully turned around 4 times, while 3 full turns are needed for the feeders with small diameters (Feeder-4, Feeder-5 and Feeder-6). The error in % is calculated for each test case by using Equation (2.1)

$$Error(\%) = \frac{\left|\sum \dot{m}_{NN} - \sum \dot{m}_{EXP}\right|}{\sum \dot{m}_{EXP}} x100 \qquad (2.1)$$

where,

$$\sum \dot{m}_{NN} = \dot{m}_{F2NN} + \dot{m}_{F3NN} + \dot{m}_{F4NN} + \dot{m}_{F5NN} + \dot{m}_{F6NN} + \dot{m}_{ECI} \qquad (2.2)$$

$$\sum \dot{m}_{EXP} = \dot{m}_{F2EXP} + \dot{m}_{F3EXP} + \dot{m}_{F4EXP} + \dot{m}_{F5EXP} + \dot{m}_{F6EXP} + \dot{m}_{ECI} \qquad (2.3)$$

2.4.2.1 TEST A

Test A has 4 cases. Test A-I is the single phase flow case. Test A-II is the two-phase flow case where nearly 28.2% inlet void fraction is introduced into the system.In Test A-III, inlet void fraction kept constant at almost 28.9% and low flow rate ECI (0.319 kg/s) is injected. Test A-IV, has 28% inlet void fraction but with a higher ECI flow rate (0.522 kg/s). Two-phase mass flowrate, the average void fraction and the normalized $\dot{m}$ for each outlet feeder are given in Table 2.4, Figure 2.10 and Figure 2.11. Normalized $\dot{m}$ for each feeder represents the flow split ratios in a test case. Each feeder flow rate is divided to the Feeder-2 mass flow rate, which is arbitrarily taken, so that a normalized value is obtained for each feeder. It is easier to observe the flow distribution using the normalized values.

Table 2.4 TEST-A Steady State Flow Distribution Through Feeders

TEST A RESULTS					
		A-I	**A-II**	**A-III**	**A-IV**
Feeder-2	α (%)	**0**	**72.6**	**70.3**	**76**
	$\dot{m}$ **(kg/s)**	**0.276**	**0.233**	**0.244**	**0.198**
	Normalized $\dot{m}$	**1.000**	**1.000**	**1.000**	**1.000**
Feeder-3	α (%)	**0**	**0**	**0**	**0**
	$\dot{m}$ **(kg/s)**	**0.352**	**0.794**	**0.852**	**0.909**
	Normalized $\dot{m}$	**1.276**	**3.407**	**3.491**	**4.578**
Feeder-4	α (%)	**0**	**36.3**	**34.5**	**24.4**
	$\dot{m}$ **(kg/s)**	**0.376**	**0.303**	**0.335**	**0.403**
	Normalized $\dot{m}$	**1.363**	**1.299**	**1.371**	**2.033**
Feeder-5	α (%)	**0**	**43.5**	**41**	**45**
	$\dot{m}$ **(kg/s)**	**0.347**	**0.300**	**0.331**	**0.349**
	Normalized $\dot{m}$	**1.260**	**1.285**	**1.356**	**1.756**
Feeder-6	α (%)	**0**	**75.7**	**5**	**6.5**
	$\dot{m}$ **(kg/s)**	**0.329**	**0.143**	**0.254**	**0.232**
	Normalized $\dot{m}$	**1.195**	**0.615**	**1.043**	**1.170**
	$\bar{\alpha}_{INLET}$	**0**	**28.2**	**28.9**	**28.0**
	$\sum \dot{m}_{NN}(kg/s)$	**1.680**	**1.773**	**2.016**	**2.091**
	$\sum \dot{m}_{EXP}(kg/s)$	**1.748**	**1.749**	**2.054**	**2.280**
	$\dot{m}_{ECI}(kg/s)$	**0**	**0**	**0.319**	**0.522**
	Error(%)	**3.89**	**1.37**	**1.85**	**8.29**

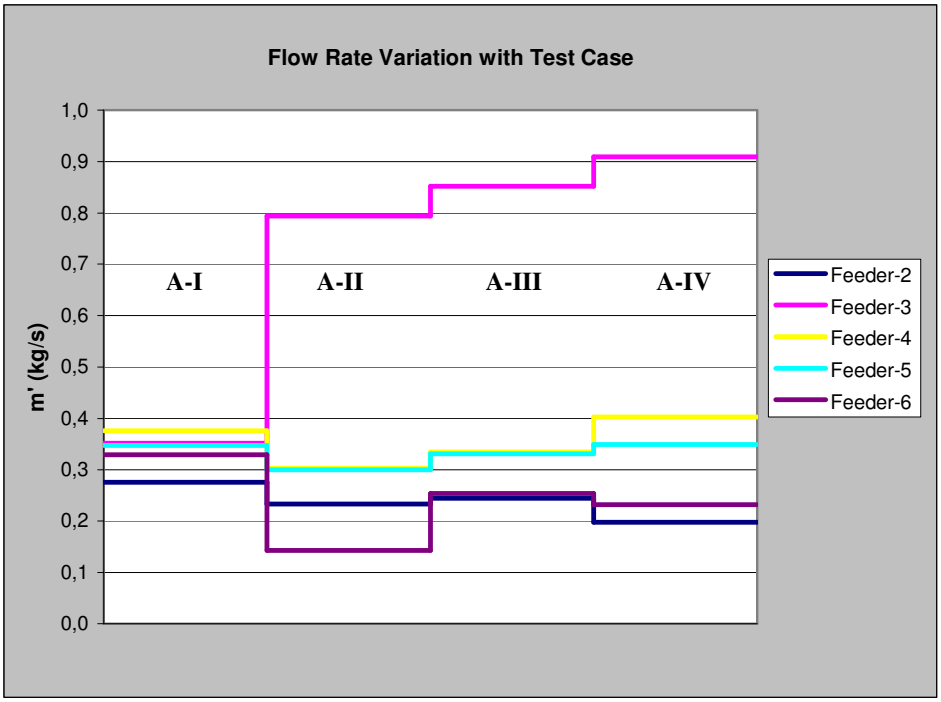

Figure 2.10 Test-A Steady State Mass Flow Rate Variation

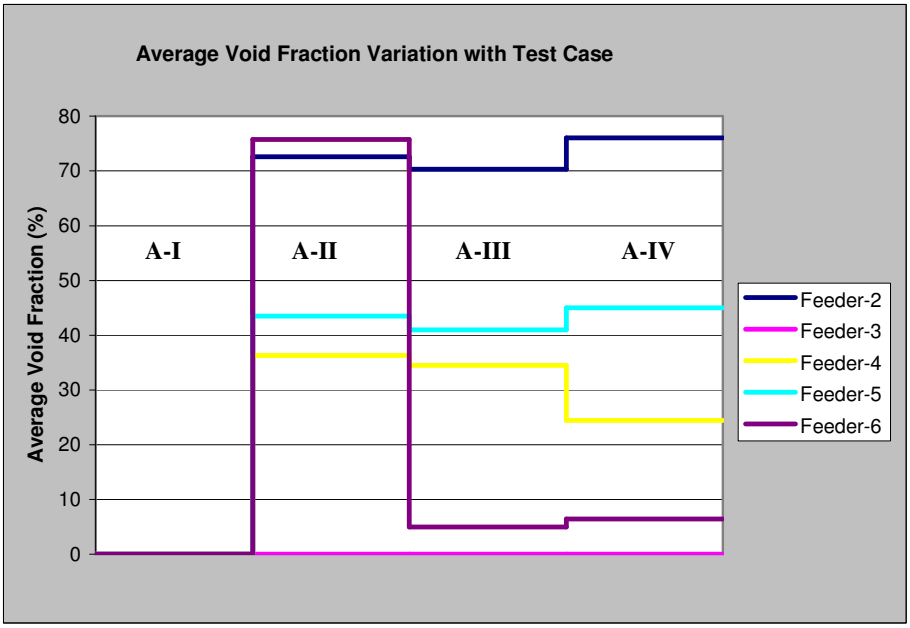

Figure 2.11 Test-A Steady State Average Void Fraction Variation

The followings are the comments on the Test-A results:

- Feeder-3, in every two-phase flow condition received more flow than other feeders. The reason might be the elevation of Feeder-3 nozzle. It exits the header from the lowest level. When air is introduced to the system, a seperated air volume at the top of the header, which results in more void fraction at higher elevated nozzles. Feeder-3 also never received air flow in any four cases of the Test A. This fact could also be related to having the lowest elevation.

- In the A-II case, Feeder-2 and Feeder-6 received higher average void fraction than other feeder. Because these two feeders are connected to the header at the highest elevation.

- In the A-III case, it is observed that, void fraction in Feeder-6 decreased suddenly to 5%, while in Feeder-2 it was kept almost constant. The increase in the flow rate of Feeder-6 can be followed in Figure 2.10. The biggest portion of the ECI water seems to be directed in Feeder-6 while Feeder-2 which is connected to the header at the same elevation is not considerably affected from ECI.

- Feeder-4 and Feeder-5 have the same diameter and are connected to the header symmetrically at the same elevation but due to the lack of the overall system symmetry, Feeder-4 seems to have more water flow than Feeder-5 while Feeder-5 receives more void than Feeder-4. Parrott[18] also observed the same behaviour in his studies done with five feeders in the RD-14M Test facility. Pezek[4] had done the experiments with dual discharge by using Feeder-4 and Feeder-5 providing fully symmetric system conditions and even observed the same behaviour. The flow conditions in this study differ from Parrott's at some points like valve opening, usage of air instead of vapor etc. Nevertheless, the whole behaviour is also observed here in this study which

was tried to be explained by Parrott[18] and Pezek[4] as the existance of centrifugal forces appearing in the inlet section of the header .

- Neural network estimation of total mass flowrate throughout the Test A both for single phase and two-phase flows are in agreement with measured values within an error range of 1.37-8.29 %.

2.4.2.2 TEST B

Test B has 4 cases. Test B-I is the single phase flow case. Test B-II is the two-phase flow case where almost 32.6% inlet void fraction is introduced into the system.In Test B-III, inlet void fraction is kept constant at nearly 32.1% and low flow rate ECI (0.322 kg/s) is injected. Test B-IV has 32.5% inlet void fraction but higher ECI flow rate (0.572 kg/s). Two-phase mass flow rate, the average void fraction and the normalized $\dot{m}$ for each feeder are given in the Table 2.5, Figure 2.12 and Figure 2.13. Normalized $\dot{m}$ for each feeder represents the flow split ratios in a test case.

Table 2.5 TEST-B Steady State Flow Distribution Through Feeders

TEST B RESULTS					
		B-I	B-II	B-III	B-IV
Feeder-2	α (%)	0	85.4	92.6	88.7
	$\dot{m}$ (kg/s)	0.266	0.14	0.131	0.147
	Normalized $\dot{m}$	1.000	1.000	1.000	1.000
Feeder-3	α (%)	0	0	0	0
	$\dot{m}$ (kg/s)	0.358	0.804	0.864	0.917
	Normalized $\dot{m}$	1.347	5.742	6.610	6.240
Feeder-4	α (%)	0	34.9	35.5	23.6
	$\dot{m}$ (kg/s)	0.384	0.311	0.34	0.411
	Normalized $\dot{m}$	1.443	2.218	2.606	2.797
Feeder-5	α (%)	0	42.8	41	39.7
	$\dot{m}$ (kg/s)	0.348	0.304	0.335	0.367
	Normalized $\dot{m}$	1.309	2.172	2.560	2.497
Feeder-6	α (%)	0	72.8	5	9
	$\dot{m}$ (kg/s)	0.337	0.152	0.25	0.268
	Normalized $\dot{m}$	1.265	1.087	1.914	1.827
	$\bar{\alpha}_{INLET}$	0	32.6	32.1	32.5
	$\sum \dot{m}_{NN}(kg/s)$	1.694	1.712	1.919	2.11
	$\sum \dot{m}_{EXP}(kg/s)$	1.744	1.743	2.055	2.309
	$\dot{m}_{ECI}(kg/s)$	0	0	0.322	0.572
	Error(%)	2.88	1.82	6.62	8.63

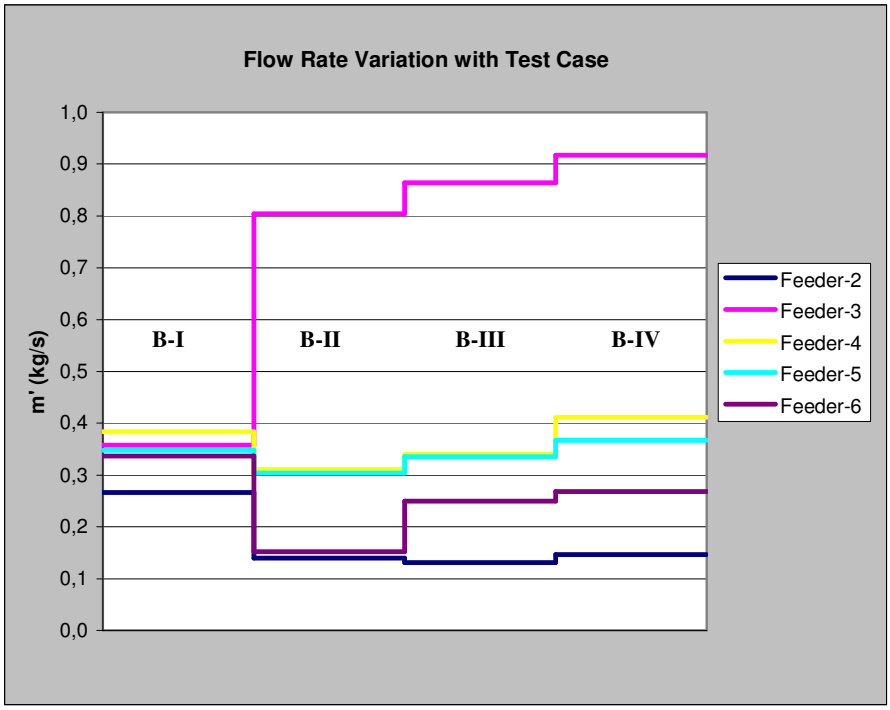

Figure 2.12 Test-B Steady State Mass Flow Rate Variation

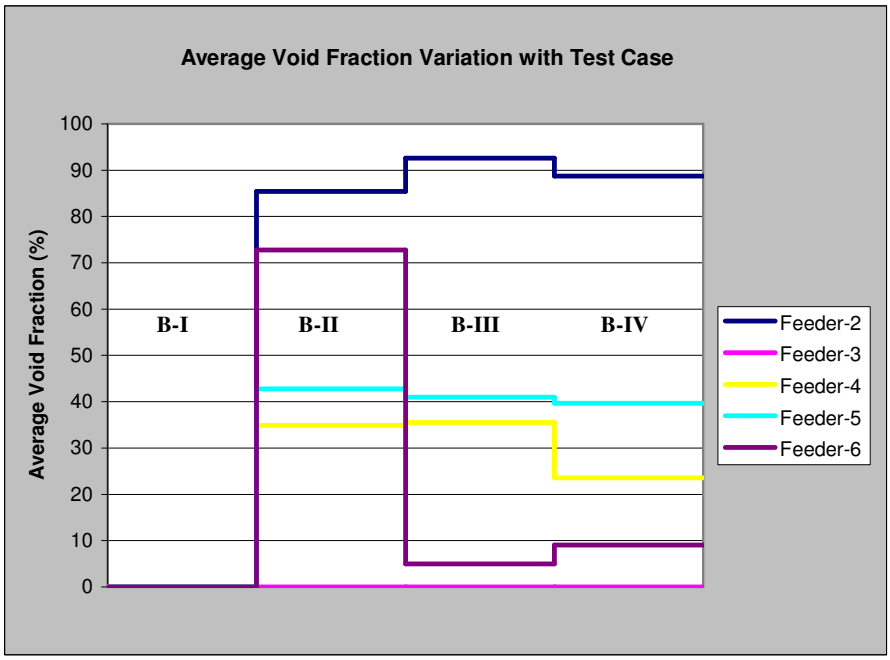

Figure 2.13 Test-B Steady State Average Void Fraction Variation

The followings are the comments on the Test-B results:

- Feeder-3 received the most of the flow rate in two-phase conditions. Again no void was observed in Feeder-3 during any of the three two-phase flow test cases.

- Feeder-2 and Feeder-6 received higher void fraction (85.4% and 72.8% respectively) than other feeders just like Test-A, due to their nozzle elevation. When emergency coolant injection is introduced into the system the decremental change in void fraction(from 72.8% to 5% - 9% levels) is the most for Feeder-6, while some small increase occured in Feeder-2 as observed in Test-A. Between B-II and B-IV case, Feeder-6 received the most of the ECI water supply to the system which resulted in the biggest decrease in the void fraction.

- Feeder-5 received more void fraction than Feeder-4 just like in Test-A where Feeder-4 received more water flow rate than Feeder-5 in all test cases.

- Neural network estimations of total mass flow rate in all cases of Test B is in agreement with the measurements within an error range of 1.82-8.63 %.

- In the two phase tests, (B-II, B-III and B-IV) when the total input flow rate (inlet + ECI) increases, a less homogeneous flow distribution is obtained among the feeders when compared with the initial single-phase conditions.

- As in Test-A, feeders closer to the inlet nozzle (Feeders-3, 4, 5) received more flow rate than the others (Feeders 2 and 6).

- Increasing inlet void fraction from 28% in Test A to 32.5% in Test B caused a more nonhomogeneous flow distribution among the feeders. It can be easily

seen when normalized flow rate values are compared. For example, normalized flow rate for Feeder-3 was 4.578 in Test A, while for Test B this value is measured as 6.240.

2.4.2.3 TEST C

Test C has 4 cases. Test C-I is the single phase flow case. Test C-II is the two-phase flow case where nearly 38.3% inlet void fraction is introduced into the system. In Test C-III, inlet void fraction is kept almost constant at 37% and low flow rate ECI (0.325 kg/s) is injected. Test C-IV has 38.8% inlet void fraction but higher ECI flow rate (0.544 kg/s). Two-phase mass flow rate, the average void fraction and normalized $\dot{m}$ for each outlet feeder is given in the Table 2.6, Figure 2.14 and Figure 2.15. Normalized $\dot{m}$ for each feeder represents the flow split ratios in a test case.

Table 2.6 TEST- C Steady State Flow Distribution Through Feeders

TEST C RESULTS					
		C-I	C-II	C-III	C-IV
Feeder-2	α (%)	0	86.8	87.6	87.8
	$\dot{m}$ (kg/s)	0.274	0.138	0.142	0.148
	Normalized $\dot{m}$	1.000	1.000	1.000	1.000
Feeder-3	α (%)	0	0	0	0
	$\dot{m}$ (kg/s)	0.360	0.816	0.888	0.926
	Normalized $\dot{m}$	1.314	5.921	6.241	6.266
Feeder-4	α (%)	0	36.8	34.6	23.7
	$\dot{m}$ (kg/s)	0.379	0.285	0.358	0.416
	Normalized $\dot{m}$	1.382	2.066	2.516	2.817
Feeder-5	α (%)	0	42.8	45.1	40
	$\dot{m}$ (kg/s)	0.342	0.299	0.337	0.366
	Normalized $\dot{m}$	1.247	2.171	2.365	2.476
Feeder-6	α (%)	0	73.5	3.6	5
	$\dot{m}$ (kg/s)	0.333	0.149	0.247	0.271
	Normalized $\dot{m}$	1.215	1.082	1.736	1.834
	$\bar{\alpha}_{INLET}$	0	38.3	37.0	38.8
	$\sum \dot{m}_{NN}(kg/s)$	1.688	1.687	1.972	2.127
	$\sum \dot{m}_{EXP}(kg/s)$	1.754	1.741	2.093	2.284
	$\dot{m}_{ECI}(kg/s)$	0	0	0.325	0.544
	Error(%)	3.75	3.09	5.80	6.87

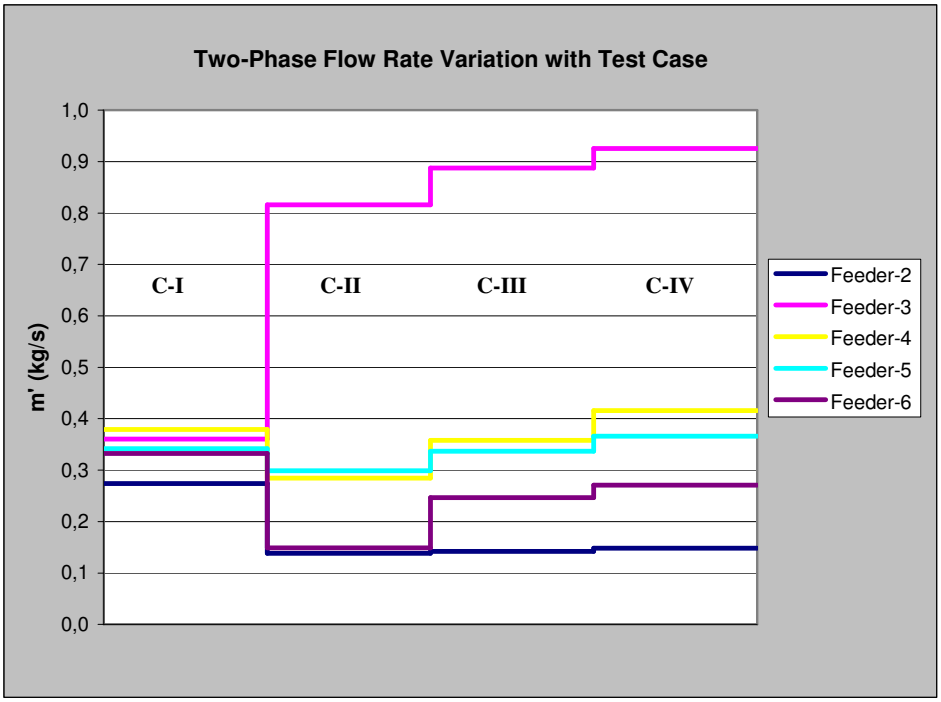

Figure 2.14 Test-C Steady State Mass Flow Rate Variation

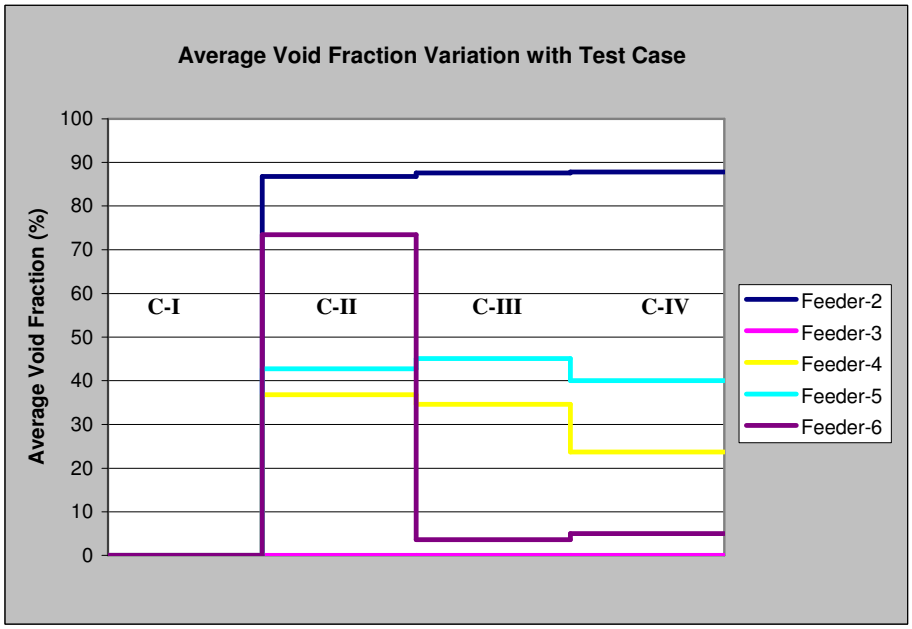

Figure 2.15 Test-C Steady State Average Void Fraction Variation

The followings are the comments on the Test-C results:

- In two-phase cases (C-II, C-III and C-IV) Feeder-3 again received the highest flow rate than the others as in Test-A and Test-B.

- ECI water supply is received mostly by Feeder-6 in low ECI case. An increase of 0.98 kg/s in the flow rate is observed in Feeder-6 between case C-II and C-III.

- When compared the same elevation feeders, it can be said that, more void (40% - 45%) was observed in Feeder-5 while more flow (0.358 and 0.416 kg/s) was observed in Feeder-4 in ECI cases (C-III and C-IV).

- As observed in Test A and Test B, in the two phase tests (C-II, C-III and C-IV), when the total input flow rate (inlet + ECI) increases, a less homogeneous flow distribution was obtained among the feeders.

- When ECI is introduced into the system, as observed in the previous tests, Feeder-6 void fraction is decreased suddenly from 73.5% to 3.6% and 5% respectively, while in Feeder-2 it was kept nearly constant at about 87%.

- Neural network estimation of total mass flow rate in all cases of Test C is in agreement with measurements within an error range of 3.09 – 6.87 %.

As a summary of all tests:

- Two-phase tests revealed less homogeneous flow distribution among the feeders compared to single-phase tests.

- Neural network estimations of total mass flow rate are in good agreement with measured values with a maximum error of 8.63% (Test B-IV).

- When A-II, B-II and C-II cases are compared, the inlet void fraction in C-II was the highest and in A-II it was the lowest. It can be observed from the Table 2.4, 2.5 and 2.6 that when the inlet void fraction is increased in A-II through B-II, the void fraction in Feeder-2 is increased as expected(from 72.6% to 85.4%) and the mass flow rate in the same feeder is decreased. However, when B-II and C-II test cases are compared, the aforementioned variables remained nearly constant for Feeder-2 (86.8%).

- The mass flow rate increased mostly in Feeder-3 and no air flow is detected when A-II, B-II and C-II are compared. This situation can be explained by the lowest elevation of this feeder's connection to the header.

- It is observed in every test that Feeder-6 received most of the ECI water flow compared to Feeder-2 which has the same nozzle elevation. This phenomenon resulted a sudden decrease in Feeder-6 void fraction in the 3rd cases of all tests.

CHAPTER 3

COMPUTATIONAL STUDY

3.1 Introduction

A computational simulation study was carried out after completion of the experimental work. Throughout the computational study, every test case was simulated by "CATHENA Mod-3.5c/Rev 0".

The primary focus of CATHENA has been on the analysis of the sequence of events which occur during a postulated loss-of-coolant accident (LOCA) in a CANDU reactor. Although it has been developed for CANDU reactors, CATHENA has found a wide range of applications. These applications include the analysis of thermal-hydraulic experiments conducted in several laboratories like Whiteshell and Chalk River and analysis of upset conditions in the MAPLE class of research reactors. As a result, a large number of conference publications, AECL and CANDU Owners Group(COG) reports and AECL technical notes have been produced concerning the application and validation of the code [2].

In the year 2000, Middle East Technical University was given a "registered user" license of CATHENA regarding the Joint Research Project, signed between AECL, TAEK and METU.

A description of the code is given in following sections.

3.2 CATHENA Computer Code

The CATHENA's thermal-hydraulic model uses a one-dimensional, two-fluid non-equilibrium representation of gas-liquid flow in a piping network. The model consists of individual mass, momentum, and energy equations for the gas and liquid phases together with flow-regime dependent constitutive relations that describe mass, momentum, and energy transfers across the interface and between each phase and the piping walls (energy). In addition, a noncondensable gas component may optionally be included in the description of the gas phase. The code contains thermophysical property relations for both H_2O and D_2O as well as for a number of noncondensable gases (Air, N_2, H_2, He, Ar, and CO_2) [24].

3.2.1 CATHENA Input

CATHENA needs a couple of main sections in the input file (see Appendix B). These cards are inserted in an input file with a syntax and order. The main sections can be identified as:

3.2.1.1 Control Parameters Section:

Input from the Control Group is used to specify beginning and end simulation times, frequency and nature of printed output, etc. CATHENA performs a simulation by integrating the fluid flow equations in time using a finite-difference formulation. At each simulation time, an appropriate new time step is selected automatically by the code between the limits defined by the user in this section[2].

3.2.1.2 Components and Geometry Section:

For a system's idealization, several components/elements are provided in CATHENA by which the user can model the system. These are PIPE, RESERVOIR,

TANK, VOLUME and TEE-JUNCTION components. Pipes can be circular, square; can also be in bundles. Flow resistance, roughness and the projected flow regime can also be modeled with the geometric features. PIPE's can be divided into segments by a given node quantity. Boundary conditions can be set by using RESERVOIR component. TANK components are used when two distinct regions are considered or when the water level is to be observed. TEE-JUNCTION's are components where at least three pipes are met.

3.2.1.3 Connections Section:

All the components defined in COMPONENTS section are connected in the CONNECTIONS section, so that a flow network is created. Each pipe component has a left and a right end. Connecting these left and right ends of pipes in a system, a model of the whole flow system is created. Components like VOLUME, RESERVOIR, TANK and TEE-JUNCTION has no left or right ends and they can only be connected to pipe components.

3.2.1.4 Boundary Conditions Section:

There are three types of boundary conditions that can be specified in CATHENA. They are RESERVOIR Boundary Condition, FLOW Boundary Condition and HEAT INPUT Boundary Condition. In the RESERVOIR boundary condition, thermal-hydraulic conditions in a reservoir component are described. They are the liquid pressure, vapor enthalpy, liquid enthalpy, vapor void fraction and non-condensible fraction where applicable. FLOW boundary condition is set between any components' connection where a mixture flow rate is specified. HEAT INPUT boundary condition is not used in this study since no thermal considerations take place in the tests [2].

3.2.1.5 System Models Section:

Components used in reactor systems or test facilities can be modeled in this section. They can be listed in Table 3.1;

Table 3.1 CATHENA System Models

1. Boil Length Average- CHF	7. Heat Exchanger
2. Crept Pressure Tube	8. Junction Resistance
3. Delay Line	9. Reactor Kinetics
4. Discharge/Break	10. Pump
5. ECI Accumulator	11. Seperator
6. Heat Balance	12. Valve/Orifice

Only VALVE/ORIFICE model is used from this system models section, for the valves on each feeder line in the test facility.

3.2.1.6 System Control Section :

In this section, system control models are provided to simulate the control systems used in reactors and test facilities. Most of the input sections described above have controllable variables (nodal pressure, flowrate, valve area etc). These variables can be made time dependent if the time history of a CATHENA input parameter is known. Therefore a “trip” transient can be modeled by the aid of the system control part.

3.2.1.7 Initial Conditions Section:

For all defined components and connections, initial conditions have to be set in the input file. The inital condition parameters consist of pressure, vapor enthalpy, liquid enthalpy, void fraction of the vapor or non-condensable fraction where appropriate. For pipe components, a mixture mass flow rate or phase velocities can be specified. Finally for each connection specified in the CONNECTIONS list, phase velocities should be given.

3.2.1.8 GEN HTP (Heat Transfer Package) :

This section describes the thermal-hyraulic input specifications required to model piping networks [1]. In this study GEN HTP is not used as no heat transfer is taken into consideration in the experiments. The whole experiments were carried out at room temperature.

3.3 CATHENA Model of the Test Facility

The test facility is modeled by using PIPE components and connections between them. Fig. 3.1 shows the CATHENA model of the METU-TPFTF. Boundary conditions are set with RESERVOIR components. The header itself is also composed of 6 connected pipes having larger diameters. The five feeder outlets are connected to the header from certain distances measured from the right end of HEAD1 pipe.

While preparing the input file of the code, some systematic assumptions were made because of the limits of CATHENA. These assumptions simplify the solution and reduces the runtime. Some of the assumptions can be listed as :

- Whole 3-D geometry is degraded to 1-D geometry as CATHENA solves mass, momentum and energy equations in 1-D geometry.

- The header is modeled as a network of big diameter six unequal lenght pipes connected end to end. Most of these connection points were selected to use also for the feeder connection points.

- The pipes that carry water from the pump and air from the tanks were not modelled entirely. Instead, the flow rates of air and water are given as flow boundary conditions at the mixing section pipe inlet. The header inlet pipe which carries the air-water mix to the header is modelled after the mixing section.

- Two reservoirs are defined before the mixing section, which are for defining inlet pressure and temperature for air and water.

- There are also five reservoirs defined at the end of each feeder's discharge points. Five of each are representing the tank where the water is collected and where the atmospheric pressure is valid. Atmospheric pressure boundary conditions are defined for these reservoirs. Each feeder is ending at a different elevation from the tank water surface (max difference of 200 mm). If all the feeders were connected to one reservoir as in the test facility, they all would have to end at the same elevation; that's why each feeder is connected to a seperate reservoir.

- In METU-TPFTF, water from the ECI line is injected into the system with the aid of the same pump's driving force as the main water inlet line. In CATHENA, ECI line is modelled as a different reservoir, connected to one end of the header with the appropriate flow boundary conditions at the connection.

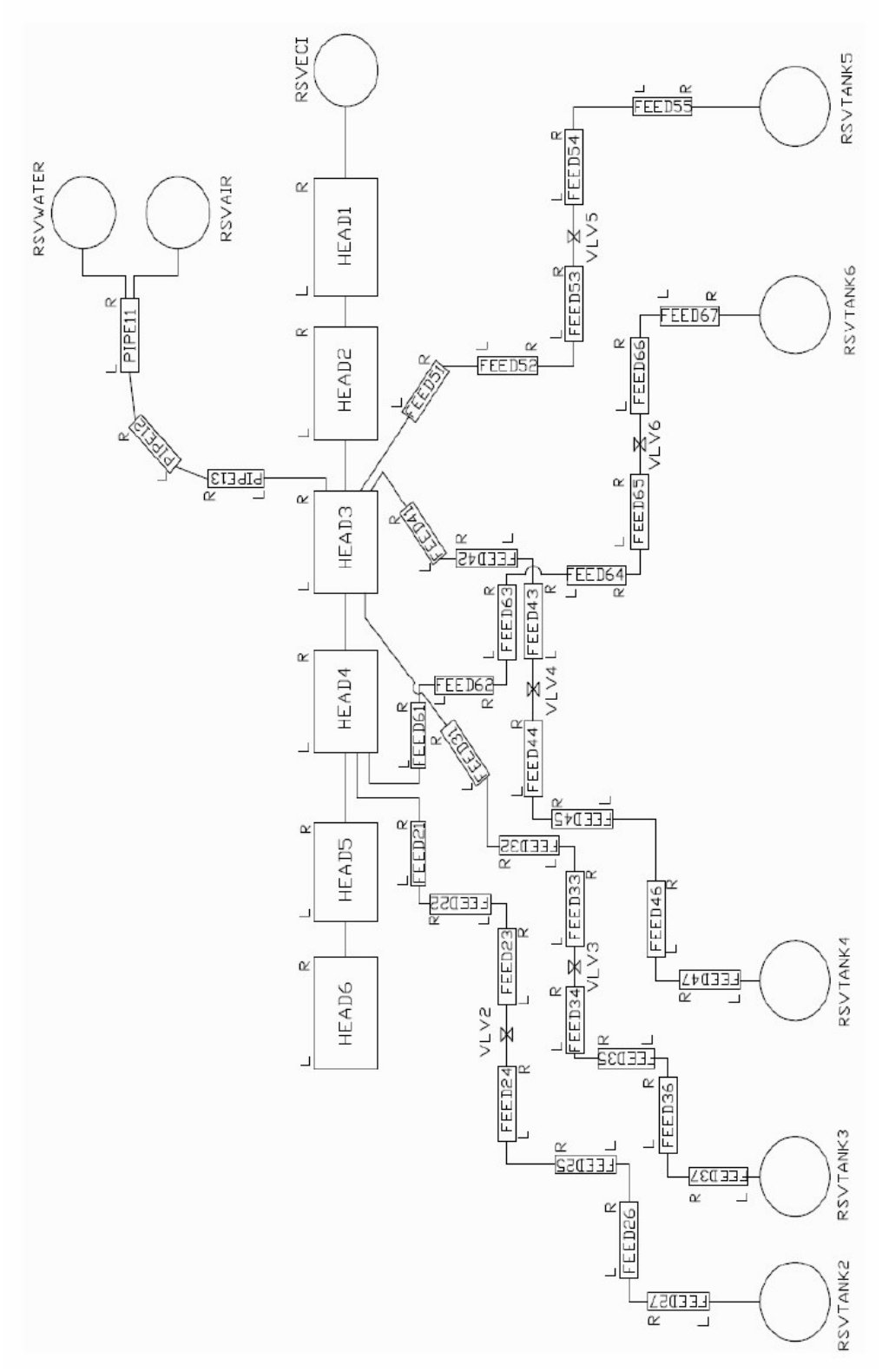

Figure 3.1 Geometrical Modeling of Test Facility in CATHENA

As seen from Figure 3.1, the feeders mounted in opposite directions are connected to the header from the same header pipe end but in reverse directions. For example R-FEED41 is connected to the R-HEAD3 while L-FEED51 is connected to the same side. FEED21 and FEED61 are other examples of the same logic.

The elevation of the feeder connections in actual test setup are different as mentioned in Chapter 2. A deficiency of geometrical modeling is that, the elevations of feeder connections can not be defined in CATHENA. The elevation mostly determines how much void is received into the feeder because a stratified air region is formed in the upper part of the header in two-phase tests. Feeders connected to the header at a higher elevation would eventually receive more void than the feeders at lower elevation.

The height of the header components (PIPE's centerline) were defined at about 1,75 m elevation. Where the lower ends of FEED27, FEED37, FEED47, FEED55 and FEED67 come down to an elevation of 0 meter level.

The valve model in the system input needs the total flow area, the discharge coefficient and valve opening ratio. By receiving these values, CATHENA solves an orifice equation for each valve and valve opening. The pressure drop occuring on each valve actually determines the flow rate on each feeder.

There are five valves on the system. Three of them are on the small diameter feeders which are to be 100% opened if 3 full turns are made. Two of the valves are on the large diameter feeders which are to be turned 4-full turns to reach 100% opening. The flow area for any globe valve on the system is not known with respect to valve opening. 18.75% valve opening ratio for the large diameter feeders and 25% valve opening for the small diameter feeders were used which normally resulted in different flow areas across the two types of valves. The computational modeling approach for the unknown valve flow areas was to go for a trial solution. Single phase results (A-I, B-I, C-I) were provided to CATHENA as initial conditions for the given inlet flow rate. By trying different valve/orifice flow areas:

- The flow rate results of the code for each feeder is recorded and flow split ratios are calculated.

- It is observed that more than one set of valve opening ratio's could ensure the normalized flow rates calculated and given in Tables 2.3, 2.4 and 2.5 .

- The system absolute pressure values had been recorded in the tests and the pressure results coming from the code output were compared with the ones from the experiments.

- When the flow split ratio's and the pressure values all matched with the experimental ones on the single phase section, the two phase test cases were simulated by keeping these valve/orifice flow areas constant. Providing the stated valve flow areas shown in Table 3.2, the normalized water flow rates in each test result is obtained. The increase in pressure (see Table 2.3) between tests A, B and C is tried to be simulated with arranging relatively small flow areas at the orifices.

Table 3.2 Orifice Flow Area of the Valves

	Orifice Flow Area of the Valves ($x10^4 m^2$)		
	Test A	Test B	Test C
Feeder-2	0.888	0.837	0.794
Feeder-3	1.206	1.197	1.103
Feeder-4	2.042	2.042	1.626
Feeder-5	1.404	1.363	1.170
Feeder-6	1.419	1.424	1.216

Two types of boundary conditions are set in the code. RESERVOIR boundary condition was defined for each reservoir specified in the components section. The RSVWATER represents the reservoir which holds $24^0 C$ of water at about atmospheric pressure. The RSVAIR represents the reservoir that contains air at $24^0 C$ and P~150 kPa. RSVECI represents the Emergency Coolant Injection reservoir where $24^0 C$ water at about atmospheric pressure is contained. All RSVTANK reservoirs are used to collect the water coming down from the feeders.

Atmospheric pressure boundary condition is applied for those reservoirs which is the reality in all tests.

Flow boundary conditions were also defined at some connections to set constant inlet flow rates of fluids. A flowrate of water at the junction between RSVWATER and R-PIPE11, air flow at the junction between RSVAIR and R-PIPE11 and ECI water flowrate at the connection between RSVECI and R-HEAD1 were specified.

In the SOLUTION CONTROL section of the input (see Appendix B), some variables are controlled for arbitrarily taken time intervals. Enough time is given to the code for each test case to reach the steady state. The defined time intervals can be listed as:

Time Arrival(s)	Test Case Simulation
0-40	Introducing single phase water to the system and reaching steady state
40-200	Introducing air into the system and reaching steady state
200-300	Introducing low flow rate ECI into the header and reaching steady state
300-400	Introducing high flow rate ECI into the header and reaching steady state

The code runs are carried out in a Windows Vista environment Pentium Core2 Duo processor 2 GB RAM computer.

All desired data from the output of the code is written into text files and plotted. The converged values are stated in the Table 3.1, Table 3.2, Table 3.3. The graphical representations of the computational results are given in Chapter 4 together with the experimental results.

3.4 Simulation Results and Discussions

3.4.1 TEST A

Values in the Table 3.1 are the steady state values for each case.The test cases can be defined as:

A-I : Single Phase Flow

A-II : Two Phase Flow

A-III : Two Phase Flow + Low Flow rate ECI

A-IV : Two Phase Flow + High Flow rate ECI

Table 3.3 Test A CATHENA Simulation Results

TEST A CATHENA RESULTS		**A-I**	**A-II**	**A-III**	**A-IV**
Feeder-2	α (%)	0	71.9	58.7	52.8
	$\dot{m}$ **(kg/s)**	0.286	0.272	0.323	0.352
	Normalized $\dot{m}$	1.000	1.000	1.000	1.000
Feeder-3	α (%)	0	0	0	0
	$\dot{m}$ **(kg/s)**	0.367	0.536	0.584	0.618
	Normalized $\dot{m}$	1.283	1.971	1.808	1.756
Feeder-4	α (%)	0	36.6	31.2	25.6
	$\dot{m}$ **(kg/s)**	0.391	0.343	0.411	0.460
	Normalized $\dot{m}$	1.367	1.261	1.272	1.307
Feeder-5	α (%)	0	42.3	35.7	31.3
	$\dot{m}$ **(kg/s)**	0.362	0.329	0.393	0.439
	Normalized $\dot{m}$	1.266	1.210	1.217	1.247
Feeder-6	α (%)	0	61.3	48.2	42.0
	$\dot{m}$ **(kg/s)**	0.342	0.270	0.344	0.390
	Normalized $\dot{m}$	1.196	0.993	1.065	1.108
	$\bar{\alpha}_{INLET}$	0	28.2	28.2	28.2
	$\sum \dot{m}_{CATHENA}(kg/s)$	1.748	1.750	2.055	2.259
	$\sum \dot{m}_{EXP}(kg/s)$	1.748	1.749	2.054	2.280
	$\dot{m}_{ECI}(kg/s)$	0	0	0.319	0.522

The following comments can be made on Test A CATHENA Results :

- In A-II case, air is introduced into the system. Feeder-2 and Feeder-6 received higher void fraction (71.9% and 61.3%, respectively) than other feeders.

- In all two-phase cases, due to its connection elevation and angle, Feeder-3 received the highest amount of mass flow rate with zero average void fraction. The normalized flow rate value for Feeder-3 decreased from 1.971 to 1.756 with the increasing ECI flow rate.

- Feeder-6 received the highest ratio (23.2%) of ECI water supplied in the A-III case. In A-IV case, the distribution of ECI is more even between all feeders.

- It is seen in Table 3.2 that, Feeder-4 received more mass flowrate than its equivalence Feeder-5 while Feeder-5 always received more void than Feeder-4.

- More void was generally observed in Feeder-2 with respect to the void in Feeder-6. CATHENA supplied good data on the total mass conservation of water and air as seen in Table 3.3 .

3.4.2 TEST B

Table 3.4 Test B CATHENA Simulation Results

TEST B CATHENA RESULTS		B-I	B-II	B-III	B-IV
Feeder-2	α (%)	0	76.2	67.1	57.4
	$\dot{m}$ **(kg/s)**	0.274	0.259	0.309	0.347
	Normalized $\dot{m}$	1.000	1.000	1.000	1.000
Feeder-3	α (%)	0	0	0	0
	$\dot{m}$ **(kg/s)**	0.369	0.546	0.595	0.637
	Normalized $\dot{m}$	1.347	2.108	1.926	1.836
Feeder-4	α (%)	0	40.9	34.8	30.8
	$\dot{m}$ **(kg/s)**	0.395	0.360	0.432	0.49
	Normalized $\dot{m}$	1.442	1.390	1.398	1.412
Feeder-5	α (%)	0	47.9	39.8	35.1
	$\dot{m}$ **(kg/s)**	0.360	0,320	0.387	0.439
	Normalized $\dot{m}$	1.314	1.236	1.252	1.265
Feeder-6	α (%)	0	66.8	55.2	46.4
	$\dot{m}$ **(kg/s)**	0.347	0.260	0.334	0.394
	Normalized $\dot{m}$	1.266	1.004	1.081	1.135
	$\bar{\alpha}_{INLET}$	**0**	**32.6**	**32.8**	**32.8**
	$\sum \dot{m}_{CATHENA}(kg/s)$	**1.745**	**1.745**	**2.057**	**2.307**
	$\sum \dot{m}_{EXP}(kg/s)$	**1.744**	**1.743**	**2.055**	**2.309**
	$\dot{m}_{ECI}(kg/s)$	**0**	**0**	**0.322**	**0.572**

For the Test B Simulation following comments can be made:

- Feeder-3 did not receive any air flow in any cases of two phase tests (B-II, B-III, B-IV). Compared to the normalized mass flow rate value of Test A-II Section, the Feeder-3 normalized mass flow rate is higher .

- Feeder-2 and Feeder-6 received the highest void fraction in all two phase cases, for example in A-II case Feeder-2 void fraction is 76.2 and Feeder-6 void fraction is 66.8.

- Feeder-5 again received more void than Feeder-4, while Feeder-4 received more flow rate than Feeder-5.

- In Test B simulation, Feeder-4 and Feeder-5 received a more water flow rate from the ECI compared to the Test A simulations.

3.4.3 TEST C

Table 3.5 Test C CATHENA Simulation Results

TEST C CATHENA RESULTS					
		C-I	**C-II**	**C-III**	**C-IV**
Feeder-2	α (%)	0	86.7	69.0	63.8
	$\dot{m}$ **(kg/s)**	0.285	0.256	0.321	0.354
	Normalized $\dot{m}$	1.000	1.000	1.000	1.000
Feeder-3	α (%)	0	0	0	0
	$\dot{m}$ **(kg/s)**	0.375	0.552	0.610	0.644
	Normalized $\dot{m}$	1.316	2.156	1.900	1.819
Feeder-4	α (%)	0	44.6	37.6	34.7
	$\dot{m}$ **(kg/s)**	0.394	0.357	0.435	0.477
	Normalized $\dot{m}$	1.382	1.395	1.355	1.347
Feeder-5	α (%)	0	51.8	43.3	39.6
	$\dot{m}$ **(kg/s)**	0.355	0.318	0.390	0.429
	Normalized $\dot{m}$	1.246	1.242	1.215	1.212
Feeder-6	α (%)	0	70.0	58.8	53.2
	$\dot{m}$ **(kg/s)**	0.346	0.260	0.339	0.382
	Normalized $\dot{m}$	1.214	1.016	1.056	1.079
	$\bar{\alpha}_{INLET}$	**0**	**38.3**	**37.9**	**38.3**
	$\sum \dot{m}_{CATHENA}(kg/s)$	**1.755**	**1.743**	**2.095**	**2.286**
	$\sum \dot{m}_{EXP}(kg/s)$	**1.754**	**1.741**	**2.093**	**2.284**
	$\dot{m}_{ECI}(kg/s)$	**0**	**0**	**0.325**	**0.544**

For the Test C Simulation following comments can be made:

- Feeder-3 did not receive any air in any case of two phase tests (C-II, C-III, C-IV). Compared to the normalized mass flow rate value of Test B-II case, the

Feeder-3 normalized mass flow rate is higher in C-II case, which are 2.108 and 2.156, respectively.

- Feeder-5 again received more void than Feeder-4, while Feeder-4 received more flowrate than Feeder-5. The void fraction in Feeder-4 in C-II case was 44.6% while it was 51.8% in Feeder-5.

- Feeder-2 and Feeder-6 always received the highest void fraction. Feeder-2 seemed to have more void fraction compared to Feeder-6. For example void fraction in C-II was 86.7% for Feeder-2 while it was 70.0% for Feeder-6. The same behaviour can be followed in the following two-phase test cases.

As a conclusion to the computational simulation section, some general comments on the results can be made:

- Feeder-5 received more void than Feeder-4 in all two phase test cases in all simulations. This may be due to the fact that air tends to move through the feeder in which there is lower friction losses. Feeder-5, from the exit of the header till the end in the RSVTANK5 is shorter than Feeder-4 and has less 90^0 elbows than Feeder-4. Also in the input, to simulate the geometrical pressure effects on each feeder, different valve openings were defined. Here the orifice area of Feeder-5 is smaller than Feeder-4 which is shown in Table 3.2. So a smaller flow area might have resulted in a flow resistance for water flow. The air might have restored the place of resisted water in Feeder-5. The same phenomenon was also observed by Pezek[4] and Parrott[18] in their studies, which was thought to be resulted from the effect of centrifugal forces appearing in the inlet nozzle of the header.

- The same idea might be true for Feeder-2 and Feeder-6 couple. Feeder-2 has higher flow resistance since it has a smaller defined amount of orifice area shown in Table 3.2. The void fraction in Feeder-2 is higher than that of

Feeder-6. Generally speaking, water flow tends to move towards the large orifice opening where the flow resistance is lower, while air flows in the opposite path at the same instance.

- Although the average void fraction at the inlet is increased in all tests, Feeder-3 never received any void in any test.

CHAPTER 4

COMPARISON of the EXPERIMENTAL & COMPUTATIONAL RESULTS

4.1 Introduction

In this chapter, experimental and computational results are compared and discussed. The results are firstly given in tables and then in graphs for both of the studies. The effect of average inlet void fraction, the amount of ECI flow and the geometrical effects are observed on each feeder connected to the header.

Generally speaking, when the results emerging from the computational and experimental studies are compared, the amount of error seems to be relatively high in some feeders. Moreover, the main behaviour both in computational and experimental studies show similar trends which may indicate the consistency between the two different studies.

A more detailed discussions section takes place after the graphs. At the end of this chapter, suggestions for future work are given.

4.2 Results

4.2.1 Results on Tables

In Test A, average void fraction at the inlet, $\overline{\alpha}_{IN}$ is set to 0.28, approximately. The inlet mass flowrate of water is 1.748 kg/s at the inlet in A-I case. In A-II, air is introduced into the header and 28.2% inlet void fraction is provided. In A-III, ECI

water flowrate at 0.319 kg/s is released into the system. The ECI flow rate is increased to 0.522 kg/s in the case, A-IV (see Table 4.1).

In Test B, average void fraction at the inlet, $\bar{\alpha}_{IN}$ is set to 0.32, approximately. The inlet mass flowrate of water is 1.744 kg/s at the inlet in B-I case. In B-II, air is introduced into the header and 32.6% inlet void fraction is provided. In B-III, ECI water at 0.322 kg/s is released into the system. The ECI flow rate is increased to 0.572 kg/s in the case, B-IV (see Table 4.2).

In Test C, average void fraction at the inlet, $\bar{\alpha}_{IN}$ is set to 0.38, approximately. The inlet mass flowrate of water is 1.754 kg/s at the inlet in C-I case. In C-II, air is introduced into the header and 38.3% inlet void fraction is provided. In C-III, ECI water at 0.325 kg/s is released into the system. The ECI flow rate is increased to 0.544 kg/s in the case, C-IV (see Table 4.3).

Table 4.1 Experimental and Computational (CATHENA) Results of TEST A

TEST A RESULTS		EXPERIMENTAL RESULTS				COMPUTATIONAL RESULTS			
		A-I	A-II	A-III	A-IV	A-I	A-II	A-III	A-IV
Feeder-2	α (%)	0	72.6	70.3	76	0	71.9	58.7	52.8
	$\dot{m}$ (kg/s)	0.276	0.233	0.244	0.198	0.286	0.272	0.323	0.352
	Normalized $\dot{m}$	1.000	1.000	1.000	1.000	1.000	1.000	1.000	1.000
Feeder-3	α (%)	0	0	0	0	0	0	0	0
	$\dot{m}$ (kg/s)	0.352	0.794	0.852	0.909	0.367	0.536	0.584	0.618
	Normalized $\dot{m}$	1.276	3.407	3.491	4.578	1.283	1.971	1.808	1.756
Feeder-4	α (%)	0	36.3	34.5	24.4	0	36.6	31.2	25.6
	$\dot{m}$ (kg/s)	0.376	0.303	0.335	0.403	0.391	0.343	0.411	0.460
	Normalized $\dot{m}$	1.363	1.299	1.371	2.033	1.367	1.261	1.272	1.307
Feeder-5	α (%)	0	43.5	41	45	0	42.3	35.7	31.3
	$\dot{m}$ (kg/s)	0.347	0.300	0.331	0.349	0.362	0.329	0.393	0.439
	Normalized $\dot{m}$	1.260	1.285	1.356	1.756	1.266	1.210	1.217	1.247
Feeder-6	α (%)	0	75.7	5	6.5	0	61.3	48.2	42.0
	$\dot{m}$ (kg/s)	0.329	0.143	0.254	0.232	0.342	0.270	0.344	0.390
	Normalized $\dot{m}$	1.195	0.615	1.043	1.170	1.196	0.993	1.065	1.108
$\bar{\alpha}_{INLET}$		0	28.2	28.9	28.0	0	28.2	28.2	28.2
$\sum \dot{m}_{NN}(kg/s)$ & $\sum \dot{m}_{CATHENA}(kg/s)$		1.680	1.773	2.016	2.091	1.748	1.750	2.055	2.259
$\sum \dot{m}_{EXP}(kg/s)$		1.748	1.749	2.054	2.280	1.748	1.749	2.054	2.280
$\dot{m}_{ECI}(kg/s)$		0	0	0.319	0.522	0	0	0.319	0.522

Table 4.2 Experimental and Computational (CATHENA) Results of TEST B

TEST B RESULTS		EXPERIMENTAL RESULTS				COMPUTATIONAL RESULTS			
		B-I	B-II	B-III	B-IV	B-I	B-II	B-III	B-IV
Feeder-2	α (%)	0	85.4	92.6	88.7	0	76.2	67.1	57.4
	$\dot{m}$ (kg/s)	0.266	0.140	0.131	0.147	0.274	0.259	0.309	0.347
	Normalized $\dot{m}$	1.000	1.000	1.000	1.000	1.000	1.000	1.000	1.000
Feeder-3	α (%)	0	0	0	0	0	0	0	0
	$\dot{m}$ (kg/s)	0.358	0.804	0.864	0.917	0.369	0.546	0.595	0.637
	Normalized $\dot{m}$	1.347	5.742	6.61	6.24	1.347	2.108	1.926	1.836
Feeder-4	α (%)	0	34.9	35.5	23.6	0	40.9	34.8	30.8
	$\dot{m}$ (kg/s)	0.384	0.311	0.340	0.411	0.395	0.360	0.432	0.490
	Normalized $\dot{m}$	1.443	2.218	2.606	2.797	1.442	1.390	1.398	1.412
Feeder-5	α (%)	0	42.8	41	39.7	0	47.9	39.8	35.1
	$\dot{m}$ (kg/s)	0.348	0.304	0.335	0.367	0.360	0.320	0.387	0.439
	Normalized $\dot{m}$	1.309	2.172	2.560	2.497	1.314	1.236	1.252	1.265
Feeder-6	α (%)	0	72.8	5	9	0	66.8	55.2	46.4
	$\dot{m}$ (kg/s)	0.337	0.152	0.250	0.268	0.347	0.26	0.334	0.394
	Normalized $\dot{m}$	1.265	1.087	1.914	1.827	1.266	1.004	1.081	1.135
$\bar{\alpha}_{INLET}$		0	32.6	32.1	32.5	0	32.6	32.8	32.8
$\sum \dot{m}_{NN}(kg/s)$ & $\sum \dot{m}_{CATHENA}(kg/s)$		1.694	1.712	1.919	2.110	1.745	1.745	2.057	2.307
$\sum \dot{m}_{EXP}(kg/s)$		1.744	1.743	2.055	2.309	1.744	1.743	2.055	2.309
$\dot{m}_{ECI}(kg/s)$		0	0	0.322	0.572	0	0	0.322	0.572

Table 4.3 Experimental and Computational (CATHENA) Results of TEST C

TEST C RESULTS		EXPERIMENTAL RESULTS				COMPUTATIONAL RESULTS			
		C-I	C-II	C-III	C-IV	C-I	C-II	C-III	C-IV
Feeder-2	α (%)	0	86.8	87.6	87.8	0	86.7	69.0	63.8
	$\dot{m}$ **(kg/s)**	0.274	0.138	0.142	0.148	0.285	0.256	0.321	0.354
	Normalized $\dot{m}$	1.000	1.000	1.000	1.000	1.000	1.000	1.000	1.000
Feeder-3	α (%)	0	0	0	0	0	0	0	0
	$\dot{m}$ **(kg/s)**	0.360	0.816	0.888	0.926	0.375	0.552	0.610	0.644
	Normalized $\dot{m}$	1.314	5.921	6.241	6.266	1.316	2.156	1.900	1.819
Feeder-4	α (%)	0	36.8	34.6	23.7	0	44.6	37.6	34.7
	$\dot{m}$ **(kg/s)**	0.379	0.285	0.358	0.416	0.394	0.357	0.435	0.477
	Normalized $\dot{m}$	1.382	2.066	2.516	2.817	1.382	1.395	1.355	1.347
Feeder-5	α (%)	0	42.8	45.1	40	0	51.8	43.3	39.6
	$\dot{m}$ **(kg/s)**	0.342	0.299	0.337	0.366	0.355	0.318	0.390	0.429
	Normalized $\dot{m}$	1.247	2.171	2.365	2.476	1.246	1.242	1.215	1.212
Feeder-6	α (%)	0	73.5	3.6	5	0	70.0	58.8	53.2
	$\dot{m}$ **(kg/s)**	0.333	0.149	0.247	0.271	0.346	0.260	0.339	0.382
	Normalized $\dot{m}$	1.215	1.082	1.736	1.834	1.214	1.016	1.056	1.079
$\bar{\alpha}_{INLET}$		0	38.3	37.0	38.8	0	38.3	37.9	38.3
$\sum \dot{m}_{NN}(kg/s)$ **&** $\sum \dot{m}_{CATHENA}(kg/s)$		1.688	1.687	1.972	2.127	1.755	1.743	2.095	2.286
$\sum \dot{m}_{EXP}(kg/s)$		1.754	1.741	2.093	2.284	1.754	1.741	2.093	2.284
$\dot{m}_{ECI}(kg/s)$		0	0	0.325	0.544	0	0	0.325	0.544

4.2.2 Results in Graphs

4.2.2.1 TEST A Experimental and Computational Results

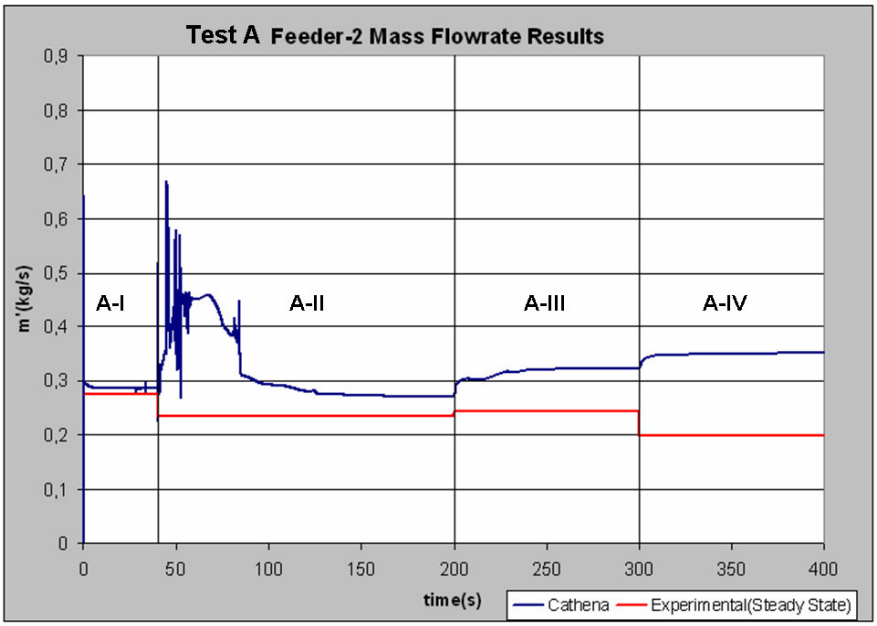

Figure 4.1 Test A Feeder-2 Two-Phase Mass Flow Rate

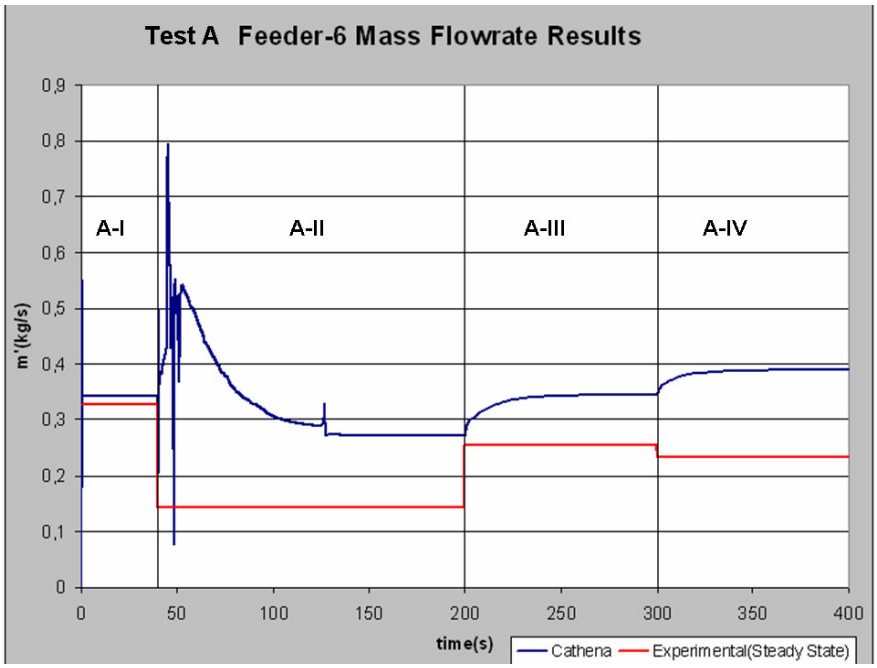

Figure 4.2 Test A Feeder-6 Two-Phase Mass Flow Rate

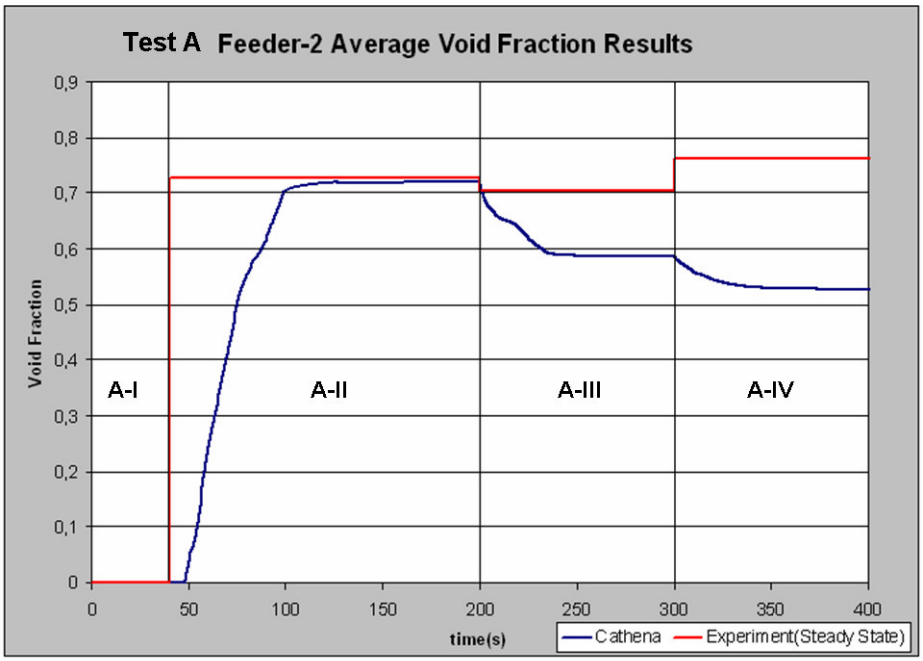

Figure 4.3 Test A Feeder-2 Average Void Fraction

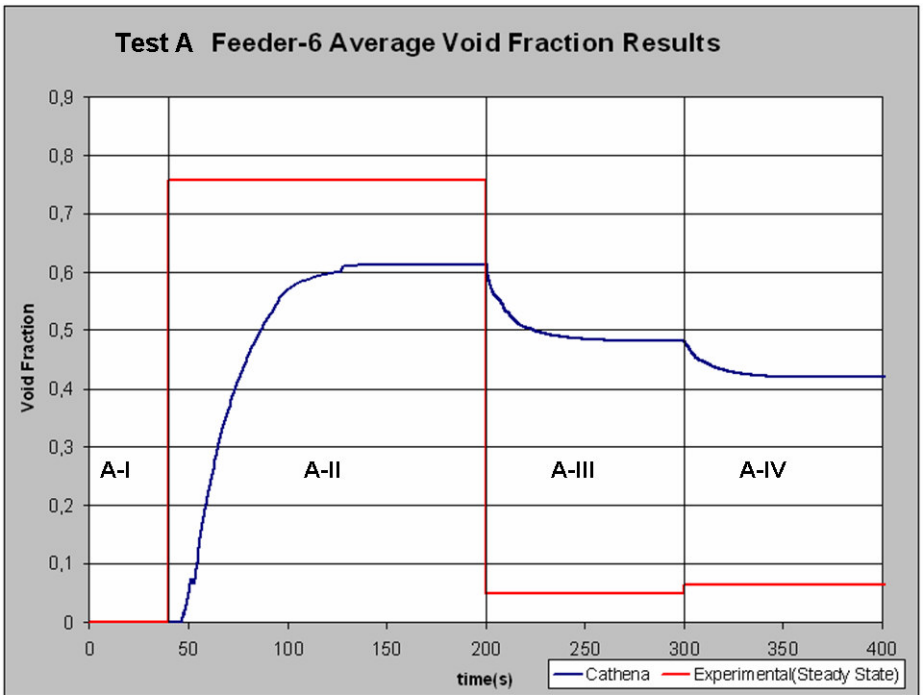

Figure 4.4 Test A Feeder-6 Average Void Fraction

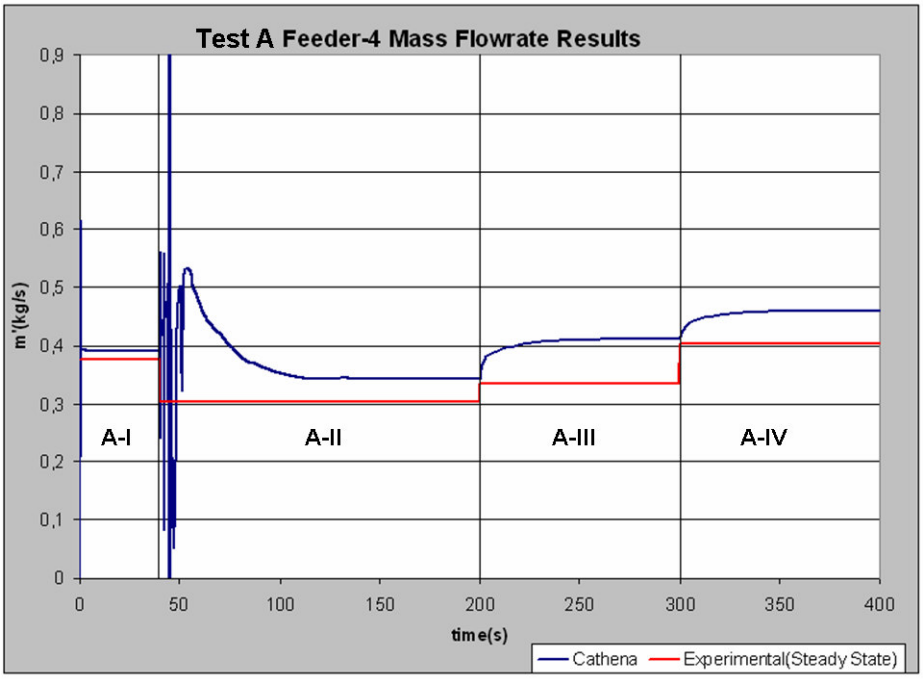

Figure 4.5 Test A Feeder-4 Two-Phase Mass Flow Rate

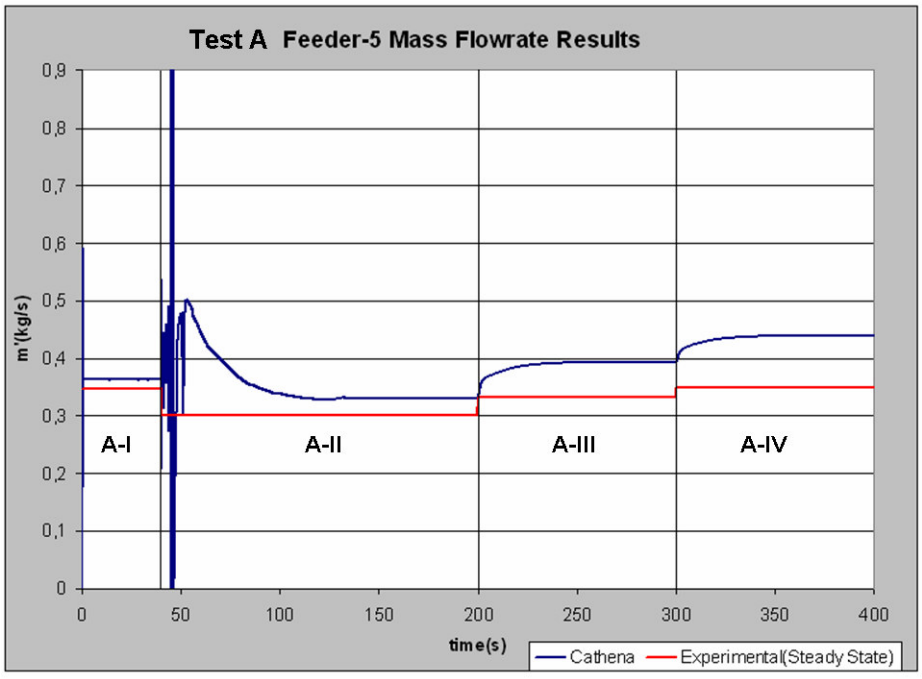

Figure 4.6 Test A Feeder-5 Two-Phase Mass Flow Rate

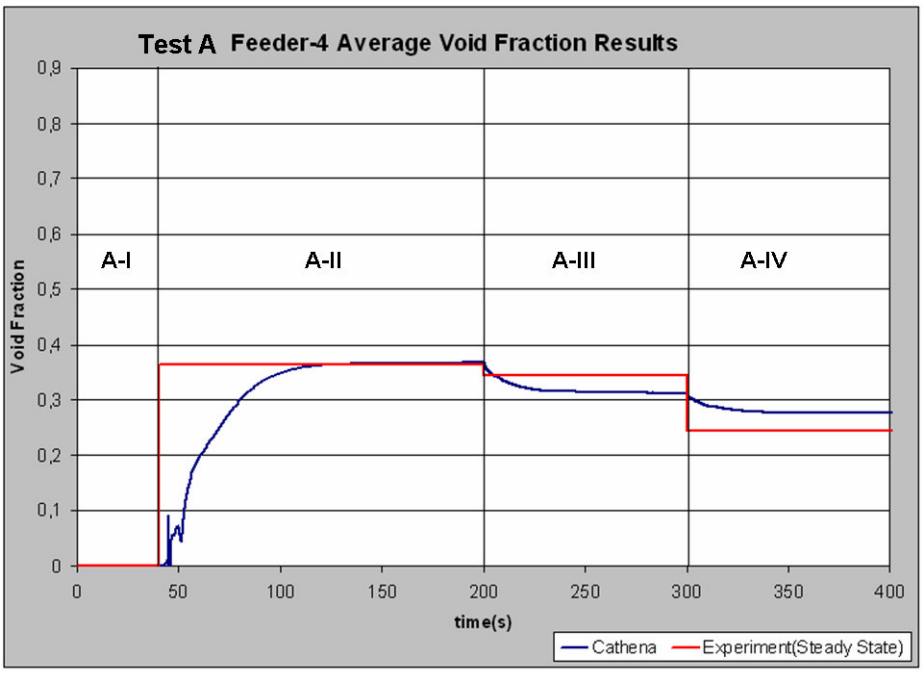

Figure 4.7 Test A Feeder-4 Average Void Fraction

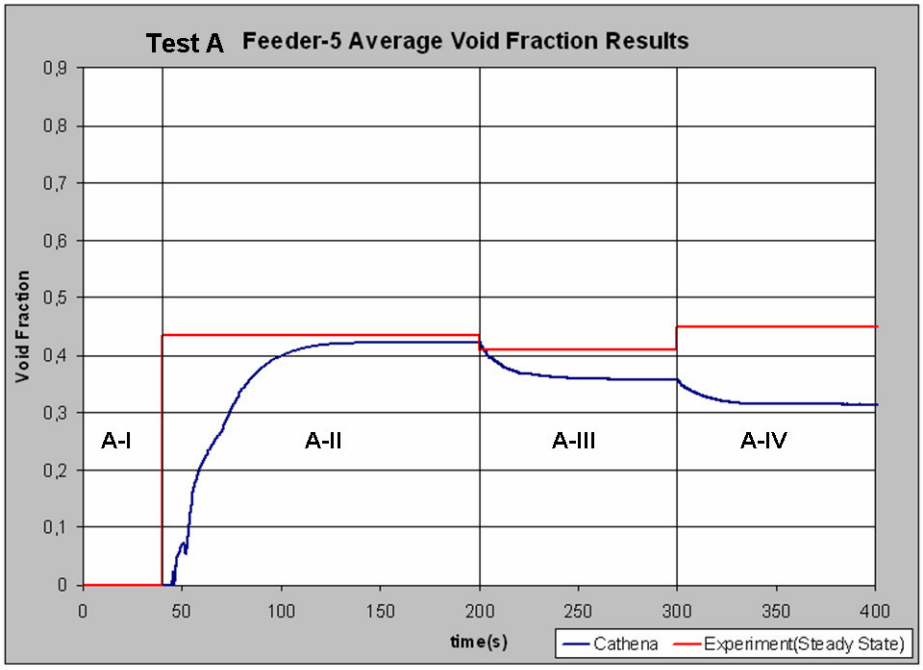

Figure 4.8 Test A Feeder-5 Average Void Fraction

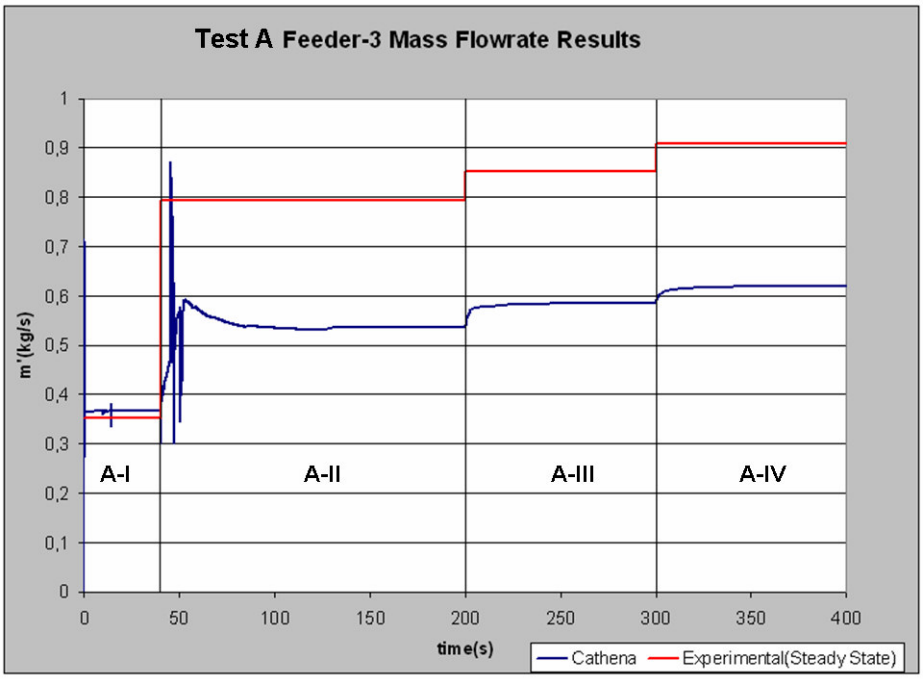

Figure 4.9 Test A Feeder-3 Mass Flow Rate

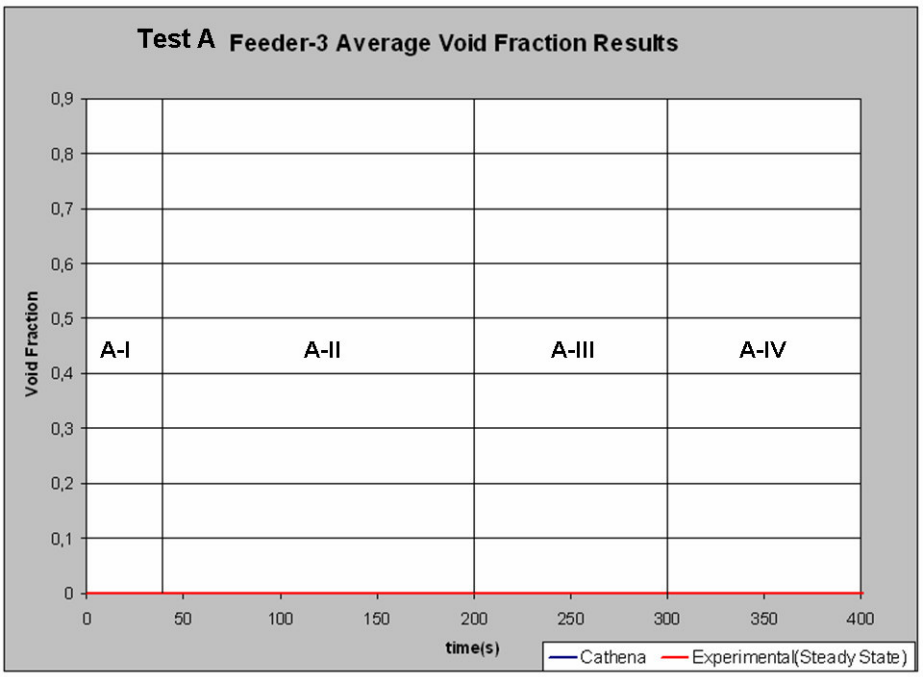

Figure 4.10 Test A Feeder-3 Average Void Fraction

4.2.2.2 TEST B Experimental and Computational Results

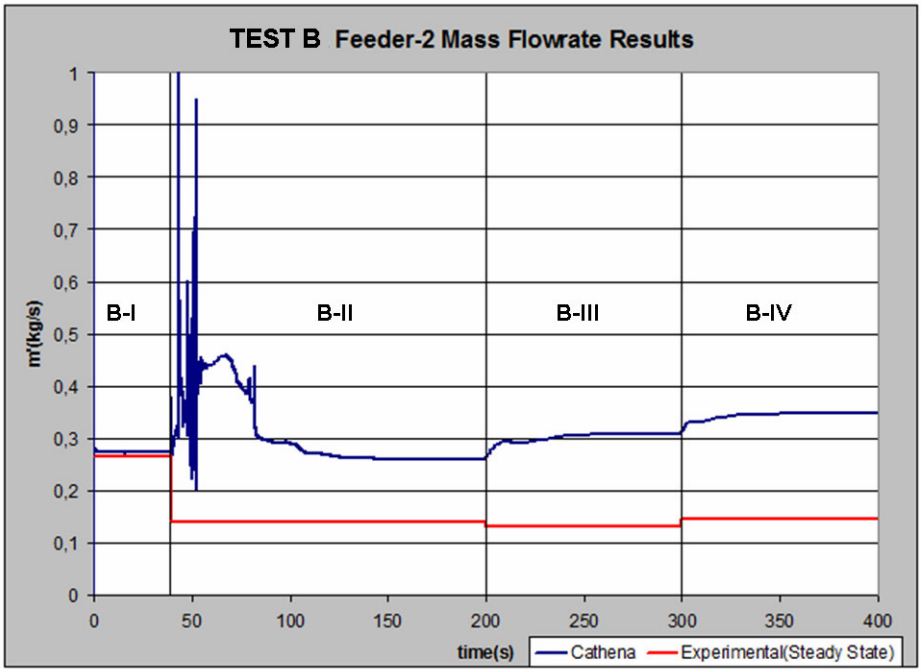

Figure 4.11 Test B Feeder-2 Two-Phase Mass Flow Rate

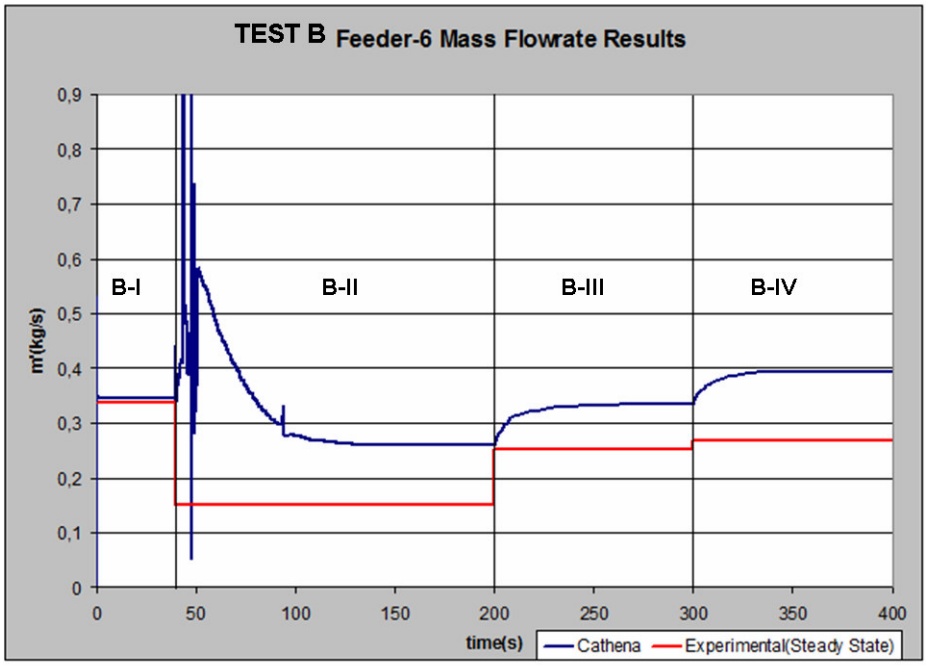

Figure 4.12 Test B Feeder-6 Two-Phase Mass Flow Rate

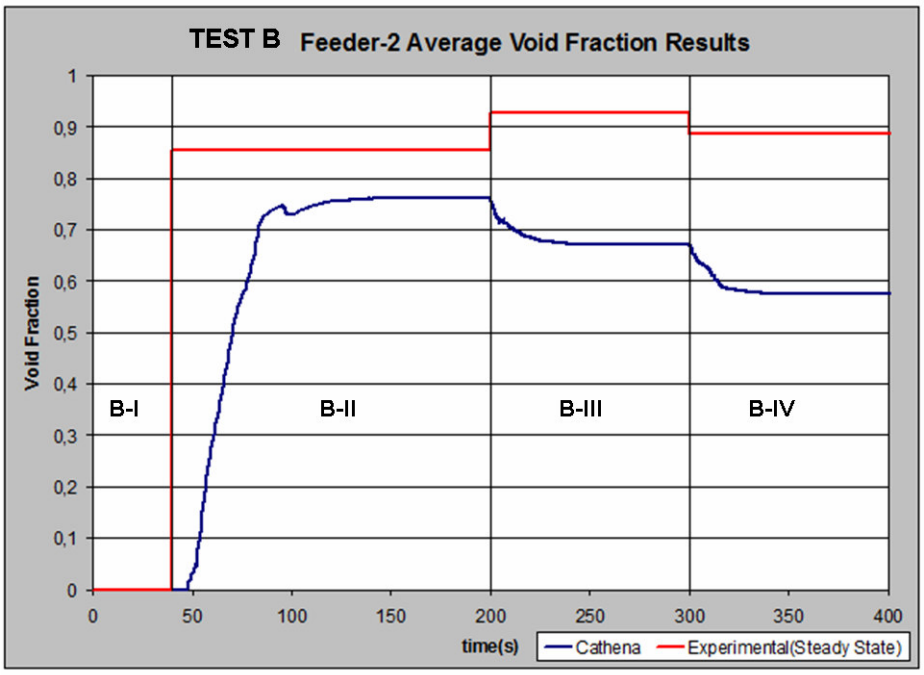

Figure 4.13 Test B Feeder-2 Average Void Fraction

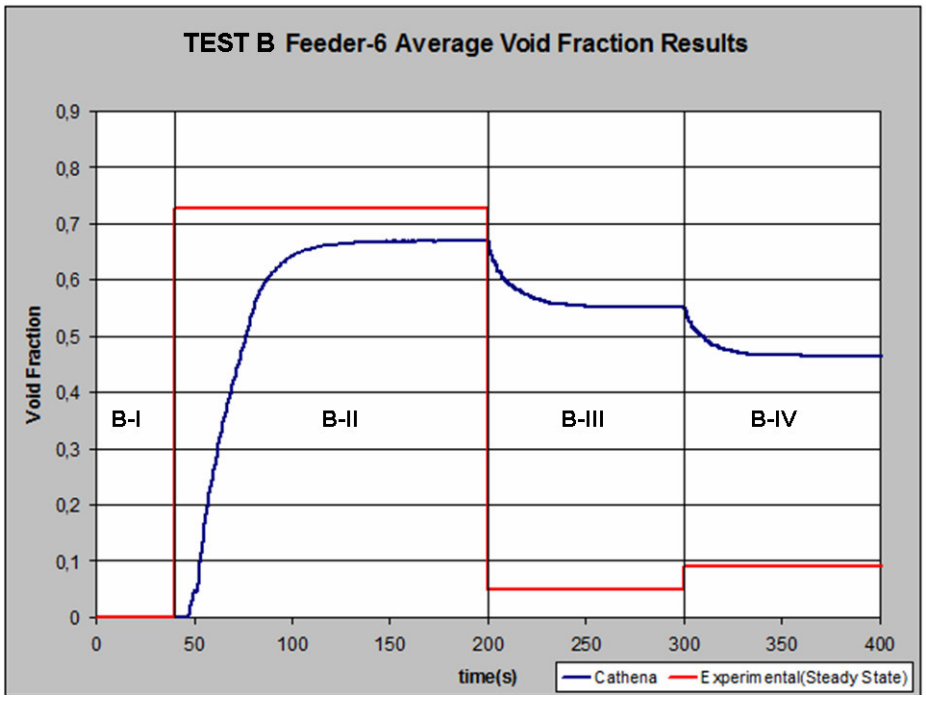

Figure 4.14 Test B Feeder-6 Average Void Fraction

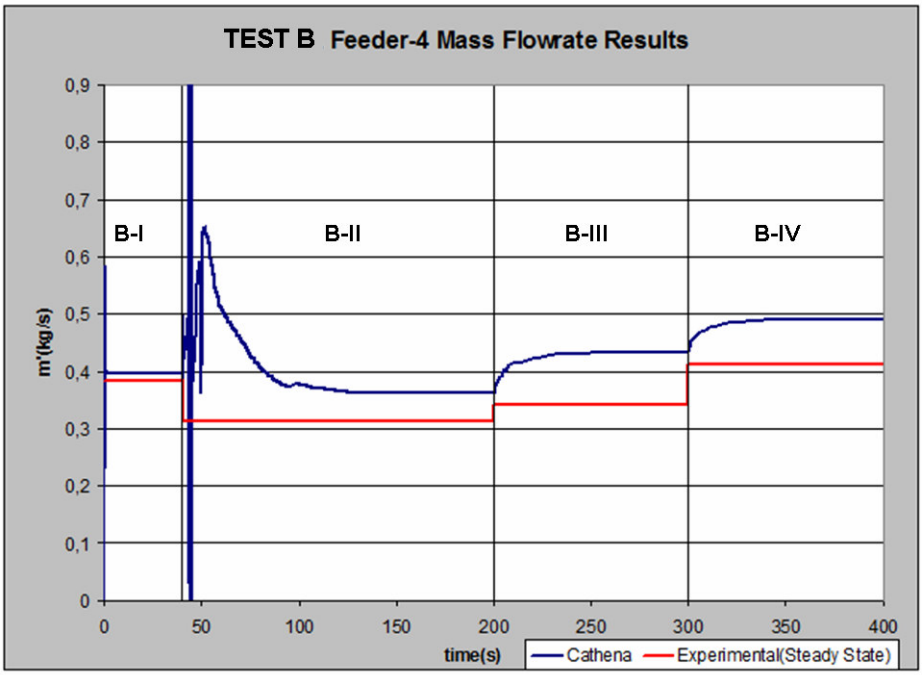

Figure 4.15 Test B Feeder-4 Two-Phase Mass Flow Rate

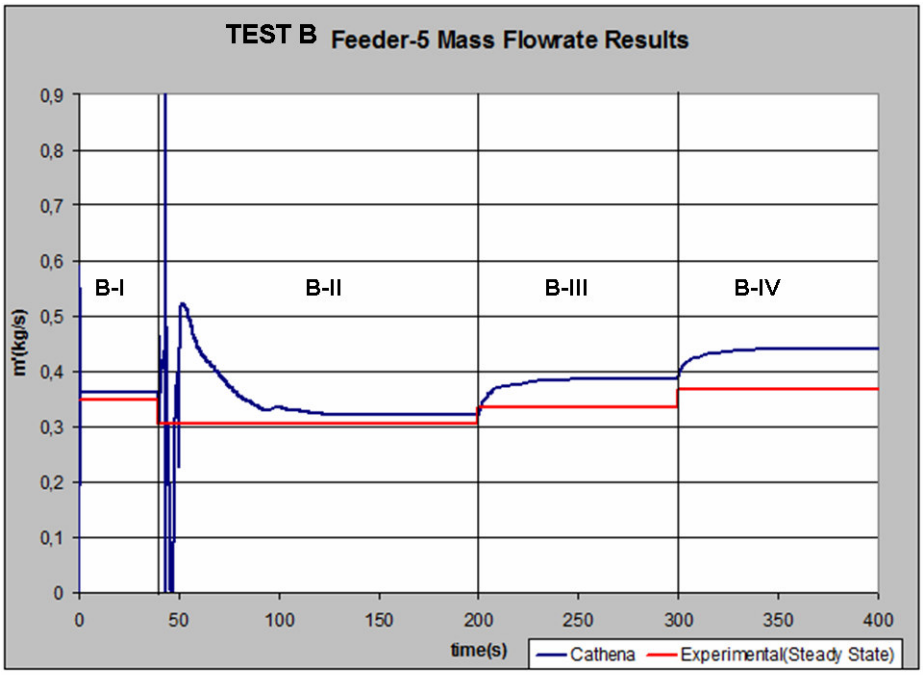

Figure 4.16 Test B Feeder-5 Two-Phase Mass Flow Rate

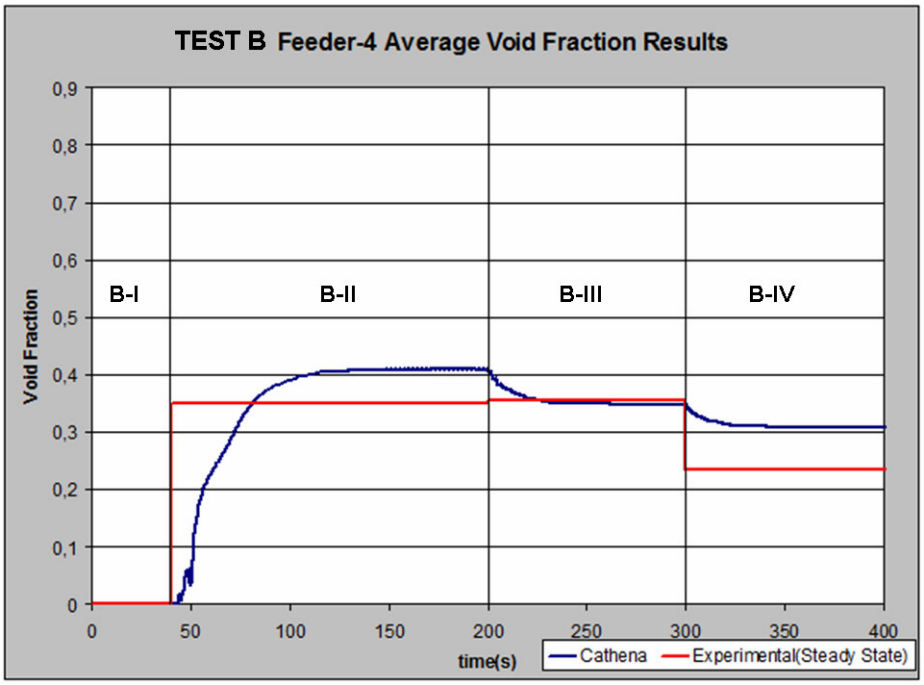

Figure 4.17 Test B Feeder-4 Average Void Fraction

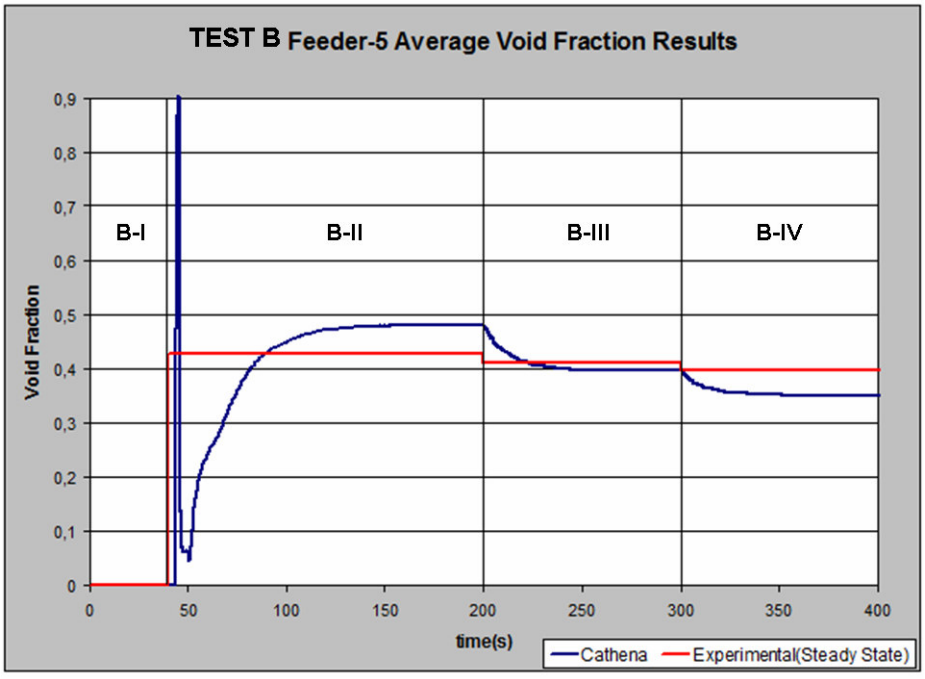

Figure 4.18 Test B Feeder-5 Average Void Fraction

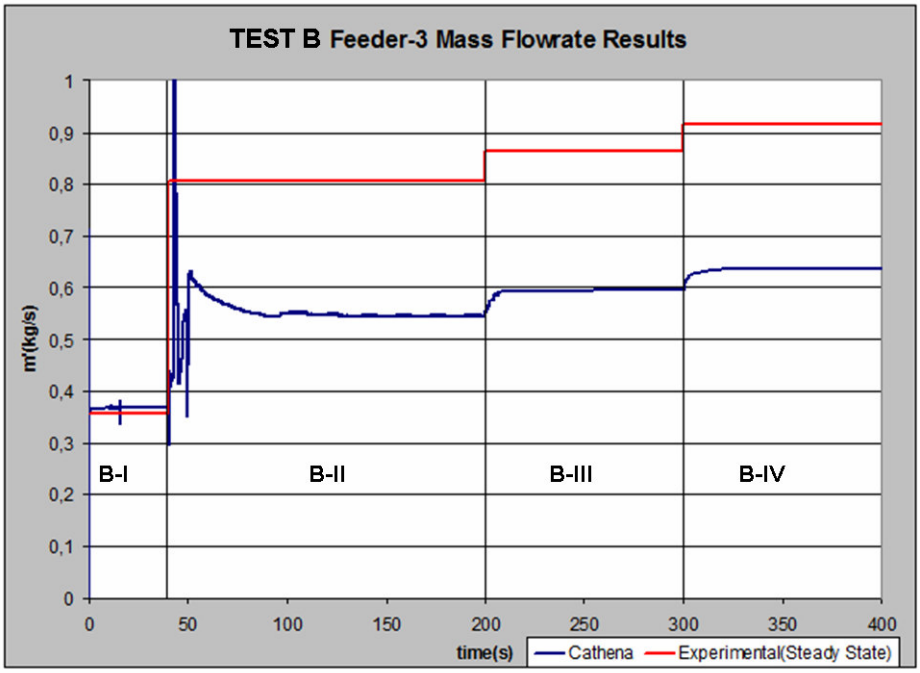

Figure 4.19 Test B Feeder-3 Mass Flow Rate

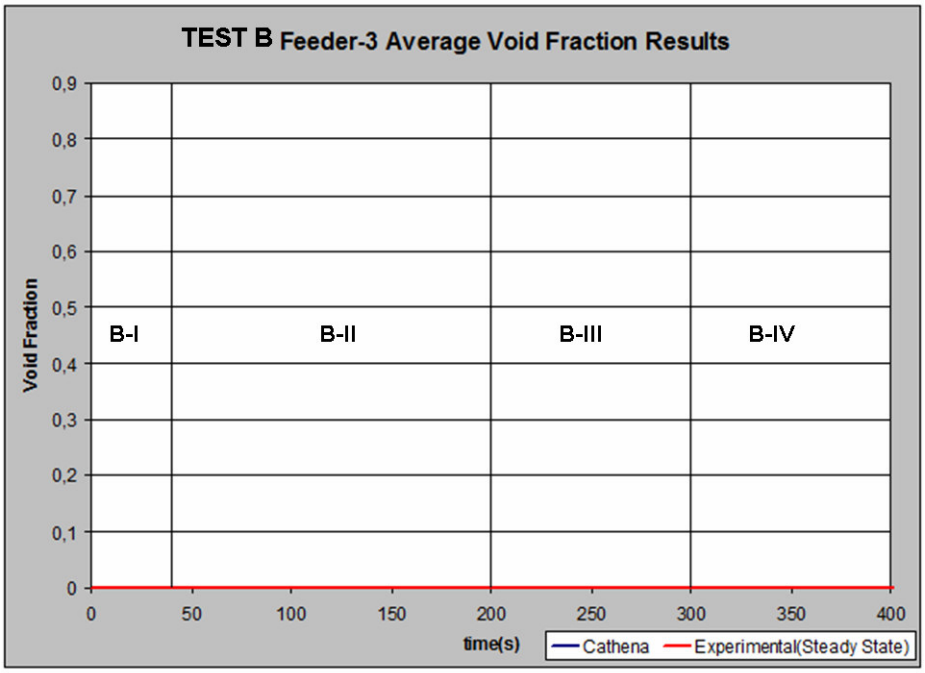

Figure 4.20 Test B Feeder-3 Average Void Fraction

4.2.2.3 TEST C Experimental and Computational Results

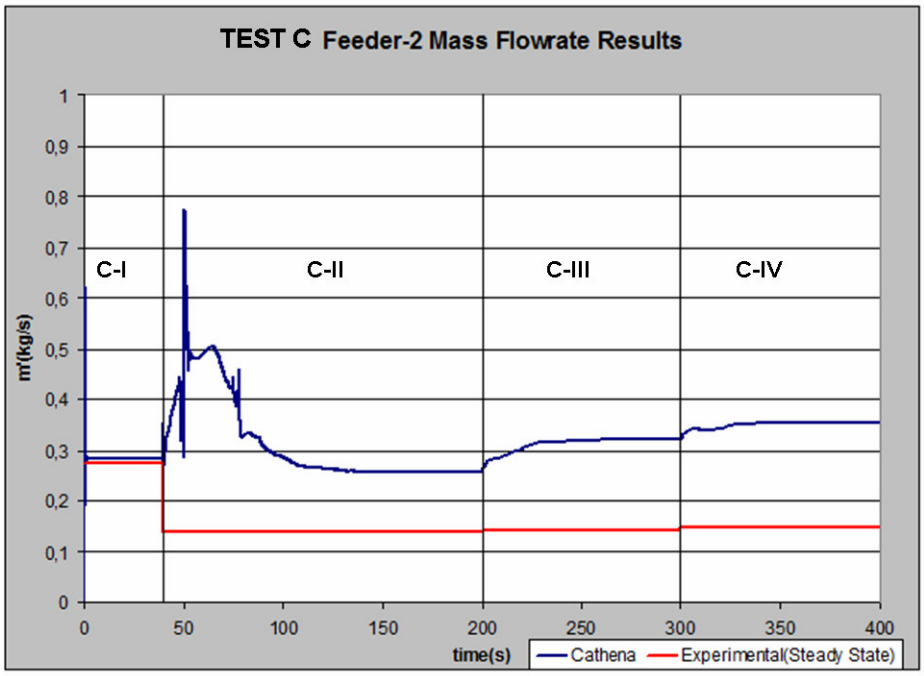

Figure 4.21 Test C Feeder-2 Two-Phase Mass Flow Rate

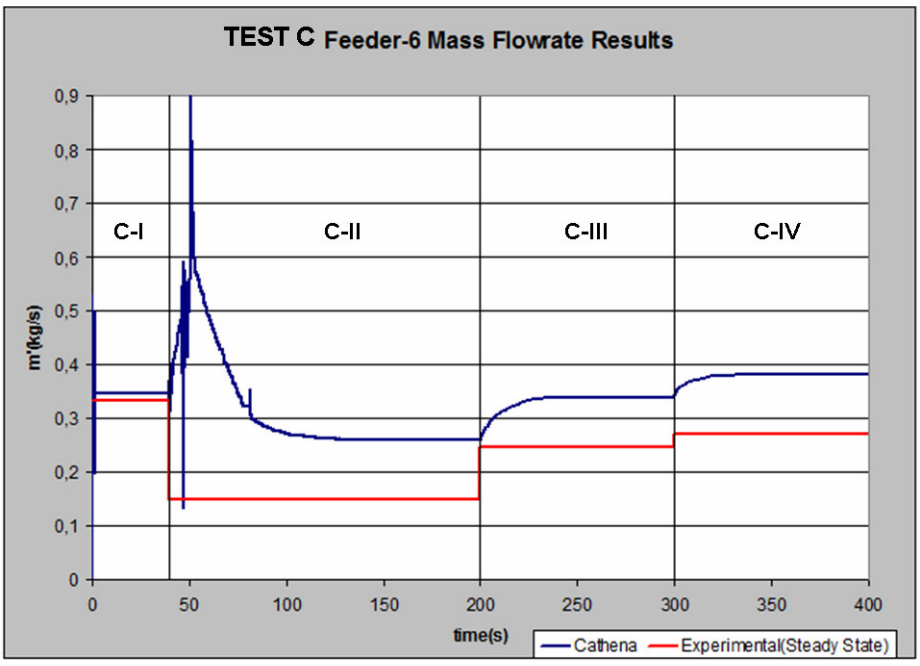

Figure 4.22 Test C Feeder-6 Two-Phase Mass Flow Rate

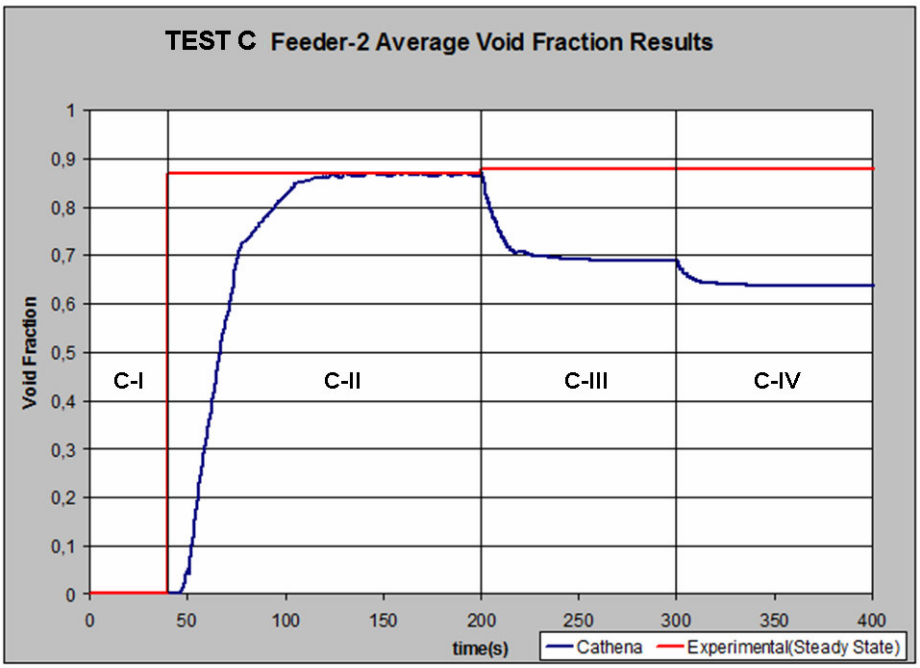

Figure 4.23 Test C Feeder-2 Average Void Fraction

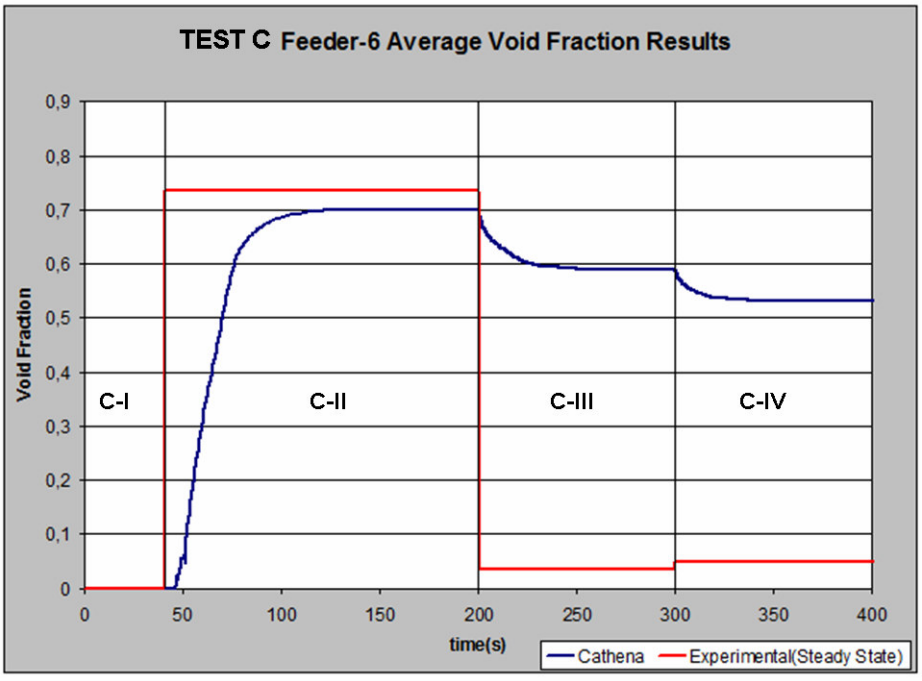

Figure 4.24 Test C Feeder-6 Average Void Fraction

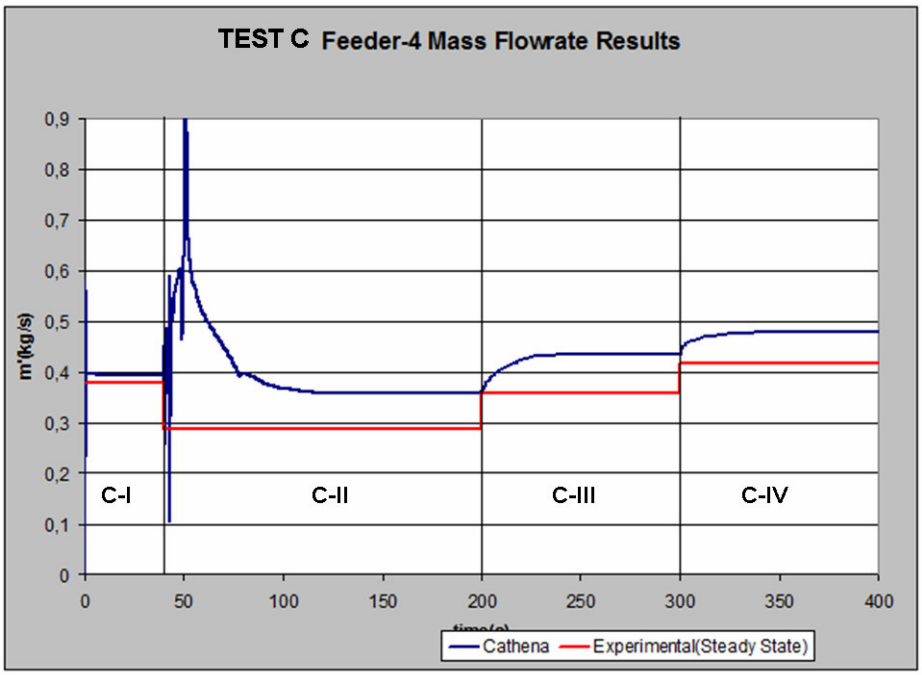

Figure 4.25 Test C Feeder-4 Two-Phase Mass Flow Rate

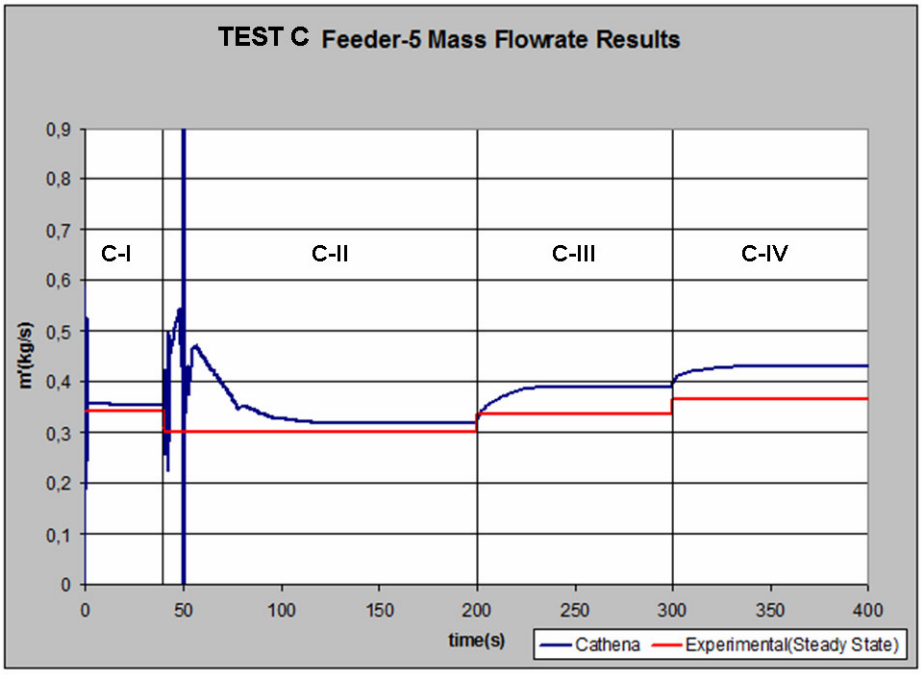

Figure 4.26 Test C Feeder-5 Two-Phase Mass Flow Rate

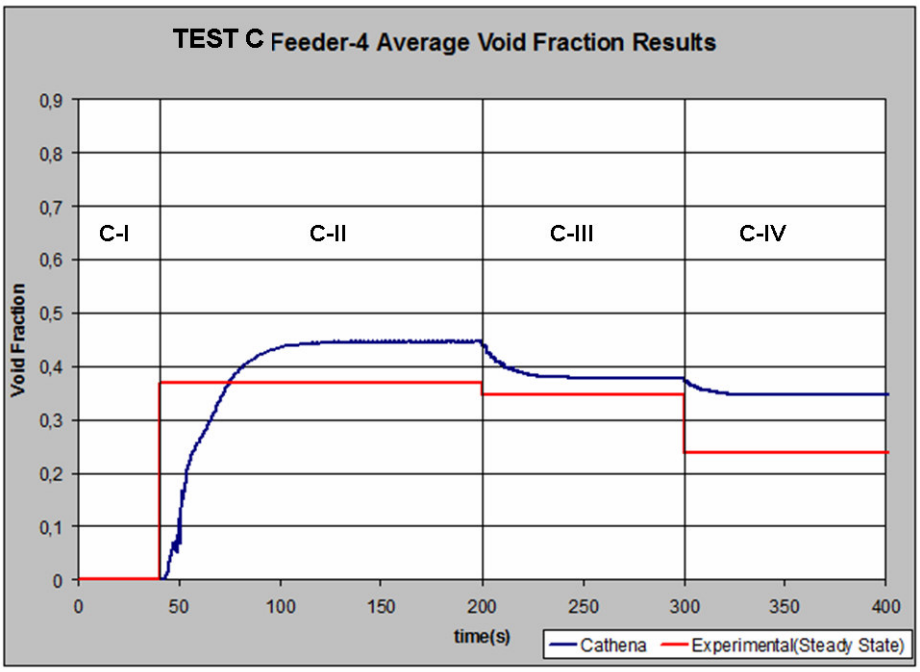

Figure 4.27 Test C Feeder-4 Average Void Fraction

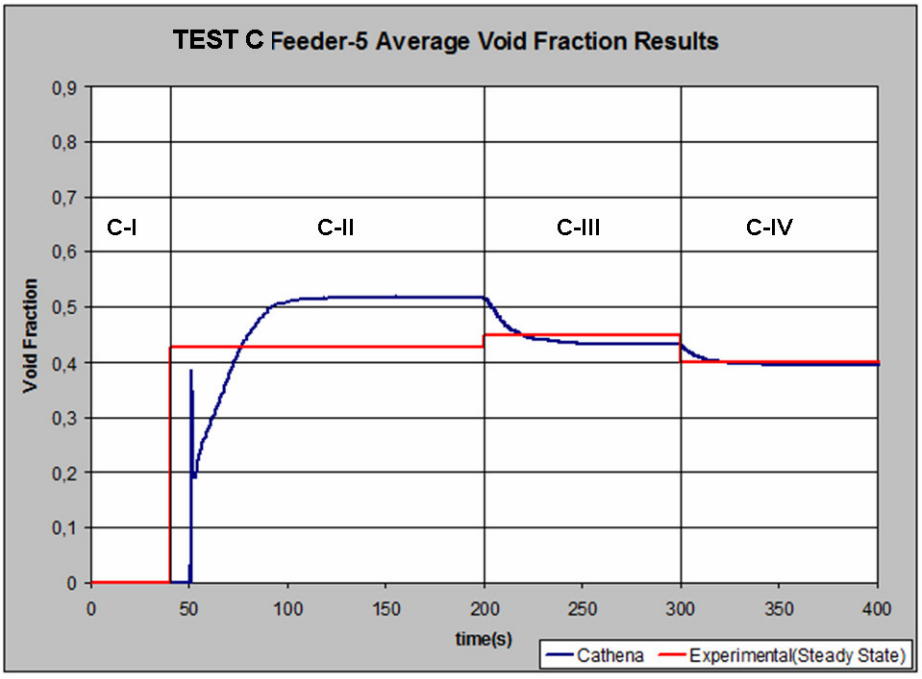

Figure 4.28 Test C Feeder-5 Average Void Fraction

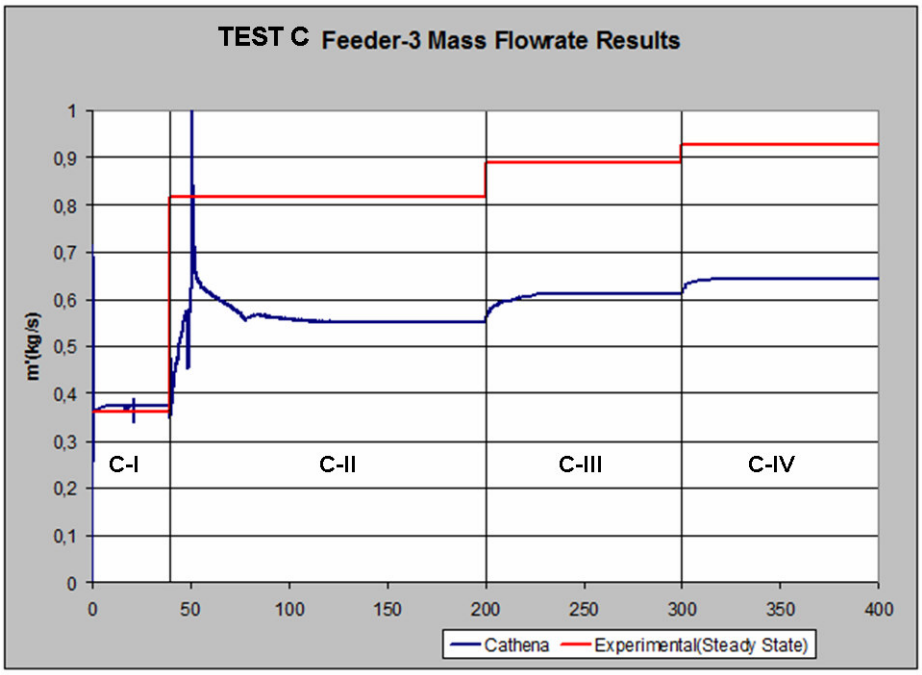

Figure 4.29 Test C Feeder-3 Mass Flow Rate

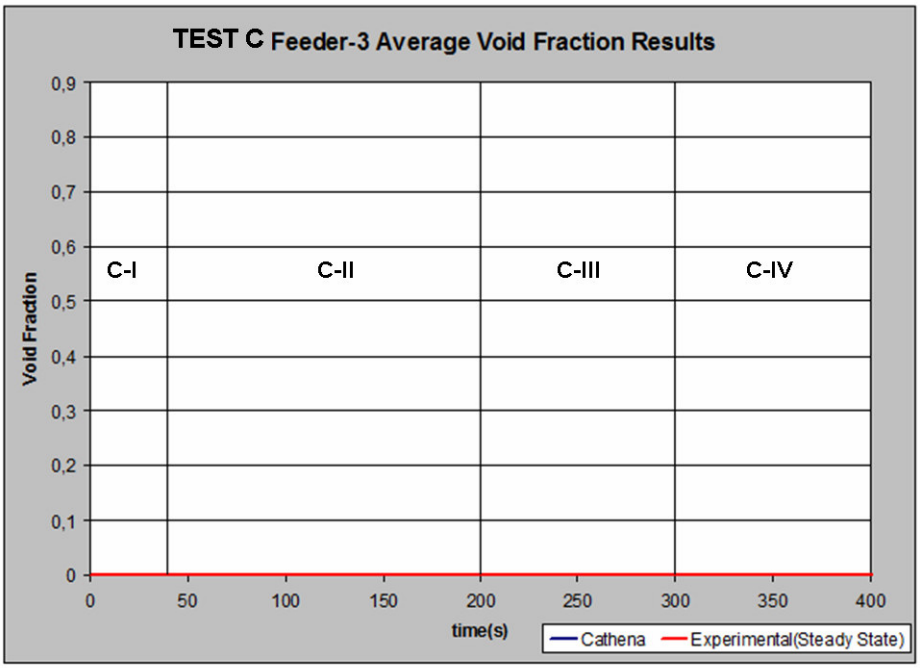

Figure 4.30 Test C Feeder-3 Average Void Fraction

4.3 Discussions and Conclusions

During the study, three sets of experiments were carried out in METU TPFTF. The test were named as Test A, B and C. The tests then, are simulated in a computer environment almost with the same conditions, such as inlet void fraction, inlet mass flow rate, ECI flow rate etc. This section represents the explanation and comparison of the results of experimental and computational.

The results given in the Tables 4.1 through 4.3 are steady state values for each test case for both experimental and computational studies. The graphs show the same test cases with time varying results. These graphs are direct outputs of CATHENA and fed with time variable behaviour to check out for the convergence to steady-state in the simulation and also for consistence between the experimental steady state results.

Throughout different tests (A, B, C), the inlet void fraction $\bar{\alpha}_{INLET}$ values were changed. The inlet water flowrate was tried to be kept at a constant level for a healthy comparison between the tests as well as the ECI flow rates. Thereby, in each test, the two-phase mass flowrate and average void fraction are measured or computed by CATHENA for each feeder.

According to the limitations of the test facility, the aforementioned inlet water flow rate values in each test were hardly kept constant throughout each case. Nevertheless the fluctuation on those values were limited at minimal degree.

In the following discussions, experimental and computational results are compared and comments are given :

- In both computational and experimental work, Feeder-3 never received air in any test cases.

- A sharp increase in the flow rate of Feeder-3 for Case II in every test (A, B, C) was not observed in CATHENA simulations. Anyhow, the increase in the normalized flow rates in Feeder-3 between all Case II and all Case I was maximum in CATHENA results, just like the experiments. Both in the experimental and computational study, there has always been a considerable water flow rate increase in Feeder-3, after air input.

- Feeder-2 and Feeder-6 in all computational and experimental tests, received the highest amount of void fraction rate. The main reason might be the exiting elevations of these feeders. The water level in the header in all of the two phase test cases, dropped down. Air which stayed on the top of water formed a stratified region in the header and this phenomenon forced the air to leak from the nearest feeder exit which was eventually the feeders with highest elevation (Feeder-2, 6). It is observed that the division of the air flow was actually dependent on how the water flow is distributed between Feeder-2 and Feeder-6. In the computational results, it is seen that more water flows though the feeder with a bigger orifice area on its valve, which is Feeder-6 among these two feeders. A higher amount of water flow is obtained in Feeder-6, while more void is observed in Feeder-2. The same phenomena is also observed in some of the experimental tests. In all of the tests except the Case II of Test A, Feeder-2 received more void while Feeder-6 received relatively a higher flow rate.

- In experimental results, it is seen that the ECI water introduction into the header decreased the void fraction in Feeder-6 considerably. The void fraction of Feeder-6 in Test A was decreased from 75.7% to 5%, in Test B it was decreased from 72.8% to 5% and in Test C it was decreased from 73.5% to 3.6% (See Table 4.1,4.2 and 4.3). A reason for such a sharp decrease observed in experiments might be the positions of the impedance probes on Feeder-6 and Feeder-2 which causes a possible misreading. The exiting pipe portions of these two feeders are horizontal, so a stratified flow is easily observed during low flow rates. At an instance like this, measuring tip of the

impedance probe is submerged in water while a considerable amount of air passes over the water region. In the CATHENA simulation results, this event could not be followed obviously but anyhow Feeder-6 still received the highest portion of the ECI water which is in agreement with the experimental results.

- The predictions of mass flowrate and the average void fraction by CATHENA for Feeder-4 and Feeder-5 seemed to be reasonable. The experimental results shows that (Fig. 4.5-4.8, Fig. 4.15-4.18, Fig.4.25-4.28) more water flow is directed into Feeder-4 while more void fraction is observed in Feeder-5 in nearly all of the test cases. This scheme could be seen in the computational study results in the aforementioned tables and graphs. The same phenomenon was also observed by Pezek[4] whose experimental study was also carried out in METU TPFTF. He reasoned this behaviour with the possibility of centrifugal force effects in the header. Same behaviour between Feeder-4 and Feeder-5 was also noted by Parrott[18] in the tests in RD-14M facility. The void and flow rate split into other feeders and the frictional loss effects through the feeders may be other explanations of this inequality between Feeder-4 and Feeder-5.

- In the computational study, when ECI water was introduced into the system, the void fraction in all feeders seemed to be decreasing. In some cases of the experimental study, the void fraction in some feeders did not decrease. As it is seen in Table 4.2 the void fraction in Feeder-2 in Test B Case II is 85.4%. With the ECI water, the void fraction increases to 92.6% which were not observed in the computational study.

- ECI water flow distribution between the feeders in the third and fourth cases of the tests can be shown in Table 4.4 and Table 4.5 as normalized flow rates:

Table 4.4 Experimental Results on Normalized Flow Rates of ECI in Case III and IV of all Tests

	Experimental Results on Normalized Flow Rates of ECI Water in Case III and IV of all Tests					
	A-III	**B-III**	**C-III**	**A-IV**	**B-IV**	**C-IV**
Feeder-2	0.344	*	0.055	*	0.070	0.076
Feeder-3	1.813	2.069	0.986	1.150	1.130	0.840
Feeder-4	1.000	1.000	1.000	1.000	1.000	1.000
Feeder-5	0.969	1.069	0.521	0.490	0.630	0.511
Feeder-6	3.469	3.379	1.342	0.890	1.160	0.931

* No increase in the flow rate. It was not normalized.

Table 4.5 Computational Results on Normalized Flow Rates of ECI in Case III and IV of all Tests

	CATHENA Results on Normalized Flow Rates of ECI Water in Case III and IV of all Tests					
	A-III	**B-III**	**C-III**	**A-IV**	**B-IV**	**C-IV**
Feeder-2	0.750	0.694	0.833	0.684	0.677	0.817
Feeder-3	0.706	0.681	0.744	0.701	0.700	0.767
Feeder-4	1.000	1.000	1.000	1.000	1.000	1.000
Feeder-5	0.941	0.931	0.923	0.940	0.915	0.925
Feeder-6	1.088	1.028	1.013	1.026	1.031	1.017

	CATHENA Results on Percentage Flow Rates of ECI Water in Case III and IV of all Tests					
	A-III(%)	**B-III(%)**	**C-III(%)**	**A-IV(%)**	**B-IV(%)**	**C-IV(%)**
Feeder-2	15.98	15.53	20.00	15.33	15.38	18.01
Feeder-3	15.04	15.22	17.84	15.71	15.91	16.91
Feeder-4	21.32	22.36	24.00	22.41	22.73	22.06
Feeder-5	20.06	20.81	22.15	21.07	20.80	20.40
Feeder-6	23.20	22.98	24.31	22.99	23.43	22.43

a. As seen from the Table 4.5, in CATHENA results, the ECI flow is distributed evenly when the average inlet void fraction is increased (from Test A to Test C)

b. In CATHENA results, Feeder-6 in all test cases seems to get more flow than other feeders (See Table 4.5). This was generally observed in the experimental study in A-III, B-III and C-III cases. In the fourth case of the experiments Feeder-6, Feeder-3 and Feeder-4 received approximately the same ECI flow rate.

c. If Feeder-4 and Feeder-5 normalized flow rates are compared in experimental study, it is seen that Feeder-4 utilizes from the ECI more than Feeder-5 does in every case except B-III. CATHENA results also follow the same behaviour.

4.4 Suggestions for Future Work

Present work can be extended with the following studies:

- Experimental tests covering a wider range may be done with multiple discharge conditions.

- For a better flow rate measurement, the calibration with the Neural Network might cover a higher number of calibration test points which would result in more accurate guesses, especially for two-phase flow cases.

- The impedance probes (which are used to measure the void fraction) on Feeder-2 and Feeder-6 are submerged in the horizontal pipe near the connection to the header. These two probes can be moved to the vertical pipe connected to the horizontal one which will reduce the amount of fluctuation in the pipe and eventually result in a more stable void fraction reading. Because when stratified flow regime is active in the feeders, the tip of the probe is submerged in the water flow, while actually a serious amount of air flows through the upper region. Also, in some flow conditions, annular flow was observed in Feeder-2 and Feeder-6. In this kind of a flow, the tip of the

probe stays in the air which generates a 100% void fraction voltage signal while a considerable amount of water flows over the peripherical surface of the feeder.

- The ECI line might be fed with a separate pump. This will provide a wider range of water flow rates in the experiments.

- A new pump with a higher flow rate capacity should be installed, which would provide making two-phase flow tests with lower inlet void fractions.

- A correlation between valve opening percentage and valve flow area should be defined.

- The design of the impedance probes might be developed so that a more stable void fraction reading can be obtained.

- The test results might be compared with other two-fluid codes like FLUENT, CFX etc.

REFERENCES

[1] B.N. Hanna, M.E. Lavack,and T.G. Beuthe, "AECL CATHENA MOD-3.5c/Rev 0 GENHTP Input Reference" , *COG-98-340-R1, AECL*, Dec 2000.

[2] B.N. Hanna, M.E. Lavack, and T.G. Beuthe,"CATHENA Input Manual MOD35c Rev0", *AECL COG-98-339-R1*, Dec. 2000.

[3] Cho Y.J., Jeun G.D., " Assessments of RELAP5/MOD3.2 and RELAP5/CANDU in a Reactor Inlet Header Break Experiment B9401 of RD-14M", *Journal of the Korean Nuclear Society, Volume 35, Number 5, pp.426-441,* Oct 2003.

[4] E. Pezek, "Numerical and Experimental Investigation of Two Phase Flow Distribution Through Multiple Outlets from a Horizontal Drum", *Ph.D Thesis, METU*, March 2006.

[5] Hosanoğlu, T., "Void Fraction Measurement in a Two-Phase Flow System With Impedance Probe Technique", *M.Sc. Thesis, METU*, Jan 2002.

[6] Hassan I.G., Soliman H.M, Sims G.E, Kowalski J.E, " Single and Multiple Discharge from a Stratified Two-Phase Region Through Small Branches", *Nuclear Engineering and Design,176, pp.233-245*,1997.

[7] H. Demuth, M. Beale, M. Hagan, "Neural Network Toolbox, for use with MATLAB", *Mathworks*, 2006.

[8] IAEA, "Analysis of Severe Accidents in Pressurized Heavy Water Reactors", *IAEA-TEC-DOC-1594*, June 2008.

[9] J.Y. Lee, G.S Hwang, M.Kim, H.C. NO, "Experimental analysis of off-take phenomena at the header–feeder system of CANDU", *Annals of Nuclear Energy 33 (2006) 1–12*, 2005.

[10] Kaya M.B., "Flow Rate Measurements in a Two Phase Flow System", *M.Sc. Thesis, METU*, Sept 2001.

[11] Kowalski, J.E. and Hanna, B.N., "Studies of Two-Phase Flow Distribution in a CANDU Type Header Feeder System", *Proceedings of the Fourth International Topical Meeting on Nuclear Reactor Thermalhyraulics, Karlsruhe, Germany, VOL 1, pp. 28-33*, October, 1989.

[12] Kowalski, J.E. and Krishnan, V.S., 'Two-Phase Fiow Distribution from a Large Manifold", *AIChE Annual Meeting, New York*, November 15-20, 1987.

[13] Lamari M.L., "An Experimental Investigation of Two-Phase (Air-water) Flow Regimes in a Horizontal Tube at Near Atmospheric Conditions", *Ph.D Thesis, Carleton University,Ottawa*, May 2001.

[14] Lee S., Kim M., "RELAP5 Simulation of the Small Inlet Header Break Test B8604 Conducted in the RD-14M Test Facility", *Journal of the Korean Nuclear Society, Volume 32, Number 1, pp.57-66*, Feb 2000.

[15] Malayeri M.R., Steinhagenier H.M., Smith J.M., "Neural Network Analysis of Void Fraction in Air/Water Two-Phase Flows At Elevated Temperatures", *Chemical Engineering and Processing, 42, pp. 587-597*, 2003.

[16] N.H. Kim, S.P Han, "Distribution of air–water annular flow in a header of a parallel flow heat exchanger", *International Journal of Heat and Mass Transfer 51 (2008) pp. 977–992*, Aug 2007

[17] Osakabe M.,Hamada T., Hiroki S., "Water Flow Distribution in Horizontal Header Contaminated with Bubbles", *International Journal of Multiphase Flow, 25, pp.827-840*, 1999.

[18] S.D Parrott, "WPIR 1503: Draft Report on Characterization of Flow and Phase Distribution in an RD-14M Inlet Header Under Two-Phase Steam-Water Conditions", *AECL Memo STHB-99-033*,Mar 1999.

[19] Song C.H., Chung M.K., No H.C. "Measurements of Void Fraction by An Improved Multi-Channel Conductance Void Meter", *Nuclear Engineering and Design, 184, pp.269-285*, 1998.

[20] T.G. Beuthe, B.N. Hanna "COG-00-00 Theory_Mod35cr0", *AECL*, Nov 2000.

[21] Yonomoto, T. and Tasaka, K., "New Theoretical Model for Two-Phase Flow Discharged from Stratified Two-Phase Region through Small Break", *Journal of Nuclear Science and Technology, Vol. 25, pp. 441-455*, 1988.

[22] Z. Teclemariam,"Two-Phase (Gas- Liquid) Flow Distribuiton in the Outlet Bracnhes of a Horizontal Multi-Branch Header", *M.Sc. Thesis, University of Manitoba*, 2000.

[23] Z. Teclemariam, Soliman H.M., Sims G.E., Kowalski J.E, "Experimental Investigation of Two-Phase Flow Distribution in the Outlets of a Horizontal Multi-Branch Header", *Nuclear Engineering and Design , 222, pp. 29-39*, 2003

[24] T. Beuthe, B.N Hanna, "COG-00-008 Theory_Mod35cr0", *COG*, November 2000

[25] Taylor, J. R., "An Introduction To Error Analysis: The Study of Uncertainties In Physical Measurements", *University Science Books, Mill Valley, California*, 1982.

APPENDIX A

Specifications of the Test Setup Instrumentation

A.1 Water Circulation Pump

Manufacturer……: WILO

Type……..: Multi-stage normal suction, horizontal, high pressure centrifugal pump.

Supply Voltage….: 1~200 V (± 10%) / 50 Hz

Fluid Temperature…: -15 ^{o}C to 110 ^{o}C with gaskets- EPDM,

-15 ^{o}C to 80 ^{o}C version with gaskets- VITON

Max. Permissible Working Pres..: 10 Bar

Max. Permissible Inlet Pres…….: 6 Bar

Max. Flow Rate : 8 m^3 / hr

Max. ambient temperature…….: 40 ^{o}C

A.2 Air Compressor

Manufacturer……: KOMSAN KOMPRESÖR

Type……..: T-175 KDT-15

Number of Cylinder……..: 1

Tank Volume …...…….: 100 liter

Stroke Volume…….: 216 lt/min

Motor Power……..……: 1.5 kW

Revolution……..……: 700 rpm

Operating Pressure…….…: 15 kgf/ cm2

Piston Displacement……...: 13 m3/h

Max. Pressure…….....: 10 kg/cm2

Weight……....: 110 kg

A.3 Pressure Gage

Manufacturer: PAKKENS

Type: Bourdon Gage

Measuring Range: 0 - 2.5 Bar

Sensitivity: 0.05 Bar

Working Medium: Liquid/gas/steam

A.4 Temperature Gage

Manufacturer: PAKKENS LTD. ŞTİ.

Measuring Range: 0 – 120 °C

Sensitivity: 2 °C

A.5 Turbine Type Flowmeter

Manufacturer: CHEMLINE PLASTIC

Model: 2110 TM & 110 TM

Supply Voltage: 12 - 24 V DC

Output: 4 to 20 mA, load resistance < 500 ohm

Velocity Range: 0.15 - 10 m/sec

Electrical Connection: 4 pole, DIN 43650,NEMA 4X

Accuracy: ±1% over calibrated flow rate range

Repeatability: ±0.5% over calibrated flow rate range

Linearity: ±1% over calibrated flow rate range

Viscosity Range: 0.5 - 20 cST (outside this range transmitter needs recalibration)

Working Medium: Liquids only

A.6 Pressure Transducer

Manufacturer: OMEGA

Model: PX 605-100 GI

Supply Voltage: 24 V DC (10 - 30 V DC)

Output: 4 - 20 mA (2 wire)

Max. Loop Resistance: $50\times(\text{supply voltage}-10)\,\Omega$

Accuracy: ±0.4% at full scale

Storage Temperature: -65°F to 250°F (-53 °C to 121 °C)

Operating Temperature: -20° to 180°F (-28 °C to 82 °C)

Compensated Temperature: -20° to 160°F (-28 °C to 71 °C)

Thermal Effect: (zero) ±0.04% full scale/ F

(span) ±0.04% full scale/ F

Proof Pressure: 15 - 2000 psi = 200 % full scale

3000 - 5000 psi=150% full scale

500 - 20000 psi=120% full scale

Burst Pressure: 15 - 2000 psi=800% full scale

3000 – 5000 psi=300% full scale

7500 - 20000 psi=150% full scale

Response Time: 1 ms.

Working Medium: Liquid/gas/steam

A.7 Differential Pressure Transmitter I

Manufacturer: OMEGA

Model: PX 711-100WDI

Output: 4 - 20 mA DC output corresponding 1 - 5 V DC through 250 ohm load resistor

Max. Pressure Range: 0 - 100 inch H_2O

Min. Pressure Range: 0 - 17 inch H_2O

Supply Voltage: 24 V DC nominal

12.5 V DC min. at transmitter

15.25 V DC min. with digital meter option

36 V DC max. at transmitter

42 V DC with external load specified

Reverse polarity protection provided

Accuracy: (Includes independent linearity, hysteresis and repeatability)

±0.15 % of calibrated span

Working Pressure: 2000 psi

Working Medium: Liquid/gas/steam

A.8 Differential Pressure Transmitter II

Manufacturer: OMEGA

Model: PX 771-100DI

Output: 4 - 20 mA DC output corresponding 1 - 5 V DC through 250 ohm load resistor

Max. Pressure Range: 0 - 100 psi

Min. Pressure Range: 0 - 17 psi

Supply Voltage: 24 V DC nominal

12.5 V DC min. at transmitter

15.25 V DC min. with digital meter option

36 V DC max. at transmitter

42 V DC with external load specified

Reverse polarity protection provided.

Accuracy: (Includes independent linearity, hysteresis and repeatability)

±0.15 % of calibrated span

Working Pressure: 2000 psi

Working Medium: Liquid/gas/steam

A.9 Multilab Digital and Analog I/O Card

Manufacturer: ADVANTECH

Type: PCL-812 PG

Analog Input Channels: 16 single-ended.

A/D Converter: 12-bit, 25 μsec. conversion time

Analog Input Range: ±(10,5,2.5,1.25,0.625,0.3125)

Analog Trigger Mode: Software, pacer or external trigger

Data Transfer: Program controlled, interrupt 2~7, 9~12, 14, 15 or DMA (Channel 1 or 3) for

Accuracy: 0.01% of reading ±1 bit

Input Impedance: >100 MΩ

Overvoltage: Continuous ±30 V DC max.

Analog Output Channels: Two doubled buffered 12-bit channels

D/A range (in V): 0~5, 0~10 w/internal reference; ±10 V max. with external AC or DC reference (accuracy for output above ±9V may vary depending on power supply used)

Settling Time: 30 μsec.

Output Current: ±5 mA max.

Linearity: ±1/2 bit

Digital Input Channels: 16, TTL level

Digital Output Channels: 16, TTL compatible

Counter: One 16-bit counter with a 20 MHz. time base

Power Consumption: +5V@500 mA typical,1.0 A max.

+12 V@ 50 mA typical ,100 mA max.

-12 V@ 14 mA typical, 20 mA max.

Operating Temperature: 0~50^{o}C (32~122^{o}F)

I/O Ports: 16 consecutive bytes

Connectors: Two 20-pin flat-cable connectors

Dimensions: 185× 100 mm

A.10 Amplifier and Multiplexer Board

Manufacturer……..……: ADVANTECH

Type……..……..: PCLD-789D

Input Channels……..…..: 16 differential

Input Range…….....: ± 10 V max., depending on selected gain

Output Range……..: ± 10 V max.

Overvoltage Protection……...: ± 30 V continuous

Cold-junction Compensation..: +24.4 mV/^{o}C, 0 V at 0^{o}C

Power Consumption…….....: +5 V @ 10 mA maximum

+12 V @ 80 mA maximum

Connectors For D/A buses…...: One DB-37 connector , two 20-pin flat cable connectors for daisy chaining

Dimensions……: 205 mm × 114 mm

APPENDIX B

CATHENA Input Text

The following input text is for the conditions of TEST A of the study.

```
'METU-TEST-FACILITY CATHENA MODEL',
'First trial run'/
'CONTROL PARAMETERS'/<<<<<<<<<<<<<<<<<<<<<<<<<<<<<<<<<<<<<<<<<<<<<<<<<<<<<<<<<<<<
'**  TEST DESCRIPTION **'/
'*   '/
'*   TEST A: Simulation of the Effect of Emergency Coolant Injection' /
'*   During a LOCA in a CANDU Inlet Header'/
'*   '/
'PRINT CONTROL'/
2*1.,,,,,,'A'/
'PROCESSING OPTION'/
'RUN'/
'NUMERIC OPTIONS'/
'#-PRESS-LOW(-150000)','#-HG-LOW(-150000)','#-TSTM-NE-TNC(-1500000)','#-HF-LOW(-
150000)','#-HG-HIGH(-150000)','#-PRESS-HIGH(-150000)','#-HF-HIGH(-150000)','#-VEL-HIGH(-
150000)'/
'RESTART CONTROL'/
,'C:/CAT/METU.RST',,1.,,,'C','C'/
'SOLUTION CONTROL'/
0.0,10000.,,,,0.03/
'END'/
'COMPONENTS'/<<<<<<<<<<<<<<<<<<<<<<<<<<<<<<<<<<<<<<<<<<<<<<<<<<<<<<<<<<<<<<<<
'PIPE11',0.4181  ,0.0     ,4.763E-3,0.0778764,4.0E-6,5.,'CIRC',2,'H2O,AIR',,,'FIX-MIXED'/
'PIPE12',0.18583 ,0.117847,4.763E-3,0.0778764,4.0E-6,5.,'CIRC',1,'H2O,AIR',,,'FIX-MIXED'/
'PIPE13',0.386313,0.386313,4.763E-3,0.0778764,4.0E-6,5.,'CIRC',1,'H2O,AIR',,,'FIX-MIXED'/
'HDR1',0.0386,0.0,0.02946,0.193675,4.0E-6,5.,'CIRC',1,'H2O,AIR',,,'FIX-MIXED'/
'HDR2',0.1361,0.0,0.02946,0.193675,4.0E-6,5.,'CIRC',3,'H2O,AIR',,,'FIX-MIXED'/
'HDR3',0.2000,0.0,0.02946,0.193675,4.0E-6,5.,'CIRC',4,'H2O,AIR',,,'FIX-MIXED'/
'HDR4',0.2503,0.0,0.02946,0.193675,4.0E-6,5.,'CIRC',5,'H2O,AIR',,,'FIX-MIXED'/
```

'HDR5',0.1560,0.0,0.02946,0.193675,4.0E-6,5.,'CIRC',3,'H2O,AIR',,,'FIX-MIXED'/
'HDR6',0.3190,0.0,0.02946,0.193675,4.0E-6,5.,'CIRC',6,'H2O,AIR',,,'FIX-MIXED'/
'PIPE61',0.715163,0.0 ,5.067075E-4,0.0254,4.0E-6,5.,'CIRC',2,'H2O,AIR',,,'FIX-MIXED'/
'PIPE62',0.813 ,-0.813,5.067075E-4,0.0254,4.0E-6,5.,'CIRC',2,'H2O,AIR',,,'FIX-MIXED'/
'PIPE63',0.97 ,0.0 ,5.067075E-4,0.0254,4.0E-6,5.,'CIRC',2,'H2O,AIR',,,'FIX-MIXED'/
'PIPE64',0.532 ,-0.532,5.067075E-4,0.0254,4.0E-6,5.,'CIRC',2,'H2O,AIR',,,'FIX-MIXED'/
'PIPE65',1.51 ,0.0 ,5.067075E-4,0.0254,4.0E-6,5.,'CIRC',2,'H2O,AIR',,,'FIX-MIXED'/
'PIPE66',0.337 ,0.0 ,5.067075E-4,0.0254,4.0E-6,5.,'CIRC',2,'H2O,AIR',,,'FIX-MIXED'/
'PIPE67',0.445 ,-0.445,5.067075E-4,0.0254,4.0E-6,5.,'CIRC',1,'H2O,AIR',,,'FIX-MIXED'/
'PIPE31',0.56 ,0.5329,9.3482E-4,0.0345,4.0E-6,5.,'CIRC',2,'H2O,AIR',,,'FIX-MIXED'/
'PIPE32',0.644 ,0.644 ,9.3482E-4,0.0345,4.0E-6,5.,'CIRC',2,'H2O,AIR',,,'FIX-MIXED'/
'PIPE33',2.686 ,0.0 ,9.3482E-4,0.0345,4.0E-6,5.,'CIRC',3,'H2O,AIR',,,'FIX-MIXED'/
'PIPE34',0.653 ,0.0 ,9.3482E-4,0.0345,4.0E-6,5.,'CIRC',1,'H2O,AIR',,,'FIX-MIXED'/
'PIPE35',0.152 ,0.152 ,9.3482E-4,0.0345,4.0E-6,5.,'CIRC',1,'H2O,AIR',,,'FIX-MIXED'/
'PIPE36',2.1687,0.0 ,9.3482E-4,0.0345,4.0E-6,5.,'CIRC',3,'H2O,AIR',,,'FIX-MIXED'/
'PIPE37',0.369 ,0.369 ,9.3482E-4,0.0345,4.0E-6,5.,'CIRC',1,'H2O,AIR',,,'FIX-MIXED'/
'PIPE51',0.6245144,-0.36708,5.067075E-4,0.0254,4.0E-6,5.,'CIRC',2,'H2O,AIR',,,'FIX-MIXED'/
'PIPE52',0.997 ,-0.997 ,5.067075E-4,0.0254,4.0E-6,5.,'CIRC',2,'H2O,AIR',,,'FIX-MIXED'/
'PIPE53',1.537 ,0.0 ,5.067075E-4,0.0254,4.0E-6,5.,'CIRC',2,'H2O,AIR',,,'FIX-MIXED'/
'PIPE54',1.203 ,0.0 ,5.067075E-4,0.0254,4.0E-6,5.,'CIRC',2,'H2O,AIR',,,'FIX-MIXED'/
'PIPE55',0.369 ,-0.369 ,5.067075E-4,0.0254,4.0E-6,5.,'CIRC',1,'H2O,AIR',,,'FIX-MIXED'/
'PIPE41',0.6245144,0.36708,5.067075E-4,0.0254,4.0E-6,5.,'CIRC',1,'H2O,AIR',,,'FIX-MIXED'/
'PIPE42',0.541 ,0.541 ,5.067075E-4,0.0254,4.0E-6,5.,'CIRC',2,'H2O,AIR',,,'FIX-MIXED'/
'PIPE43',1.306 ,0.0 ,5.067075E-4,0.0254,4.0E-6,5.,'CIRC',2,'H2O,AIR',,,'FIX-MIXED'/
'PIPE44',0.555 ,0.0 ,5.067075E-4,0.0254,4.0E-6,5.,'CIRC',1,'H2O,AIR',,,'FIX-MIXED'/
'PIPE45',0.456 ,0.456 ,5.067075E-4,0.0254,4.0E-6,5.,'CIRC',1,'H2O,AIR',,,'FIX-MIXED'/
'PIPE46',1.0054 ,0.0 ,5.067075E-4,0.0254,4.0E-6,5.,'CIRC',2,'H2O,AIR',,,'FIX-MIXED'/
'PIPE47',0.369 ,0.369 ,5.067075E-4,0.0254,4.0E-6,5.,'CIRC',1,'H2O,AIR',,,'FIX-MIXED'/
'PIPE21',0.715163,0.0 ,9.3482E-4,0.0345,4.0E-6,5.,'CIRC',1,'H2O,AIR',,,'FIX-MIXED'/
'PIPE22',0.813 ,0.813,9.3482E-4,0.0345,4.0E-6,5.,'CIRC',1,'H2O,AIR',,,'FIX-MIXED'/
'PIPE23',2.206 ,0.0 ,9.3482E-4,0.0345,4.0E-6,5.,'CIRC',3,'H2O,AIR',,,'FIX-MIXED'/
'PIPE24',0.885 ,0.0 ,9.3482E-4,0.0345,4.0E-6,5.,'CIRC',2,'H2O,AIR',,,'FIX-MIXED'/
'PIPE25',0.608 ,0.608,9.3482E-4,0.0345,4.0E-6,5.,'CIRC',1,'H2O,AIR',,,'FIX-MIXED'/
'PIPE26',2.53355 ,0.0 ,9.3482E-4,0.0345,4.0E-6,5.,'CIRC',3,'H2O,AIR',,,'FIX-MIXED'/
'PIPE27',0.369 ,0.369,9.3482E-4,0.0345,4.0E-6,5.,'CIRC',1,'H2O,AIR',,,'FIX-MIXED'/
'RSVTANK2',,,,,,,,,'H2O,AIR'/
'RSVTANK3',,,,,,,,,'H2O,AIR'/
'RSVTANK4',,,,,,,,,'H2O,AIR'/

'RSVTANK5',,,,,,,,,'H2O,AIR'/
'RSVTANK6',,,,,,,,,'H2O,AIR'/
'RSVMIX',,,,,,,,,'H2O'/
'RSVMIX2',,,,,,,,,'H2O,AIR'/
'RSVECI',,,,,,,,,'H2O'/
'END'/
'CONNECTIONS'/<<<<<<<<<<<<<<<<<<<<<<<<<<<<<<<<<<<<<<<<<<<<<<<<<<<<<<<<
'RSVECI','R-HDR1','FIX-MIXED'/
'L-HDR1','R-HDR2','FIX-MIXED'/
'L-HDR2','R-HDR3','FIX-MIXED'/
'L-HDR3','R-HDR4','FIX-MIXED'/
'L-HDR4','R-HDR5','FIX-MIXED'/
'L-HDR5','R-HDR6','FIX-MIXED'/
'L-HDR6'/
'RSVMIX','R-PIPE11','FIX-MIXED'/
'RSVMIX2','R-PIPE11','FIX-MIXED'/
'L-PIPE11','R-PIPE12','FIX-MIXED'/
'L-PIPE12','R-PIPE13','FIX-MIXED'/
'L-PIPE13','R-HDR3','FIX-MIXED'/
'L-HDR4','L-PIPE61','FIX-MIXED'/
'R-PIPE61','L-PIPE62','FIX-MIXED'/
'R-PIPE62','L-PIPE63','FIX-MIXED'/
'R-PIPE63','L-PIPE64','FIX-MIXED'/
'R-PIPE64','L-PIPE65','FIX-MIXED'/
'R-PIPE65','L-PIPE66','FIX-MIXED'/
'R-PIPE66','L-PIPE67','FIX-MIXED'/
'R-PIPE67','RSVTANK6','FIX-MIXED,CHOKED=HOMOG'/
'L-HDR3','R-PIPE31','FIX-MIXED'/
'L-PIPE31','R-PIPE32','FIX-MIXED'/
'L-PIPE32','R-PIPE33','FIX-MIXED'/
'L-PIPE33','R-PIPE34','FIX-MIXED'/
'L-PIPE34','R-PIPE35','FIX-MIXED'/
'L-PIPE35','R-PIPE36','FIX-MIXED'/
'L-PIPE36','R-PIPE37','FIX-MIXED'/
'L-PIPE37','RSVTANK3','FIX-MIXED,CHOKED=HOMOG'/
'R-HDR3','L-PIPE51','FIX-MIXED'/
'R-PIPE51','L-PIPE52','FIX-MIXED'/
'R-PIPE52','L-PIPE53','FIX-MIXED'/

```
'R-PIPE53','L-PIPE54','FIX-MIXED'/
'R-PIPE54','L-PIPE55','FIX-MIXED'/
'R-PIPE55','RSVTANK5','FIX-MIXED,CHOKED=HOMOG'/
'R-HDR3','R-PIPE41','FIX-MIXED'/
'L-PIPE41','R-PIPE42','FIX-MIXED'/
'L-PIPE42','R-PIPE43','FIX-MIXED'/
'L-PIPE43','R-PIPE44','FIX-MIXED'/
'L-PIPE44','R-PIPE45','FIX-MIXED'/
'L-PIPE45','R-PIPE46','FIX-MIXED'/
'L-PIPE46','R-PIPE47','FIX-MIXED'/
'L-PIPE47','RSVTANK4','FIX-MIXED,CHOKED=HOMOG'/
'L-HDR4','R-PIPE21','FIX-MIXED'/
'L-PIPE21','R-PIPE22','FIX-MIXED'/
'L-PIPE22','R-PIPE23','FIX-MIXED'/
'L-PIPE23','R-PIPE24','FIX-MIXED'/
'L-PIPE24','R-PIPE25','FIX-MIXED'/
'L-PIPE25','R-PIPE26','FIX-MIXED'/
'L-PIPE26','R-PIPE27','FIX-MIXED'/
'L-PIPE27','RSVTANK2','FIX-MIXED,CHOKED=HOMOG'/
'END'/
'BOUNDARY CONDITIONS'/<<<<<<<<<<<<<<<<<<<<<<<<<<<<<<<<<<<<<<<<<<<<<<<<
'RESERVOIR B.C.','BC1'/
'RSVMIX'/
0.101E6,24.,24.,0.0,'HG-BY-TEMP','HF-BY-TEMP'/
'RESERVOIR B.C.','BC0'/
'RSVMIX2'/
0.151E6,24.,24.,1.0,1.0,'HG-BY-TEMP','HF-BY-SAT'/
'RESERVOIR B.C.','BCECI'/
'RSVECI'/
0.101E6,24.,24.,0.0,'HG-BY-TEMP','HF-BY-TEMP'/
'FLOW B.C.','FLWMIX'/
'RSVMIX','R-PIPE11'/
1.748/
'FLOW B.C.','FLWMIX2'/
'RSVMIX2','R-PIPE11'/
0.0/
'FLOW B.C.','FLWECI'/
'RSVECI','R-HDR1'/
```

```
0.0/
'RESERVOIR B.C.','BC2'/
'RSVTANK2'/
0.101E6,24.,24.,0.99,1.0,'HG-BY-TEMP','HF-BY-TEMP'/
'RESERVOIR B.C.','BC3'/
'RSVTANK3'/
0.101E6,24.,24.,0.99,1.0,'HG-BY-TEMP','HF-BY-TEMP'/
'RESERVOIR B.C.','BC4'/
'RSVTANK4'/
0.101E6,24.,24.,0.99,1.0,'HG-BY-TEMP','HF-BY-TEMP'/
'RESERVOIR B.C.','BC5'/
'RSVTANK5'/
0.101E6,24.,24.,0.99,1.0,'HG-BY-TEMP','HF-BY-TEMP'/
'RESERVOIR B.C.','BC6'/
'RSVTANK6'/
0.101E6,24.,24.,0.99,1.0,'HG-BY-TEMP','HF-BY-TEMP'/
'END'/
'SYSTEM MODELS'/<<<<<<<<<<<<<<<<<<<<<<<<<<<<<<<<<<<<<<<<<<<<<<<<<<<<<<<<<<<<
'VALVE','VALVE6'/
'R-PIPE65','L-PIPE66'/
5.067075E-4,0.6,1.0,/
'VALVE','VALVE3'/
'L-PIPE33','R-PIPE34'/
9.3482E-4,0.6,1.0,/
'VALVE','VALVE5'/
'R-PIPE53','L-PIPE54'/
5.067075E-4,0.6,1.0,/
'VALVE','VALVE4'/
'L-PIPE43','R-PIPE44'/
5.067075E-4,0.6,1.0,/
'VALVE','VALVE2'/
'L-PIPE23','R-PIPE24'/
9.3482E-4,0.6,1.0,/
'END'/
'SYSTEM  CONTROL
MODELS'/<<<<<<<<<<<<<<<<<<<<<<<<<<<<<<<<<<<<<<<<<<<<<<<<<<<<<<<<<<<<<<<<<<<
'INPUT TABLE','VAREA2'/  VALVE AREA VS. TIME TABLE
1,3/
```

'TIME','AREA2'/
0.,0.095/
0.1,0.095/
50.,0.095/
'TIME VAR.','ARB2'/ VALVE AREA APPLICATION
'VAREA2','AREA2'/
/
'VALVE2','OPENFR',.TRUE./
/
'INPUT TABLE','VAREA3'/ VALVE AREA VS. TIME TABLE
1,3/
'TIME','AREA3'/
0.,0.129/
0.1,0.129/
50.,0.129/
'TIME VAR.','ARB3'/ VALVE AREA APPLICATION
'VAREA3','AREA3'/
/
'VALVE3','OPENFR',.TRUE./
/
'INPUT TABLE','VAREA4'/ VALVE AREA VS. TIME TABLE
1,3/
'TIME','AREA4'/
0.,0.403/
0.1,0.403/
50.,0.403/

'TIME VAR.','ARB4'/ VALVE AREA APPLICATION
'VAREA4','AREA4'/
/
'VALVE4','OPENFR',.TRUE./
/
'INPUT TABLE','VAREA5'/ VALVE AREA VS. TIME TABLE
1,3/
'TIME','AREA5'/
0.,0.277/
0.1,0.277/
50.,0.277/

```
'TIME VAR.','ARB5'/ VALVE AREA APPLICATION
'VAREA5','AREA5'/
/
'VALVE5','OPENFR',.TRUE./
/
'INPUT TABLE','VAREA6'/  VALVE AREA VS. TIME TABLE
1,3/
'TIME','AREA6'/
0.,0.28/
0.1,0.28/
50.,0.28/
'TIME VAR.','ARB6'/ VALVE AREA APPLICATION
'VAREA6','AREA6'/
/
'VALVE6','OPENFR',.TRUE./
/
'INPUT TABLE','FLWCH'/
1,7/
'TIME','MDOT'/
0.,1.748/
0.1,1.748/
40.,1.748/
40.1,1.749/
200.0,1.749/
200.1,1.735/
4000.,1.735/
'TIME VAR.','FLW'/ VALVE AREA APPLICATION
'FLWCH','MDOT'/
/
'FLWMIX','MFLO',.FALSE./
/
'INPUT TABLE','FLWCHA'/
1,6/
'TIME','MDOTA'/
0.,0.0/
0.1,0.0/
40.,0.0/
50.0,0.00124/
```

```
50.1,0.00124/
4000.,0.00124/
'TIME VAR.','FLWA'/ VALVE AREA APPLICATION
'FLWCHA','MDOTA'/
/
'FLWMIX2','MFLO',.FALSE./
/
'INPUT TABLE','FLWE'/
1,7/
'TIME','MDOTE'/
0.,0./
0.1,0./
200.,0.0/
200.1,0.319/
300.,0.319/
300.1,0.522/
4000.,0.522/
'TIME VAR.','FLWB'/ VALVE AREA APPLICATION
'FLWE','MDOTE'/
/
'FLWECI','MFLO',.FALSE./
/
'OUTPUT','OUT6'/
2,'C:/CAT/LINE6.OUT','(2X,F13.6,2X,F13.4,2X,F13.4)',1/
'MFLO:R-PIPE67>RSVTANK6',1.0/
/
'VOID:PIPE61(0.56)',1.0/
/
'OUTPUT','OUT61'/
5,'C:/CAT/PRESS.OUT','(2X,F13.6,2X,F13.4,2X,F13.4,2X,F13.4,2X,F13.4,2x,F13.4)',1/
'PRESS:PIPE21(0.01)',1.0/
/
'PRESS:PIPE31(0.01)',1.0/
/
'PRESS:PIPE41(0.01)',1.0/
/
'PRESS:PIPE51(0.01)',1.0/
/
```

'PRESS:PIPE61(0.01)',1.0/
/
'OUTPUT','OUT3'/
2,'C:/CAT/LINE3.OUT','(2X,F13.6,2X,F13.4,2X,F13.4)',1/
'MFLO:L-PIPE37>RSVTANK3',1.0/
/
'VOID:PIPE31(0.29)',1.0/
/
'OUTPUT','OUT5'/
2,'C:/CAT/LINE5.OUT','(2X,F13.6,2X,F13.4,2X,F13.4)',1/
'MFLO:R-PIPE55>RSVTANK5',1.0/
/
'VOID:PIPE52(0.46)',1.0/
/
'OUTPUT','OUT4'/
2,'C:/CAT/LINE4.OUT','(2X,F13.6,2X,F13.4,2X,F13.4)',1/
'MFLO:L-PIPE47>RSVTANK4',1.0/
/
'VOID:PIPE41(0.46)',1.0/
/
'OUTPUT','OUT2'/
2,'C:/CAT/LINE2.OUT','(2X,F13.6,2X,F13.4,2X,F13.4)',1/
'MFLO:L-PIPE27>RSVTANK2',1.0/
/
'VOID:PIPE21(0.19)',1.0/
/
'OUTPUT','OUT7'/
2,'C:/CAT/INPFLW.OUT','(2X,F13.6,2X,F13.4,2X,F13.4)',1/
'MFLO:RSVMIX>R-PIPE11',1.0/
/
'VOID:PIPE11(0.01)',1.0/
/
'OUTPUT','OUT8'/
1,'C:/CAT/INPECI.OUT','(2X,F13.6,2X,F13.4,2X,F13.4)',1/
'MFLO:RSVECI>R-HDR1',1.0/
/
'END'/
'INITIAL CONDITIONS'/<<<<<<<<<<<<<<<<<<<<<<<<<<<<<<<<<<<<<<<<<<<<<<<<<<<<<<<<<<<<

'PIPE11','BY-ENDS','HG-BY-TEMP','HF-BY-TEMP'/
1.8E5,24.0,24.0,0.0,0.0/
1.8E5,24.0,24.0,0.0,0.0/
'PIPE12','BY-ENDS','HG-BY-TEMP','HF-BY-TEMP'/
1.8E5,24.0,24.0,0.0,0.0/
1.8E5,24.0,24.0,0.0,0.0/
'PIPE13','BY-ENDS','HG-BY-TEMP','HF-BY-TEMP'/
1.8E5,24.0,24.0,0.0,0.0/
1.8E5,24.0,24.0,0.0,0.0/
'HDR1','BY-ENDS','HG-BY-TEMP','HF-BY-TEMP'/
1.8E5,24.0,24.0,0.0,0.0/
1.8E5,24.0,24.0,0.0,0.0/
'HDR2','BY-ENDS','HG-BY-TEMP','HF-BY-TEMP'/
1.8E5,24.0,24.0,0.0,0.0/
1.8E5,24.0,24.0,0.0,0.0/
'HDR3','BY-ENDS','HG-BY-TEMP','HF-BY-TEMP'/
1.8E5,24.0,24.0,0.0,0.0/
1.8E5,24.0,24.0,0.0,0.0/
'HDR4','BY-ENDS','HG-BY-TEMP','HF-BY-TEMP'/
1.8E5,24.0,24.0,0.0,0.0/
1.8E5,24.0,24.0,0.0,0.0/
'HDR5','BY-ENDS','HG-BY-TEMP','HF-BY-TEMP'/
1.8E5,24.0,24.0,0.0,0.0/
1.8E5,24.0,24.0,0.0,0.0/
'HDR6','BY-ENDS','HG-BY-TEMP','HF-BY-TEMP'/
1.8E5,24.0,24.0,0.0,0.0/
1.8E5,24.0,24.0,0.0,0.0/
'PIPE61','BY-ENDS','HG-BY-TEMP','HF-BY-TEMP'/
1.8E5,24.0,24.0,0.0,0.0/
1.8E5,24.0,24.0,0.0,0.0/
'PIPE62','BY-ENDS','HG-BY-TEMP','HF-BY-TEMP'/
1.8E5,24.0,24.0,0.0,0.0/
1.8E5,24.0,24.0,0.0,0.0/
'PIPE63','BY-ENDS','HG-BY-TEMP','HF-BY-TEMP'/
1.8E5,24.0,24.0,0.0,0.0/
1.8E5,24.0,24.0,0.0,0.0/
'PIPE64','BY-ENDS','HG-BY-TEMP','HF-BY-TEMP'/

1.8E5,24.0,24.0,0.0,0.0/
1.8E5,24.0,24.0,0.0,0.0/
'PIPE65','BY-ENDS','HG-BY-TEMP','HF-BY-TEMP'/
1.8E5,24.0,24.0,0.0,0.0/
1.8E5,24.0,24.0,0.0,0.0/
'PIPE66','BY-ENDS','HG-BY-TEMP','HF-BY-TEMP'/
1.8E5,24.0,24.0,0.0,0.0/
1.8E5,24.0,24.0,0.0,0.0/
'PIPE67','BY-ENDS','HG-BY-TEMP','HF-BY-TEMP'/
1.8E5,24.0,24.0,0.0,0.0/
1.8E5,24.0,24.0,0.0,0.0/
'PIPE31','BY-ENDS','HG-BY-TEMP','HF-BY-TEMP'/
1.8E5,24.0,24.0,0.0,0.0/
1.8E5,24.0,24.0,0.0,0.0/
'PIPE32','BY-ENDS','HG-BY-TEMP','HF-BY-TEMP'/
1.8E5,24.0,24.0,0.0,0.0/
1.8E5,24.0,24.0,0.0,0.0/
'PIPE33','BY-ENDS','HG-BY-TEMP','HF-BY-TEMP'/
1.8E5,24.0,24.0,0.0,0.0/
1.8E5,24.0,24.0,0.0,0.0/
'PIPE34','BY-ENDS','HG-BY-TEMP','HF-BY-TEMP'/
1.8E5,24.0,24.0,0.0,0.0/
1.8E5,24.0,24.0,0.0,0.0/
'PIPE35','BY-ENDS','HG-BY-TEMP','HF-BY-TEMP'/
1.8E5,24.0,24.0,0.0,0.0/
1.8E5,24.0,24.0,0.0,0.0/
'PIPE36','BY-ENDS','HG-BY-TEMP','HF-BY-TEMP'/
1.8E5,24.0,24.0,0.0,0.0/
1.8E5,24.0,24.0,0.0,0.0/
'PIPE37','BY-ENDS','HG-BY-TEMP','HF-BY-TEMP'/
1.8E5,24.0,24.0,0.0,0.0/
1.8E5,24.0,24.0,0.0,0.0/
'PIPE51','BY-ENDS','HG-BY-TEMP','HF-BY-TEMP'/
1.8E5,24.0,24.0,0.0,0.0/
1.8E5,24.0,24.0,0.0,0.0/
'PIPE52','BY-ENDS','HG-BY-TEMP','HF-BY-TEMP'/
1.8E5,24.0,24.0,0.0,0.0/
1.8E5,24.0,24.0,0.0,0.0/

'PIPE53','BY-ENDS','HG-BY-TEMP','HF-BY-TEMP'/
1.8E5,24.0,24.0,0.0,0.0/
1.8E5,24.0,24.0,0.0,0.0/
'PIPE54','BY-ENDS','HG-BY-TEMP','HF-BY-TEMP'/
1.8E5,24.0,24.0,0.0,0.0/
1.8E5,24.0,24.0,0.0,0.0/
'PIPE55','BY-ENDS','HG-BY-TEMP','HF-BY-TEMP'/
1.8E5,24.0,24.0,0.0,0.0/
1.8E5,24.0,24.0,0.0,0.0/
'PIPE41','BY-ENDS','HG-BY-TEMP','HF-BY-TEMP'/
1.8E5,24.0,24.0,0.0,0.0/
1.8E5,24.0,24.0,0.0,0.0/
'PIPE42','BY-ENDS','HG-BY-TEMP','HF-BY-TEMP'/
1.8E5,24.0,24.0,0.0,0.0/
1.8E5,24.0,24.0,0.0,0.0/
'PIPE43','BY-ENDS','HG-BY-TEMP','HF-BY-TEMP'/
1.8E5,24.0,24.0,0.0,0.0/
1.8E5,24.0,24.0,0.0,0.0/
'PIPE44','BY-ENDS','HG-BY-TEMP','HF-BY-TEMP'/
1.8E5,24.0,24.0,0.0,0.0/
1.8E5,24.0,24.0,0.0,0.0/
'PIPE45','BY-ENDS','HG-BY-TEMP','HF-BY-TEMP'/
1.8E5,24.0,24.0,0.0,0.0/
1.8E5,24.0,24.0,0.0,0.0/
'PIPE46','BY-ENDS','HG-BY-TEMP','HF-BY-TEMP'/
1.8E5,24.0,24.0,0.0,0.0/
1.8E5,24.0,24.0,0.0,0.0/
'PIPE47','BY-ENDS','HG-BY-TEMP','HF-BY-TEMP'/
1.8E5,24.0,24.0,0.0,0.0/
1.8E5,24.0,24.0,0.0,0.0/
'PIPE21','BY-ENDS','HG-BY-TEMP','HF-BY-TEMP'/
1.8E5,24.0,24.0,0.0,0.0/
1.8E5,24.0,24.0,0.0,0.0/
'PIPE22','BY-ENDS','HG-BY-TEMP','HF-BY-TEMP'/
1.8E5,24.0,24.0,0.0,0.0/
1.8E5,24.0,24.0,0.0,0.0/
'PIPE23','BY-ENDS','HG-BY-TEMP','HF-BY-TEMP'/
1.8E5,24.0,24.0,0.0,0.0/

1.8E5,24.0,24.0,0.0,0.0/
'PIPE24','BY-ENDS','HG-BY-TEMP','HF-BY-TEMP'/
1.8E5,24.0,24.0,0.0,0.0/
1.8E5,24.0,24.0,0.0,0.0/
'PIPE25','BY-ENDS','HG-BY-TEMP','HF-BY-TEMP'/
1.8E5,24.0,24.0,0.0,0.0/
1.8E5,24.0,24.0,0.0,0.0/
'PIPE26','BY-ENDS','HG-BY-TEMP','HF-BY-TEMP'/
1.8E5,24.0,24.0,0.0,0.0/
1.8E5,24.0,24.0,0.0,0.0/
'PIPE27','BY-ENDS','HG-BY-TEMP','HF-BY-TEMP'/
1.8E5,24.0,24.0,0.0,0.0/
1.8E5,24.0,24.0,0.0,0.0/
'RSVECI','R-HDR1'/
0.0/
'L-HDR1','R-HDR2'/
0.0/
'L-HDR2','R-HDR3'/
0.0/
'L-HDR3','R-HDR4'/
0.0/
'L-HDR4','R-HDR5'/
0.0/
'L-HDR5','R-HDR6'/
0.0/
'RSVMIX','R-PIPE11'/
1.748/
'RSVMIX2','R-PIPE11'/
0.0/
'L-PIPE11','R-PIPE12'/
1.748/
'L-PIPE12','R-PIPE13'/
1.748/
'L-PIPE13','R-HDR3'/
1.748/
'L-HDR4','L-PIPE61'/
0.0/
'R-PIPE61','L-PIPE62'/

0.0/
'R-PIPE62','L-PIPE63'/
0.0/
'R-PIPE63','L-PIPE64'/
0.0/
'R-PIPE64','L-PIPE65'/
0.0/
'R-PIPE65','L-PIPE66'/
0.0/
'R-PIPE66','L-PIPE67'/
0.0/
'R-PIPE67','RSVTANK6'/
0.0/
'L-HDR3','R-PIPE31'/
0.0/
'L-PIPE31','R-PIPE32'/
0.0/
'L-PIPE32','R-PIPE33'/
0.0/
'L-PIPE33','R-PIPE34'/
0.0/
'L-PIPE34','R-PIPE35'/
0.0/
'L-PIPE35','R-PIPE36'/
0.0/
'L-PIPE36','R-PIPE37'/
0.0/
'L-PIPE37','RSVTANK3'/
0.0/
'R-HDR3','L-PIPE51'/
0.0/
'R-PIPE51','L-PIPE52'/
0.0/
'R-PIPE52','L-PIPE53'/
0.0/
'R-PIPE53','L-PIPE54'/
0.0/
'R-PIPE54','L-PIPE55'/

0.0/
'R-PIPE55','RSVTANK5'/
0.0/
'R-HDR3','R-PIPE41'/
0.0/
'L-PIPE41','R-PIPE42'/
0.0/
'L-PIPE42','R-PIPE43'/
0.0/
'L-PIPE43','R-PIPE44'/
0.0/
'L-PIPE44','R-PIPE45'/
0.0/
'L-PIPE45','R-PIPE46'/
0.0/
'L-PIPE46','R-PIPE47'/
0.0/
'L-PIPE47','RSVTANK4'/
0.0/
'L-HDR4','R-PIPE21'/
0.0/
'L-PIPE21','R-PIPE22'/
0.0/
'L-PIPE22','R-PIPE23'/
0.0/
'L-PIPE23','R-PIPE24'/
0.0/
'L-PIPE24','R-PIPE25'/
0.0/
'L-PIPE25','R-PIPE26'/
0.0/
'L-PIPE26','R-PIPE27'/
0.0/
'L-PIPE27','RSVTANK2'/
0.0/
'END'/

APPENDIX C

Uncertainty Analysis

C.1 Definition

The total uncertainty in a dependent variable can be defined in terms of the uncertainties associated with the independent variables. For example if there is a function Q, which depends on x_1, x_2,..., x_n, then the total uncertainty in Q can be found with the following relationship [25]:

$$\sigma_Q = \left[\left(\frac{\partial Q}{\partial x_1} \right)^2 (\sigma_{x_1})^2 + \left(\frac{\partial Q}{\partial x_2} \right)^2 (\sigma_{x_2})^2 + \ldots + \left(\frac{\partial Q}{\partial x_n} \right)^2 (\sigma_{x_n})^2 \right]^{\frac{1}{2}} \qquad \text{(C.1)}$$

where σ_Q is the total uncertainty in Q and σ_{x_i} is the error associated with each of measured variables x_1, x_2,..., x_n. The relative uncertainty in Q can be found by dividing this expression by Q:

C.2 Uncertainty in Pressure Drop Measurement

OMEGA PX771 type differential pressure transmitters were utilized in the tests which have an accuracy of ±0.15 % of the calibrated span. Therefore, there is ±1 kPa uncertainty in each pressure drop measurement.

C.3 Uncertainty in Valve Opening

In the tests, valve opening was arranged manually with the help of visual inspection. Fully open 1 ¼" globe valves make 4 turn to be fully closed .The uncertainty

associated with valve opening was assumed to be 1/20 of 1 turn which corresponds to ±1.3% valve opening.

C.4 Uncertainty in Void Fraction

Void fraction parameter can be defined as :

$$\alpha = \frac{\text{Volume of gas}}{\text{Total volume of mixture}} \tag{C.2}$$

or

$$\alpha = \frac{\dot{V}_{air}}{\dot{V}_{air} + \dot{V}_{water}} \tag{C.3}$$

According to the Equation G.1, the total uncertainty in a result α which is a function of measured independent variables $\dot{V}_{air}$ and $\dot{V}_{water}$ can be obtained as;

$$\sigma_{\alpha} = \left[\left(\frac{\partial \alpha}{\partial \dot{V}_{water}} \right)^2 * (\sigma_{\dot{V}_{water}})^2 + \left(\frac{\partial \alpha}{\partial \dot{V}_{air}} \right)^2 * (\sigma_{\dot{V}_{air}})^2 \right]^{\frac{1}{2}} \tag{C.4}$$

Volume flow rate of water was measured with a turbine type flowmeter. Volumetric flow rate passing through the flowmeter was calibrated by collecting the passing water within certain periods and dividing it by the density of water. Therefore, the uncertainty in the water flow rate is a function of mass flow rate and density:

$$\dot{V}_{water} = \frac{\dot{m}_{water}}{\rho_{water}} \tag{C.5}$$

Since ρ_{water} is constant throughout the measurements and has no relative uncertainty. The uncertainty associated with the volumetric flow rate of water is same as the uncertainty associated with mass flow rate of water.

Mass flow rate measurement in the calibration of the turbine flowmeter depends on collected water and time duration. The uncertainty in measuring the weight of collected water was due to the accuracy of electronic balance which has an uncertainty of ±20 gram in full scale. The uncertainty associated with the time measurement obtained by chronometer was assumed to be ±0.5 s. Then the total uncertainty in the mass flow rate of water can be defined as [10];

$$\sigma_{\dot{m}_{water}} = \sqrt{\left(\frac{\partial \dot{m}_{water}}{\partial m} * \sigma_m\right)^2 + \left(\frac{\partial \dot{m}_{water}}{\partial t} * \sigma_t\right)^2} = \sqrt{\left(\frac{\sigma_m}{t}\right)^2 + \left(\frac{-m * \sigma_t}{t^2}\right)^2} \qquad \text{(C.6)}$$

Collected mass (kg)	Time (s)	Mass flow rate (kg/s)	$\sigma_{\dot{m}_{water}}$ (kg/s)
14.360	12.23	1.174	0.048
9.980	8.29	1.204	0.073
8.860	8.02	1.105	0.069
4.740	4.09	1.159	0.142
9.960	6.14	1.622	0.132
4.960	8.81	0.563	0.032
11.040	10.27	1.074	0.052
9.560	6.57	1.455	0.111
5.960	3.21	1.857	0.289
12.98	9.98	1.300	0.065
4.66	16.61	0.280	0.009

In Table C.1, the total uncertainties associated with water flow rate are shown for each data set. The mean of the total uncertainties in water mass flow rate was ±0.093 kg/s or ±0.3348 m^3 / h in volumetric flow rate .

Volumetric flow rate of air was measured by the orificemeter which consists of a orifice and a differential pressure transmitter. The orificemeter was calibrated by the aid of a rotameter connected to the air line in series. The uncertainty associated with the volumetric flow rate of air is 0.425 m^3 / h.

As a result, the total uncertainty in the void fractioncan be calculated by using Equation C.7 [10]:

$$\sigma_\alpha = \sqrt{\left(\frac{\dot{V}_{water} * \sigma_{\dot{V}_{water}}}{\left(\dot{V}_{water} + \dot{V}_{air} \right)^2} \right)^2 + \left(\frac{-\dot{V}_{air} * \sigma_{\dot{V}_{air}}}{\left(\dot{V}_{water} + \dot{V}_{air} \right)^2} \right)^2} \qquad \text{(C.7)}$$

Using the data in the calibration experiments, the total uncertainty of the void fraction was calculated for each data via Equation C.7 and the mean of these values was found to be ±0.0459 (±4.59%).

C.5 Uncertainty in Two-Phase Mass Flow Rate Prediction

Two-phase mass flow rate in this study is predicted by neural network approach in which the input variables were the voltage(V) generated with respect to the differential pressure across the valve and the void fraction(α). The total uncertainty in the void fraction was found to be $\pm 0.0459 (\pm 4.59\%)$, previously. The uncertainty in the voltage generated by the DP-transmitter was given by the supplier as $\pm 0.15\%$ for 1-5V range(See Appendix A.7). Due to the limitations of the test setup, 0.5-2.5V range was used in the experiments, which actually means, the uncertainty in the voltage was doubled to $\pm 0.3\%$.

Uncertainty in the neural network estimations of two-phase mass flow rate was determined by the use of the calibration test results. The trained neural network was questioned with the same training inputs (voltage and void fraction) by taking the previously defined total uncertainties for each variable. For example, for each training data for the two-phase mass flow rate, the void fraction introduced to the neural network system was given as $\alpha \pm 0.0459$ and the DP Voltage value was given as $V \pm 0.3\%$. The two-phase mass flow rate results are obtained for each test data and the mean of the maximum and minimum errors associated within these neural network runs are taken as the uncertainty in two-phase mass flow rate estimations. Since Feeder-5 has a higher amount of training points, the uncertainty in this feeder seems to be relatively smaller than Feeder-2 uncertainty. The Table C.1 shows the uncertainty in the mass flow rate estimations for two different diameter feeders which are used in the mass flow rate predictions throughout the experiments. The uncertainties are not symmetrical in the negative and positive parts.

Table C.1 Uncertainties in the Mass Flow Rate Prediction in Neural Network

		Total Uncertainty (± %)
Feeder-2	Single Phase Mass Flow Rate	+5.73% −7.70%
	Two Phase Mass Flow Rate	+4.09% −8.05%
Feeder-5	Single Phase Mass Flow Rate	+3.02% −3.38%
	Two Phase Mass Flow Rate	+3.35% −1.54%